2009

ROLE OF FDCs AND FDC ACTIVATION IN PROMOTING HUMORAL IMMUNITY INCLUDING RESPONSES TO T-DEPENDENT ANTIGENS IN THE ABSENCE OF T CELLS

Sayed Rania El
Virginia Commonwealth University

School of Medicine
Virginia Commonwealth University

This is to certify that the Dissertation prepared by **Rania Mohamed El Sayed** entitled **"ROLE OF FDCs AND FDC ACTIVATION IN PROMOTING HUMORAL IMMUNITY INCLUDING RESPONSES TO T-DEPENDENT ANTIGENS IN THE ABSENCE OF T CELLS"** has been approved by her committee as satisfactory completion of the dissertation requirement for the degree of Doctor of Philosophy

Dr. Tew, John G., Ph.D., Director of Dissertation

Dr. Conrad, Daniel H., Ph.D, School of Medicine

Dr. Smeltz, Ronald B., Ph.D., School of Medicine

Dr. Szakal, Andras K., Ph.D., School of Medicine

Dr. White, Kimber L., Ph.D., School of Medicine

Dr. Ohman, Dennis E., Ph.D., Chair, Department of Microbiology and Immunology

Dr. Jerome F.Strauss, III, M.D., Ph.D., Dean, School of Medicine

Dr. F. Douglas Boudinot, Ph.D., Dean, Graduate School

Date

ROLE OF FDCs AND FDC ACTIVATION IN PROMOTING HUMORAL IMMUNITY INCLUDING RESPONSES TO T-DEPENDENT ANTIGENS IN THE ABSENCE OF T CELLS

A Dissertation submitted in partial fulfillment of the requirements for the degree of Doctor of Philosophy at Virginia Commonwealth University.

By

RANIA MOHAMED EL SAYED
Bachelor of Science, Ain Shams University, Cairo, Egypt, 1996

Director: Dr. John G. Tew, Ph.D.
Professor, Department of Microbiology and Immunology

Virginia Commonwealth University
Richmond, Virginia
June, 2009

Dedication

This work is dedicated to my beloved husband Mohey El Shikh, my everlasting support and my safest shelter; to the soul of my father the greatest man, father and teacher; to my mother, the lady with the kindest heart in the whole world and to my dearest brother Wael El Sayed. I am blessed to be having such a perfect family.

Acknowledgement

“In the name of ALLAH the Merciful and the Compassionate”

I would like to deeply thank my primary advisor Dr. John G. Tew for giving me an opportunity to learn and pursue my research in his laboratory. I would also like to thank him for his guidance, support and encouragement.

I would like to express my deep appreciation to all the members of my committee: Dr. Daniel H. Conrad, Dr. Ronald B. Smeltz, Dr. Andras K. Szakal and Dr. Kimber L. White for their continuous support and encouragement. I would like to thank Dr. Andras K. Szakal for his invaluable expertise and his guidance. I was really fortunate to have many talented scientists and gentlemen work with me.

My deapest thanks and gratitude goes to my beloved husband and colleague Dr. Mohey El Shikh for his continuous help and support, for sharing the suffering and the joy during those past years of my studies. He was always there for me, pushing me forward, encouraging me, supporting me and putting me back on the track whenever I get tired during the race, to him I owe my achievement.

I would like to thank the old and present members of my laboratory for the pleasant time we spent together working with our Follicular Dendritic Cells, which Dr. Wu used to describe as, “Not Easy”.

I would like to thank the administrative staff of the department of Microbiology and Immunology: Mrs. Connie J. Babcock, Mrs. Martha L. VanMeter, Mrs. Roberta N.

Fogg and Mrs. Bobbie J. Fogg for their great help and for making our stay at the VCU pleasant. I would also like to thank everyone who encouraged me with a pleasant word or a simple nice smile that made the difficult easy.

Last but certainly not the least, my gratitude and sincere thanks are for my father, my mother and my dearest brother for their unconditional and undying love, prayers, encouragement and support.

Table of Contents

List of Tables

Page

List of Figures

Page

Chapter 3

Chapter 4

Chapter 5

Chapter 6

List of Abbreviations

-/-	Homozygous deletion of a gene
8D6	FDC-associated antiapoptotic molecule (CD320)
Å	Angstrom
A20	Mouse B lymphoma cell line
Ab	Antibody
Ag	Antigen
anti-rat-κ	Anti-rat kappa
Anti-δ	Anti-immuoglobulin D antibody
APC	Antigen presenting cell
ARR	Ag-retaining reticula
B-1	Non-conventional B cells which are enriched in the pleural and peritoneal cavities
BAFF	B-cell-activating factor of the TNF family
BAFF-R	BAFF receptor
BCR	B cell Receptor
Blimp-1	B lymphocyteinduced maturation protein-1
bp	Base Pair
BSA	Bovine serum albumin
BSF	B-cell Stimulatory Factor
Btk	Bruton's tyrosine kinase
C3	Complement component 3
C3b	Element formed from the cleavage of C3
C3d	Cleavage product of C3b complement fragment
C3dg	The terminal activation/processing fragment of the third complement component
C4	Complement component 4
C4b	Element formed from the cleavage of C4
C4BP	C4b binding protein
CD	Clusters of Differentiation
CD21L	CD21 ligand
CD40L	CD40 ligand
CDR	Complementarity Determining Region
CGG	Chicken Gamma Globulin
CR1/2	Complement receptor 1/2
CR2	Complement Receptor 2
CR2-CD19-CD81(TAPA-1)	B cell co-receptor complex
CXCL-13	Chemokine (C-X-C motif) ligand 13 (B-cell chemo-attractant)
CXCR5	(CD185) Burkitt lymphoma receptor 1 (BLR1); receptor for CXCL13 (BLC)
Cy5.5	Cyanine 5.5

DAB	Diaminobenzidine
DC	Dendritic cell
DMEM	Dulbecco's modified Eagle's medium
EM	Electron Microscopy
Fc	Fragment crystallizable
Fcα/μR	Receptor for IgA and IgM
FcεRII	The low affinity IgE receptor (CD23)
FcγRIIb	The otherwise inhibitory receptor for IgG
FcγRs	Receptors for immunoglobulin G
FDC	Follicular dendritic cell
FDC-M1	Mfge8
FDC-M2	C4b eptiope
FITC	Fluorescein Isothiocyanate
GC	Germinal Center
HBV	Hepatitis B Virus
HIV	Human Immunodeficiency Virus
HIV-gp120	Surface glycoprotein of the HIV envelope
HRP	Horse Radish Peroxidase
IC	Immune complex
iC3b	Inactive derivative of C3b
ICAM-1	Inter-Cellular Adhesion Molecule 1 (CD54)
ICCOSOMES	Immune Complex Coated bodies (some-s)
ICs	Immune Complexes
IgA	Immunoglobulin A
IgE	Immunoglobulin E
IgG	Immunoglobulin G
IgM	Immunoglobulin M
Igs	Immunoglobulins
IKK	IκB kinase
IL-15	Interleukin 15
IL15Rα	Interleukin 15 receptor alpha chain
IL-2/15Rβγ	Interleukin 2 and 15 common βγsubunits
IL-6	Interleukin 6
IL-7	Interleukin 7
ITIM	Immunoreceptor tyrosine-based inhibitory motif
KD	Kilo Dalton
KO	Knockout
LFA-I	Leucocyte function–associated antigen-1
LN	lymph node
LPS	Lipopolysaccharide
LT	lymphotoxin
LT-R	Lymphotoxin receptor
$LT\alpha_1\beta_2$	Lymphotoxin alpha 1 beta 2 heterotrimer

mAb	Conjugated monoclonal antibodies
MadCAM-1	Mucosal addressin cell adhesion molecule-1
mDCs	Immature monocyte-derived dendritic cells
Mfge8	Fat globule epidermal growth factor 8
MFI	Mean fluorescent intensity
MHC class II	Major histocompatibility class 2 molecules
mIg	Membrane-bound Immunoglobulins
mIgD	Membrane-bound Immunoglobulin D
MRK-1	Mouse anti-rat-κ light chain
MZ B	Marginal zone B cells
NIP	(4-hydroxy-3-iodo-5-nitrophenyl) acetyl
NK-T cell	Natural killer T cell
NP	(4-hydroxy-3-nitrophenyl)-acetyl
NSS	Nonspecific rabbit serum
PAMPs	Pathogen-associated molecular patterns
PBS	Phosphate Buffered Saline
poly I:C	Polyriboinosinic-polyribocytidylic acid (TLR-3 ligand)
PRR	Pattern recognition receptor
PWM	Pokeweed mitogen
qRT-PCR	Quantitative reverse transcriptase PCR
rPA	Recombinant protective antigen of *Bacillus anthracis*
SEM	Scanning electron microscopy
SHIP	Src homology 2 domain-containing inositol-5 phosphatase
SHM	Somatic Hypermutation
slg	Surface-bound immunoglobulin
streptavidin-HRP	Streptavidin-horseradish peroxidase
*t*1/2	Half life time
TAPA-1	Target of an Anti-Proliferative Antibody (CD81)
TCR	T cell receptor
TD	T cell (Thymic) dependant
Tg	Transgenic
TI	T cell (Thymic) independant
TI-1 antigens	T cell (Thymus) independent type 1 antigens
TI-2 antigens	T cell (Thymus) independent type 2 antigens
TLR	Toll-like receptor
TNF-α	Tumor necrosis factor alpha
TNP	Trinitrophenol
TT	Tetanus toxoid
VCAM-1	Vascular cell adhesion molecule 1 (CD106)
VLA-4	Very Late Antigen-4
WT	Wild Type
λ^+ B cells	Lambda light chain positive B cells

Abstract

ROLE OF FDCs AND FDC ACTIVATED IN PROMOTING HUMORAL IMMUNITY INCLUDING RESPONSES TO T-DEPENDENT ANTIGENS IN THE ABSENCE OF T CELLS

By Rania M. El Sayed, Ph.D.

A Dissertation submitted in partial fulfillment of the requirements for the degree of Doctor of Philosophy at Virginia Commonwealth University.

Virginia Commonwealth University, 2009

Major Director: Dr. John G. Tew, Ph.D.
Professor, Department of Microbiology and Immunology

Follicular dendritic cells (FDCs) reside in primary B-cell follicles and in the light zones of germinal centers (GCs) in secondary follicles, where their dendrites interdigitate forming extensive networks intimately interacting with B-cells. In GCs, FDCs can be found at the edges attached to the supporting reticular fibers. They trap and arrange immune complexes (ICs) in vivo and in vitro in a periodic manner with 200–500Å spacing and provide both antigen-specific and

non-specific accessory signals to B-cells. FDCs exist in resting and activated states, with two characteristically different phenotypes. In their activated state, FDCs upregulate the expression of accessory molecules and cytokines important in the FDC-B cell interaction in GCs. ***We sought to determine the mechanisms influencing the transition of FDCs from a resting to an activated state in GCs and their impact on T-cell dependent (TD) and independent (TI)-GC reactions (GCRs).***

We found that IC-FDC interactions via FDC-FcγRIIB induce the upregulation of FDC-FcγRIIB, -ICAM-1, and -VCAM-1, at both the protein and mRNA levels. We also reported for the first time the expression of TLR-4 on FDCs. Moreover, engagement of FDC-TLR4 with LPS activated NF-κB, up-regulated expression of important FDC-accessory molecules, including FcγRIIB, ICAM-1, and VCAM-1, and enhanced FDC accessory activity in promoting recall IgG responses. Moreover, IC-activated FDCs produced IL-6 and FDC-IL-6 promoted GCRs, somatic hypermutation (SHM) and IgG production.

Further, we reported that binding of FDCs to collagen coated surfaces induced restoration of their dendritic processes and networks in vitro. In addition, we designed an FDC-supported in vitro model capable of induction and assessment of primary human antibody responses to protein antigens characterized by class-switching and affinity maturation.

Uniquely, we generated TI immune responses to TD protein Ags in the complete absence of T cell help in vivo and in vitro. In the presence of FDC-associated second

signals such as BAFF and C4BP, FDC- FcγRIIB-periodically trapped-ICs induced the production of Ag-specific IgM, GC-development and plasmablast-differentiation in anti-Thy-1-pretreated nude mice. Purified murine and human B cells cultured in vitro with IC-bearing FDCs also showed the production of antigen–specific IgM within just 48 h.

General Introduction

The secondary lymphoid tissues (the Theatre)

Secondary lymphoid tissues (e.g Lymph nodes and spleen), are the theatre where players of the immune system meet to orchestrate the initiation of an immune (adaptive) response.

Under steady-state conditions, peripheral tissues are patrolled by only low numbers of lymphocytes that can potentially respond to invading microorganisms (1). Secondary lymphoid tissues facilitate the efficient interaction between the immune system and microorganisms. They possess a highly organized micro-architecture that maximize the probability of antigen encounter with an antigen-specific lymphocyte and are necessary for the compartmentalization of numerous cellular interactions, thus providing the optimal environment for initiation of immune responses, including the determination of cell fate (2). Moreover, they are remarkably well connected to the blood and lymphatic systems, allowing them to continually sample and concentrate antigens that are circulating throughout the body.

Secondary lymphoid tissues are characterized by their efficient role in reducing pathogen spread throughout the host by capturing pathogens; via the action of the strategically localized macrophages (3,4), and by the production of innate immune mediators, such as type I interferons (IFNs) (5). These rapidly induced innate immune mechanisms reduce the pathogen load in anticipation of an adaptive immune response to be mounted. They also help bring antigen presenting cells (APCs) in contact with infrequent antigen-specific lymphocytes for the induction of an efficient antigen specific

immune response (6,7). In addition, they provide the necessary factors for the survival and differentiation of lymphocytes (2,8).

Beneath the protective outer collagenous capsule of a lymph node (LN), distinct regions with unique features have been described. Underneath the subcapsular sinus, the LN cortex with the well organized aggregates of B-cells; known as follicles, can be observed. The LN follicles are considered to contain the largest population of IgM^{med} IgD^{hi} $CD21^{med}$ $CD23^{hi}$ B cells in the body. They are also sites rich in radiation-resistant follicular dendritic cells (FDCs). Adjacent to the follicles, the paracortex; which is the T-cell zone that is enriched in antigen presenting cells (APCs) and high endothelial venules (HEVs), can be detected. The HEVs mediate the recruitment of APCs that have encountered the antigen in the periphery. They are also specialized in the continuous supply and drainage of lymphocytes to the LNs and the periphery, respectively. The paracortex is also characterized by a network of collagenous conduit fibers, which permit the passage of low molecular weight molecules of the lymphatic fluid, such as lymphokines and small antigens (9). The medulla is the innermost area of the lymph node, it contains B and T cells that are organized into medullary cords as well as antibody forming cells (AFCs; plasmablasts and plasma cells) and is also rich in DCs and macrophages (10).

Germinal centers (the Stage)

The germinal center (GC) was first described in 1884 by Walther Flemming, who observed a site of large lymphocytes undergoing mitosis in the follicles of lymph nodes and other secondary lymphoid organs and proposed this site to be a major source of all

lymphocytes in the body (11,12). Although this originally proposed function of the GC was disproven, Flemming's work motivated subsequent intense studies concerning GCs.

GCs are the sites where efficient antibody affinity maturation occurs through the process of clonal proliferation, somatic hypermutation and selection (13-15). GCs are known to be associated with T dependent antibody responses, and are identified as the main sites where high-affinity antibody-secreting plasma cells and memory B cells are generated.

A T cell dependent immune response is initiated when infrequent antigen-specific T and B cells cognately interact at the boundary between B-cell follicles and T cell zones (16-18). The activated B-cells can then move to extra-follicular areas where they proliferate and differentiate into short-lived plasma cells or move into the B cell follicles and proliferate within the FDC network, giving rise to GCs (19,20). As the GC matures, two main compartments; termed dark and light zones, become evident. The light zone is mainly occupied by FDCs with their complex network of processes intimately interacting with B cells, whereas few processes extend into the dark zone, where actively proliferating lymphocytes are densely packed (12).

Follicular Dendritic Cells (FDCs) and the FDC-B-T cell interaction (the players)

1. FDCs Morphology, Phylogeny and Development

Owing to their unique morphology and follicular location, the antigen retaining cells residing in primary follicles, and light zones of germinal centers in secondary follicles, were given the name "Follicular Dendritic Cells" (FDCs). In 1968, Szakal and Hanna published the first electron micrographs and description of FDCs (21-23).

Follicular dendritic cells constitute a pleomorphic, non-phagocytic group of dendritic type cells, which possess either filiform dendrites or "beaded" dendritic processes. Filiform dendrites of FDCs, which have an average length and diameter of 15-20 and 0.1-0.3 μm, respectively, tend to branch and anastomose near the cell body forming a radiating "sunburst"-like pattern (24). Studies of FDCs at the ultrastructural level revealed that they have single, and sometimes double, lymphocyte-size cell bodies, with an irregular, lobated euchromatic nucleus (sometimes there are multiple nuclei), Golgi apparatus, numerous small vesicles, and some mitochondria which are not abundant in the dendritic processes (24). The microspheres of the "beaded" dendrites range between 0.3 and 0.6 μm in diameter and are termed ICCOSOMES [immune complex-coated bodies (some-s)] (25-28).

Information available on FDCs is based primarily on studies using humans and rodents. However, FDCs are present and functional in birds and if FDCs are defined broadly as cells with the ability to trap and retain ICs, they appear to exist in all jawed vertebrates, including amphibians, reptiles and fish. The origin of FDCs remains unclear. FDCs are radiation resistant making it difficult to study development using adoptive transfer models. At present there are some data supporting a haematopoietic origin while even more data support a stromal cell origin.

2. Immunoregulatory mechanisms involving FDCs

a. <u>Capturing, retention and periodic arrangement of antigen-antibody complexes (Immune complexes; ICs) by FDCs.</u>

Follicular dendritic cells capture and retain antigens (Ags) in the form of immune complexes (ICs), via their surface expressed FcγRIIB (CD32) and complement receptor (CR2; CD21) (29-31). Antigens trapped on FDCs remain in their native conformation, a phenomenon that was confirmed by their continued recognition by specific antibody (Ab) and, on isolation, their co-migration with native Ag when applied to sizing columns (32) Moreover, horse radish peroxidase (HRP) retained its activity and was chemically detectable on the FDC cytoplasmic membranes indicating that the native structure was conserved at the tertiary protein structure level; hence the enzymatic activity was preserved. In mice, conventional soluble protein Ag-Ab ICs are retained on FDCs with a *t*1/2 of ~2 months; nevertheless, Ags have been detected a full year after injection (33).

FDCs trap ICs in a periodic manner, a phenomenon that was discovered using scanning EM with Ag trapped *in vivo* (24), revealing an orderly, spiraling, arrangement of ICs made up of alternating light and dark bands. The same periodicity was observed in recent *in vitro* studies (34) where ICs were arranged on FDCs with a 200Å to 500Å spacing between epitopes. This spacing correlates with the 95-675 Å spacing originally described by Dintzis as optimal for B cell receptor for Ag (BCR) cross-linking and activation in thymic independent (TI) responses.

IC trapping by FDCs in primary (35) and secondary (36-38) immune responses is critical for induction of GC reactions, class switching, somatic hypermutation, affinity maturation, and regulation of IgG and IgE serum levels (35,38-53). In primary responses to thymic dependent (TD) Ags, ICs form as soon as Ab is produced and, by four days after Ag challenge, ICs may be found on splenic FDCs. The kinetics of recall responses is

dramatic. Ags are almost instantaneously converted into ICs by Ab persisting from prior immunization and by 1 min after challenge labelled Ags can be detected on cells in a chain transporting ICs to FDCs deeper in the lymph node cortex. IC retention is localized and Ag injection into a single limb of an immune mouse will be restricted to the draining lymph nodes and to a lesser extent in the spleen. With time, FDC-Ag becomes more and more focused to lymph nodes nearest the site of Ag injection and by 1 year, persisting Ag and specific Ab-forming cells are almost exclusively confined to the most proximal lymph node (51,54).

b. Molecular FDC-T-B-cell interactions.

FDC promote B-cell proliferation and survival by providing both Ag-dependent and independent signals. The ability of FDC to prolong B cell viability relates to both Ag-specific and non-specific signaling, and the FDC-mediated co-stimulatory signals are not species-restricted, as evidenced by the ability of murine FDC to provide co-stimulation to human B and T cells and vice versa (55,56). The Ag–Ab complexes trapped by FDCs provide intact Ag for interaction with BCRs on GC B cells and this Ag–BCR interaction provides a positive signal for B cell activation and differentiation (36,44). FDC-FcγRIIB binds the Fc regions of Igs, thereby inhibiting the SHIP signaling pathway and thus minimizes ITIM activation in B cells by reducing co-cross-linking of BCR and B cell-FcγRIIB (30,57,58). FDC–CD21L binds complement receptor 2 (CR2 or CD21) on the B cell via CD21 in the B cell co-receptor complex consisting of CD19/CD21/TAPA-1. Engagement of CD21 in the B cell co-receptor complex by complement-derived FDC–CD21L delivers a critical co-signal. Co-ligation of BCR and

CD21 facilitates association of the two receptors, and the cytoplasmic tail of CD19 is phosphorylated by a tyrosine kinase associated with the B cell receptor complex. This co-signal dramatically augments stimulation delivered by engagement of BCR by Ag, and blockade of FDC–CD21L reduces the immune responses considerably (typically 10- to 1000-fold (29).

In addition to the accessory signals delivered by the complement derived CD21L interacting with the CD21/CD19/TAPA-1 complex, activated forms of both C3 (C3b) and C4 (C4b) can bind C4 binding protein (C4BP), which in humans and likely in rodents, co-localizes with ICs on FDCs as well as CD40 in secondary B cell follicles. C4BP is a novel CD40 ligand capable of activating B cells through CD40. C4BP in immune complexes (ICs) trapped on FDCs has been shown to signal B cells via intact CD40 in short-lived antigen-specific TI GCs independent of the T-cell derived CD40L (CD154) expression (59). Several other FDC-associated molecules are also involved in and are critical for B-cell activation, FDC- B-cell-activating factor of the TNF family (BAFF) (60-62), engaging B cell-BAFF-R (60,63), has been reported to be involved in several immunological phenomena, such as T independent B cell responses and antibody isotype switching, CD21 & CD23 expression, peripheral B-cell and plasma cell survival, MZ B cell integrity and GC maintenance (64). FDC-8D6 and CD44 engaging their ligands on B cells are also involved as co-stimulatory signal-providing molecules in FDC-B cell interactions (65). Further, FDC-CXCL-13, which attracts B cells and helps organize follicles (66,67), IL-6 that promotes terminal B cell differentiation (68), and membrane-

bound molecules necessary for FDC-B cell synapse formation, ICAM-1 and VCAM-1 (69) are also critical in B cell activation.

c. FDC-phenotypes and major FDC-molecules (receptors, cytokines, chemokines, etc.) with known functions

FDC-phenotypes in primary and secondary follicles are very different. In secondary follicles (i.e. germinal centres), FDCs bear high levels of FcγRIIB, ICAM-1, and VCAM-1, which are involved in converting poorly immunogenic ICs into a highly immunogenic form as well as facilitating FDC-B cell interactions. In contrast, FDC-FcγRIIB, -ICAM-1, and -VCAM-1 levels are low and difficult to detect in primary follicles.

Expression of FDC accessory molecules is subject to regulation; and as reported here in projects 1-3 (70-72), engagement of ICs, TLR ligands, or collagen type 1 induces FDC activation and upregulation of these molecules. Similarly, FDC-FCγRIIB mediated trapping of ICs *in vitro*, induces the secretion of BAFF and IL-6 (projects 4 and 5 in the present work [(73) & in press]). FDC-activation by TLR agonists was generally done using lipopolysaccharide (LPS). However, FDCs express mRNA for TLR2, 3, 4 & 9 and injection of poly I:C increases FDC-FcγRIIB in draining lymph nodes similar to results for LPS (project 3 (71)). FDCs also express CD44 and CD29 and FDC binding to collagen type I *in vitro* induces regeneration of FDC processes and networks with features in common with networks *in vivo* (project 2 (72)). A major consequence of activation is a marked increase in accessory activity. For example, the number of FDCs

needed for IgG responses *in vitro* could be reduced four-fold and somatic hypermuation could be increased if FDCs were activated (project 3 (71) & (35)).

FDCs express and secrete various molecules with important immunoregulatory functions as listed below in table 1 (Reviewed in (74)).

FDC-molecules	Immunoregulatory role
FcγRIIB (CD32)	1- **Conversion of poorly immunogenic ICs into a highly immunogenic form:** FDCs express high levels of FcγRs relative to GC B cells and these receptors bind immunoglobulin-Fc in ICs and minimize binding to B cell FcγRIIB. Thus, cross-linking of BCR and B cell-FcγRIIB via ICs is minimized, ITIM signalling is reduced, and B cells are productively signalled. 2- **FDC activation:** Both wild-type (WT) and FcγRIIB$^{-/-}$ mice trap ICs but only WT mice respond to ICs by up-regulating FcγRIIB, ICAM-1, and VCAM-1. Similarly, blockade of FDC-FcγRIIB results in inhibition of IC-induced FDC-IL-6 and FDC–BAFF production indicating the importance of FDC-FcγRIIB in FDC activation and cytokine production. 3- **IC periodicity:** In the absence of complement, ICs are trapped by FDC-FcRs and are periodically arranged on FDC dendrites. ICs trapped via complement receptors do not induce the B cell activation characteristic of periodically arranged Ags. 4- **Long term IC retention:** Complement-mediated IC trapping in the draining lymph nodes of FcγRIIB$^{-/-}$ mice is normal. However, long-term retention of ICs is reduced in FcγRIIB$^{-/-}$ mice suggesting the importance of this receptor in the long-term retention of ICs. 5- **Regulation of serum IgG levels:** High IgG levels feedback on Ag retained on FDC dendrites and “zip” them together thus hiding the ICs within "ball-of-yarn"-like dendritic convolutions. When Ab levels decline, Ab dissociates from Ag-epitopes, the dendrites unravel and the persisting Ag is exposed to memory B cells. This exposure initiates a rebound in Ab and memory B cell production, thereby maintaining humoral immunity.
FcεRII (CD23)	**Immune complex retention and regulation of IgE levels:** Serum IgE is suppressed in CD23 transgenic (Tg) mice where FDC-CD23 and B cell-CD23 are elevated. Adoptive transfer studies indicated that IgE production is suppressed when normal lymphocytes are used to reconstitute Tg mice with high levels of FDC-CD23. Furthermore, isolated Tg-FDCs augment IgG production normally but IgE

	production is reduced suggesting that a high level of FDC-CD23 selectively suppresses IgE.
Fcα/μR	**Immune complex retention:** In humans FDCs are the predominant cell type expressing Fcα/μR. This Fc receptor can bind Abs of both IgM and IgA isotypes and may function in Ag presentation and B cell selection in the GC response in systemic and mucosal immunity.
CR1/2 (CD21/35)	**Immune complex retention especially in the spleen**: Splenic IC retention does not occur without Complement
CD21L (iC3b, C3d or C3dg)	**B cell co-stimulation *via* CD21:** Engagement of CD21 in the B cell co-receptor complex by complement derived FDC-CD21L delivers a critical co-signal. Co-ligation of BCR and CD21 facilitates association of the two receptors and the phosphorylation of the cytoplasmic tail of CD19 by a BCR-complex-associated tyrosine kinase. This co-signal augments stimulation delivered by Ag and blockade of FDC-CD21L reduces B cell proliferation, activation induced cytidine deaminase, and Ab production 10 to 1,000 fold.
FDC-M1 (Mfge8)	**Clearance of apoptotic bodies:** Fat globule epidermal growth factor 8 (Mfge8) "licenses" tingible body macrophages to engulf apoptotic bodies in GCs and helps minimize autoimmunity
FDC-M2 (C4b eptiope)	**Binds C4b localized with FDC-ICs:** C4b binding protein (C4BP) binds C4b and co-localizes with ICs on FDCs. FDC-C4BP has been shown to signal B cells via CD40, independent of T-cell CD40L (CD154). Injection of mice with FDC-M2 inhibits C4BP localisation and TI-GC development.
ICAM-1 (CD54)	**Stability of the FDC-B cell synapse:** Abs reactive with murine ICAM-1 and/or leukocyte functional Ag-I (LFA-I) interfere with FDC-B cell clustering resulting in reduced B cell proliferation. In addition, VLA-4 and VCAM-1 have been observed in GCs and likely also play a role in FDC-B cell interactions. These adhesion molecules are thought to stabilize the FDC-B cell synapse and promote interaction of FDC-Ag and FDC-costimulatory molecules with B cells.
VCAM-1 (CD106)	
MadCAM-1	
CXCL13	**B cell homing to lymphoid follicles *via* CXCR5:** CXCL13 is secreted by FDCs and acts as a chemoattractant for B cells via the CXCR5 chemokine receptor. FDC development and expression of this chemokine depend on $LT\alpha_1\beta_2$, TNF-α and related molecules. A persistent $LTa_1\beta_2$ stimulus is important for both the induction and the maintenance of FDC networks. Further studies suggest that the maintenance of the primary lymphoid follicle structure is mediated by a positive feedback loop: CXCL13 stimulates B cells to express high levels of $LT\alpha_1\beta_2$ and in turn $LT\alpha_1\beta_2$ stimulates FDCs to produce CXCL13.
IL-6	**GC development and terminal B cell differentiation:** FDCs are the source of IL-6 in GCs. Engaging FDC-FcγRIIB by ICs activates FDCs

	and enhances FDC-IL-6 production. FDC-IL-6 promotes GC development, IgG production, and somatic hypermutation.
IL-15	**Enhancement of GC B cell proliferation:** IL-15 is produced by FDCs and is captured by IL-15Rα on the surface of FDCs. Surface IL-15 is active and promotes GC-B cell proliferation. GC-B cells have the signal-transducing components (IL-2/15Rβγ), but not a receptor for binding of soluble IL-15 (IL-15Rα) and the IL-15 signal may be delivered by trans-presentation from FDCs to GC-B cells via cell-cell contact.
8D6 (CD320)	**B cell anti-apoptosis:** The 8D6 molecule inhibits apoptosis and influences both proliferation and Ab secretion by GC B cells. Moreover, GC B cells that are induced to differentiate into pre-plasma cells are the most sensitive to the neutralizing effects of anti-8D6.
BAFF	**Enhancement of T independent B cell proliferation:** FDC-BAFF has the ability to support TI B cell activation. The outcome of BAFF signalling is multifaceted and different receptors mediate different functions. Peripheral B cell survival, plasma cell survival, MZ B cell integrity, GC maintenance, CD21 & CD23 expression, T independent B cell responses, and Ig class switching may be influenced by BAFF.
CD40	**Regulation of FDC-CD23:** FDCs express CD40 and when incubated with either CD40L trimer or agonistic anti-CD40 Ab, the expression of FDC-CD23 is increased both at the mRNA and protein levels. As explained above, FDC-CD23 helps regulate IgE levels.
Toll-like receptors (TLRs) (2, 3, and 4)	**Engagement of Pathogen-associated molecular patterns (PAMPs) and FDC activation:** Dramatic upregulation of FDC-ICAM-1, VCAM-1, and FcγRIIB is observed after injecting LPS into animals expressing wild-type TLR4 but not in animals with mutated TLR4. Incubation of FDCs with LPS *in vitro* upregulates FcγRIIB, ICAM-1, and VCAM-1. FDC activation by TLR agonists has been largely studied with LPS. However, FDCs express mRNA for TLR2, 3, 4 & 9 as well, and injection of poly I:C increases FDC-FcγRIIB to levels comparable with LPS.
CD44	**Interaction with ECM proteins, regeneration of FDC dendrites and B cell anti-apoptosis:** FDCs express CD44 and CD29 and FDC binding to collagen type I *in vitro* induces the regeneration of FDC processes and networks. CD44 also enhances B-cell adherence to FDCs allowing delivery of the FDC-derived B cell survival signals including 8D6 and BAFF.
CD29	
TNF-α	**T cell stimulation:** FDCs produced soluble tumor necrosis factor alpha (TNFα) that increases transcription and production of HIV in GC T cells.
IL-7	Interleukin 7 has been found in isolated tonsilar FDCs using RT-PCR and intracellular staining. IL-7 signalling coupled with crosslinking of

	surface immunoglobulin receptors results in B cell proliferation.
LT-R (and TNFα)	FDC development and maturation

d. T-dependant and independent-immune responses and FDCs

By the 1950s, the lymphopoietic function of the thymus had been well established, but no one believed that it had any immunological role. It was a common principle that thymus was a useless organ that had become unnecessary during evolution; a conclusion that was based on a number of observed phenomena (75).

First, efficient immune responses were documented in mice thymectomized in adult life (76). Moreover, thymus lymphocytes were inefficient in initiating immune reactions after adoptive transfer to appropriate recipients if compared to lymphocytes from the spleen, lymph nodes and blood. Again, thoracic duct lymphocytes homed efficiently from blood into lymphoid tissues, with the thymus as 'the only exception', where only very few lymphocytes lodged (75). In addition, antibody-forming plasma cells and germinal centers were absent from thymus tissue, although so prominent in spleen and lymph nodes. However, in 1961, Miller published in *The Lancet* the first data supporting an immunological function for the thymus (77) and in 1962 Martinez et al. and Miller (78,79) provided data further supporting the direct or indirect involvement of the thymus in immunological reactions and its role as a supply of lymphocytes to other lymphoid tissues.

Inspite of the general assumption, by that time, that all the immune responses of neonatally thymectomized animals to all types of antigenic stimuli are impaired (80-82), Humphrey and Parrott in 1964 (83) showed that mice thymectomized at birth can, in

certain circumstances (e.g. in response to pneumococcal polysaccharides), produce as much or even more antibody than intact controls.

The term Thymus-dependent was first assigned to histologically delineated areas of lymphocyte depletion in secondary lymphoid tissue of neonatally thymectomized mice (immediately surrounding the central arterioles in the spleen, and constitute the mid and deep cortical zones of the lymph nodes) (84-87). The remaining areas in the peripheral lymphoid organs were all designated 'thymus-independent' (88). In 1966 Micklem et al. (89) demonstrated the presence of cells from two distinct origins in the peripheral lymphoid tissues and in 1969 Davies and co-workers (90,91) demonstrated the bone marrow origin of thymus-independent areas of the secondary lymphoid organs. This concept was further supported by proceeding studies, and the term T-cells and B-cells (i.e of bone marrow origin) was assigned to cells in thymus-dependant and thymus-independent areas of the secondary lymphoid organs, respectively (92,93). Subsequent studies showed a clear distinction between thymus-dependent and independent populations based on functional and phenotypic analysis (94).

T cell-independent antigens represent two major groups. TI type 2 (TI-2) antigens are characterized by their large molecular weight, possession of repeating immunogenic epitopes, ability to activate the complement cascade, poor *in vivo* degradability, and inability to stimulate MHC class II-dependent T cell help. TI type 1 (TI-1) antigens, on the other hand, are characterized by being mitogenic for B cells. In contrast to TI antigens, T cell-dependent antigens (TD), which comprise soluble proteins or peptides are characterized by their ability to associate with MHC molecules on an antigen presenting

cell (APC), which subsequently interact with and activate T cells, in part, through ligation of their T cell antigen receptor complex (TCR), as well as through binding of accessory and adhesion molecules (reviewed in (95-104)).

TI-2 antigens express repetitive epitopes on a stable backbone with an extended length of 460 nm. This backbone carries 48 epitopes that can engage 10-50 mIg receptors forming a small number of highly cross-linked clusters with 14-fold reduction in the diffusion coefficient of the bound mIg receptors. This conformation is critical for delivering the BCR-mediated signal in TI-2 responses and is achieved by minimizing the extent of modulation and disappearance of Ig from the surface of antigen-specific B cells thus allowing for prolonged contact of the antigen with mIg and therefore persistent B-cell signaling with relatively low antigen concentrations. In addition to the spatial density and affinity of antigens, BCR signaling in TI responses is also influenced by important regulatory molecules such as complement and Fc-receptors (97-99). In addition, Ig secretion is enhanced by additional immunostimulatory signals (second signals) such as complement fragments, C4-binding protein (C4BP), B-cell-activating factor of the TNF family (BAFF), pathogen-associated molecular patterns (PAMPs), DC-, macrophage-,α-β, γ-δ, and NK T-cell- derived factors (95-97,105-107). Antibody responses to TI antigens are characterized by the absence of a typical immunological memory, failure to induce classic GC formation, and the involvement of mIgD, Bruton's tyrosine kinase (Btk), B-1 and MZ B cells.

Studies showed that virus-specific IgM responses are mounted in athymic nude, TCRα- TCRβ- TCRαβ- and TCRαβγδ-knockout mice infected with Coxsackie,

influenza, vesicular stomatitis virus and many other viral models. Moreover, all of the antiviral TI antibody responses reported so far are directed to viral antigens repetitively displayed in the virions (108). Besides, antibodies bound to strictly ordered, but not to irregularly arranged, viral antigens dramatically enhanced the induction of anti-antibodies after a single immunization and without using adjuvants (109).

In addition to the well known role of FDCs in GC reactions of the classic TD responses, our studies revealed an important role of FDCs in augmenting and enhancing B-cell proliferation and Ab responses, respectively, in *in vitro* B cell cultures stimulated with slg-dependent (anti-δ) or -independent (LPS) polyclonal activators (40). Subsequently, molecules involved in FDC-mediated enhancement of Ab responses by B cells in Ag-driven or LPS-stimulated systems were characterized and revealed an important interaction between a complement-derived CD21 ligand on follicular dendritic cells and CD21 on B cells in the initiation of IgG responses (29,39,44). The fact that blockade of CD21 receptors on B-cells co-cultured with FDCs results in the reduction of Ab responses to the TD antigen tetanus toxoid (TT), and to the TI type 1 pokeweed mitogen (PWM), further supports the importance of FDC-associated molecules (CD21 ligand) in the enhancement of Ab responses by B-cells (56).

FDC-FcγRIIB is another important molecule that influences B-cell Ab responses. FDC- FcγRIIB binds the Fc regions of Igs thereby inhibiting the SHIP signaling pathway and thus minimizes ITIM activation in B cells by reducing co-cross-linking of BCR and B cell-FcγRIIB (57,58). The role of FDC-FcγRIIB in B cell activation has been investigated under Ag-specific and anti-BCR ligation conditions. The addition of ICs to

cultures of Ag-specific T and B cells elicited pronounced Ab responses only in the presence of FDCs. In addition, Ag-specific responses in cultures containing FDCs derived from FcγRIIB$^{-/-}$ mice or FcγRIIB$^{-/-}$ mice transplanted with wild-type Ag-specific T and B cells and challenged with specific Ag were significantly depressed compared with those of controls with wild-type FDC *in vitro* and *in vivo* (30). In another study, the addition of normal FDCs, but not FDCs lacking FcγRIIB from FcγRIIB$^{-/-}$ mice, reduced and reversed the anti-BCR-induced SHIP phosphorylation in A20 cells supporting the concept that binding Ig Fc regions by FDC-FcγRIIB could inhibit the SHIP signaling pathway and thus minimize ITIM activation in B cells by reducing co-cross-linking of BCR and B cell-FcγRIIB (57). Again, the immune response to the immunodominant Ag of *Actinobacillus actinomyctemocomitans,* which is a 150 kD polymer of disaccharide repeating units capable of maintaining immune responses for long periods of time in the absence of continuous source of the Ag, increased 3-40-fold after the addition of Ag-specific IC-bearing FDCs in *in vitro* cultures(110).

TI polysaccharide antigens activate the alternative complement pathway directly and the classical pathway indirectly by making ICs with specific IgM produced early in the immune response. In addition to the accessory signals delivered by the complement derived CD21L interacting with the CD21/CD19/TAPA-1 complex, activated forms of both C3 (C3b) and C4 (C4b) can bind C4 binding protein (C4BP), which in humans and likely in rodents, co-localizes with ICs on FDCs as well as CD40 in secondary B cell follicles. C4BP is a novel CD40 ligand capable of activating B cells through CD40. C4BP in immune complexes (ICs) trapped on FDCs has been shown to signal B cells via

intact CD40 in short-lived antigen-specific TI GCs independent of the T-cell derived CD40L (CD154) expression. Consistent with the hypothesis that ICs on FDCs can provide antigen-specific, complement-derived, and CD40-mediated signals to B cells initiating B cell proliferation in TI GCs (59).

CHAPTER 1

Follicular dendritic cell (FDC)-FcγRIIB engagement *via* immune complexes induces the activated FDC phenotype associated with secondary follicle development

Introduction

Follicular dendritic cells (FDC) are localized to the light zones of germinal centers (GC), where their dendritic processes interdigitate and form three-dimensional networks or FDC-reticula that help these non-circulating cells to remain localized (37,42). FDC functions include the capture and retention of immune complexes (IC) (30), promotion of B cell survival (111-115), and the production of high-affinity Ab (39,116). The ability to stimulate B cells depends in large measure on the ability of FDC to trap and present Ag to specific B cells. FDC capture and retain Ag in the form of IC, and starting in the early 1970s, a number of studies elegantly documented that complement and complement receptors (CR) were necessary for optimal IC trapping and retention (117-121). Although, Fc receptors may not be as important as complement and CR in IC trapping, they do appear to enhance long-term retention of IC by FDC (30).

Both FDC and B cells express FcγRIIB (57,58), but B cell activation may be inhibited by immunoreceptor tyrosine-based inhibition motif (ITIM) signaling mediated by IC coligating the B cell receptor for Ag (BCR) and B cell-FcγRIIB (reviewed in (122,123)). Engagement of BCR in the absence of such coligation induces rapid activation of tyrosine kinases, generation of inositol phosphates, elevation of cytoplasmic Ca^{2+} concentrations, and activation of mitogen-activated protein kinases (reviewed in (122,123)). These events promote B cell activation and lead to proliferation, differentiation, and Ab secretion (reviewed in (124)). In marked contrast, coligation of BCR and

FcγRIIB by IC leads to inhibition of the extracellular Ca^{2+} influx, reduction of cell proliferation, blockage of blastogenesis, and inhibition of Ig synthesis (reviewed in (122-124)). Nevertheless, on FDC, IC provide potent activation signals for B cells that result in induction of GC dark zones where B cells are proliferating and differentiating rapidly (reviewed in (125)). However, FDC lacking FcγRIIB or expressing only low levels of FcγRIIB are unable to convert poorly immunogenic IC into a highly immunogenic form for B cells, although they can trap IC using CR (30). In active GC, FDC express high levels of FcR relative to B cells, and it appears that these receptors bind Fc portions of Ab in IC and minimize their binding to FcR on B cells (30,44,57). Thus, cross-linking of BCR and FcγRIIB *via* IC is minimized, ITIM signaling is reduced, and B cell proliferation and differentiation is promoted.

In follicles lacking GC, FDC exhibit a resting phenotype with significant CR1/2 levels, but with low levels of FcγRIIB, ICAM-1, and VCAM-1, raising the issue of mechanisms involved in activating FDC adequately to productively present IC to B cells. Remarkably, challenge of actively immunized mice with Ag induces a dramatic increase in FDC-FcγRIIB expression. Up-regulation of FDC-FcγRIIB is apparent within 24 h, reaches a peak by day 3, and remains high for at least 10 days (57,58). The rapidity of this response suggested that memory T and B cells were not involved and prompted the hypothesis that interaction of IC with FcγRIIB on FDC up-regulated the expression of FcγRIIB as well as of other surface molecules that participate in the immune response,

including ICAM-1 and VCAM-1 (69,126,127). A recent paper by Victoratos *et al.* (128) provides support for the concept that IC binding of FcR on FDC can lead to up-regulation of FDC-ICAM-1 and -VCAM-1.

To test this hypothesis, mice were passively immunized with anti-OVA Ab, and the levels of FcγRIIB, ICAM-1, and VCAM-1 on FDC-reticula and purified FDC were determined 3 days after challenging wild-type (WT) and FcγRIIB$^{-/-}$ mice with OVA. Both WT and FcγRIIB$^{-/-}$ mice trapped OVA-anti-OVA Ab IC, but only the WT mice responded with dramatic up-regulation of FcγRIIB, ICAM-1 and VCAM-1. Furthermore, addition of IC to purified FDC from WT mice, but not FcγRIIB$^{-/-}$ mice, *in vitro* prompted the production of mRNA for FcγRIIB, ICAM-1, and VCAM-1 within 3 h, indicating that this Fc receptor promoted activation rather than inhibition as it is known to occur in other cells including T cell-associated dendritic cells (122,123,129). In short, the data support the concept that direct interaction of IC with FDC-FcγRIIB up-regulates FcγRIIB, as well as ICAM-1 and VCAM-1, indicating that engagement of FcγRIIB is important in initiating pathways leading to FDC activation, as indicated by the expression of molecules on FDC needed for accessory function.

Materials and methods

Animals

BALB/c mice 6-8 wk old were purchased from the National Cancer Institute, and FcγRIIB KO mice (C57BL/6; 129-*Fcγr2*^{tm1}) were obtained from Taconic Farms (Hudson, NY). Mice were housed in shoebox cages and food and water were given *ad libitum*. Animals were handled in compliance with guidelines established by VCU's institutional animal care and use committee.

Ab and other reagents

The rat anti-mouse CD16/32 (clone2.4G2), CD106 (mVCAM-1), FDC-M1, biotin labeled anti-rat kappa Ab and the DAB substrate kit were from BD PharMingen (San Diego, CA). Rat anti-mouse CD54 Ab (ICAM-1), HRP-conjugated goat anti-rat IgG, and HRP-conjugated goat anti-rabbit IgG were from Southern Biotech (Birmingham, AL). Rabbit anti-OVA Ab was purchased from Biodesign International (Saco, ME) and normal rabbit serum from Gibco (Grand Islands, NY). Anti-biotin microbeads and MACS LS columns were purchased from Miltenyi Biotec GmbH (Auburn, CA).

FDC isolation

FDC were isolated by positive selection from LN (axillary, lateral axillary, inguinal, popliteal, and mesenteric) of adult mice as described (130). Before isolation, mice were irradiated with 1000 rad to eliminate most lymphocytes. On the day of isolation, mice were killed, LN were collected, opened and treated with 1.5 mL collagenase D (22 mg/mL, C-1088882; Roche),

0.5 mL of DNase I (5000 U/mL, D-4527; Sigma), and 2 mL DMEM with 20 mM HEPES. After 45 min at 37°C in a CO_2 incubator, released cells were washed in 5 mL DMEM with 10% FCS. Cells were then sequentially incubated with FDC-specific Ab (FDC-M1) for 45 min, 1 μg of biotinylated anti-rat κ light chain for 45 min, and with 20 μL anti-biotin microbeads (Miltenyi Biotec) for 15-20 min on ice. The cells were layered on a MACS LS column and washed with 10 mL ice-cold MACS buffer. The column was removed from the VarioMACS and the bound FDC were released with 5 mL MACS buffer.

Isolation of peritoneal macrophages

DMEM (20 mL) was injected i.p. and the cells were recovered by peritoneal lavage. The cells were washed by centrifugation and resuspended in complete DMEM with 10% FCS.

Isolation of lymphocytes

Lymphocytes were suspended by grinding LN from non-irradiated mice between the frosted ends of two sterile slides in complete DMEM with 10% FCS. The suspension, containing 30-45% B cells, was washed and resuspended in complete medium.

IC preparation and cell cultures

FDC isolated from murine LN were cultured at 1×10^6 cells/mL in 5-mL polypropylene tubes containing 1 mL complete medium supplemented with 10% FCS. OVA and rabbit anti-OVA Ab IC were made at a final ratio of 1 ng/mL

OVA to 6 ng/mL anti-OVA Ab. The cultures were maintained for 12 h at 37°C in a CO_2 incubator unless otherwise indicated.

Analysis of FcγRIIB, ICAM-1, and VCAM-1 mRNA levels by qRT-PCR

Total cellular RNA was extracted by using TRIzol reagent (Invitrogen Life Technologies, Carlsbad, CA) according to the manufacturer's instructions. Then, the one-step RT-PCR reaction was achieved by using an iCycler (Bio-Rad, Hercules, CA). The TaqMan one-step RT-PCR master mix reagent kit (ABI, Foster City, CA) was used for RT-PCR. The amplification of various mRNA and 18S RNA were run in separate wells using the same amount of total RNA retrieved from the same sample. The sequences for the various oligonucleotides starting with the forward primer, followed by reverse primer, then probe and going from 5′ to 3′ are indicated in Table 1. Amplifications were performed under the following conditions: 48°C for 30 min (cDNA synthesis), initial denaturation at 95°C for 10 min followed by 40 cycles of denaturation at 95°C for 15 s and a combined annealing/extension step at 60°C for 1 min. Finally, fold differences in mRNA expression levels were calculated using the $\Delta\Delta C_T$ method (131). The PCR efficiency was first ascertained to be close to 100% by performing multiple standard curves using serial mRNA dilutions. An amplification cycle threshold value (C_T value), defined as the PCR cycle number at which the fluorescence signal crosses an arbitrary threshold, was calculated for each reaction. The fold change between mRNA expression levels was determined as follows: Fold change $= 2^{-\Delta\Delta CT}$, where $\Delta\Delta C_T = (C_{T\text{-GoI}} - C_{T\text{-Hk}})$

Sample - ($C_{T\text{-}GoI}$ - $C_{T\text{-}Hk}$) Control, where C_T: cycle threshold, GoI: gene of interest, Hk: house keeping gene.

Table 1. Primer and probe sequences used in real-time qRT-PCR analysis

FcγRIIB	Sense primer	TCCTAGTATCCTTGGTCTATCTC
	Anti-sense primer	GTGAGTAGGTGATCGTATTCTC
	Probe 50-FAM-	AAGCAGGTTCCAGACAATCCTCCT-30-BHQ-2[a)]
mICAM1	Sense primer	TTGAGAACTGTGGCACCGTG
	Anti-sense primer	CAGCTCCACACTCTCCGGAA
	Probe 50-FAM-	CGCTTCCGCTACCATCACCGTGTATTCG-30-BHQ-1[a)]
mVCAM1	Sense primer	GTGACCTGTCTGCAAAGGAC
	Anti-sense primer	AAAGGGATACACATTAGGGACTG
	Probe 50-FAM-	AAGAGAACCCAGGTGGAGGTCTACTCATTC-30-BHQ-[1a)]
18S rRNA	Sense primer	AAAATTAGAGTGTTCAAAGCAGGC
	Anti-sense primer	CCTCAGTTCCGAAAACCAACAA
	Probe 50-Cy5-	CGAGCCGCCTGGATACCGCAGC-30-BHQ-2[a)]

[a)] Black hole quencher.

Immunizations and immunohistochemistry

Three mice were subcutaneously injected in the front legs with an initial dose of 100 µL rabbit anti-OVA Ab (10 mg/mL) followed 1 h later by 100 µL OVA (1 mg/mL) (Sigma, St. Louis, MO). A final dose of 100 µL rabbit anti-OVA Ab (10 mg/mL) was injected 1 h later. Controls were injected with OVA + NSS or with rabbit anti-OVA Ab alone. At 3 days post immunization, axillary LN were collected and frozen in CryoForm embedding medium (IEC, Needham Heights, MA) and frozen sections of 10 µm thickness were cut on a Leitz (1720 Digital) cryostat and air-dried. Five representative midsagittal sections were collected and processed together for the quantitative analysis. Following acetone

fixation, the sections were rehydrated and the endogenous peroxidase activity was quenched with PBS containing 0.1% phenylhydrazine-HCl (Sigma). The sections were washed and saturated with 10% BSA, then incubated with: mouse adsorbed HRP-conjugated goat anti-rabbit IgG, unlabeled rat anti-mouse CD16/CD32 (FcγRIIB), CD106 (VCAM-1), or CD54 Ab (ICAM-1). The sections with rat Ab were washed and then incubated with mouse adsorbed HRP-conjugated goat anti-rat IgG. The sections were developed with a DAB substrate kit (BD PharMingen) and images were captured using an optronics digital camera and analyzed using Bioquant Nova software.

The rat mAb 2.4G2 recognizes murine FcγRIIB and FcγRIII. However, FDC-reticula in GC of FcγRIIB$^{-/-}$ mice do not label with 2.4G2, indicating that activated FDC have little if any FcγRIII (30). Accordingly, we attribute the histochemical labeling of FDC-reticula in WT mice with 2.4G2 to FDC-FcγRIIB.

Analyses of immunohistochemistry results

BIOQUANT NOVA Advanced Image Analysis software (R&M Biometrics, Nashville, TN) was used to analyze the immunohistochemistry as described (58). This system allowed us to determine number, position, area, and density of the labeling after setting an arbitrary threshold that was the best for the FDC-reticula. This predefined threshold was used throughout to enable reliable comparisons.

Flow cytometry

FDC were isolated from WT and FcγRIIB$^{-/-}$ mice 3 days after subcutaneous injection of Ag and Ab to form IC. Control mice were injected with saline. Except for CD32/CD16-FITC labeling, FDC were first incubated with mouse Fc-Block (BD PharMingen) for 15 min on ice, followed by anti-CD54/ICAM-1-FITC Ab, anti-CD106/VCAM-1-FITC Ab or isotype control for 60 min in the dark at 4°C. After washing, the cells were analyzed using an FC500 flow cytometer and Cytomics RXP analysis software. Histograms were gated for FDC based on their forward and side scatter properties established with FDC phenotypic markers including FDC-M1, CD21/35, and CD32 (130). The figures were plotted using WinMDI software (Scripps Research Institute).

Statistical analysis

For analysis of results including qRT-PCR data, a *t*-test (two-tailed distribution) was used. To account for multiple comparisons, a *p* value of less than 0.01 was required to conclude significance.

Results

FDC-mediated IC trapping

Increases in FDC-FcγRIIB are apparent 1-3 days after challenge of immune mice with Ag, prompting the postulate that FDC may be activated by encountering IC. If IC directly initiated up-regulation, then memory T and B cells would not be important and IC in normal mice should activate FDC. To test this, we passively immunized WT and FcγRIIB$^{-/-}$ mice with rabbit anti-OVA IgG and challenged with OVA to form IC. Localization of the IC on FDC-reticula after 3 days was determined with immunohistochemistry and morphometrically analyzed (Fig. 1A1-A5). Complement and CR are known to facilitate trapping of IC on FDC (117-121); thus, IC strongly labeled FDC-reticula in both passively immunized WT and FcγRIIB$^{-/-}$ mice. In contrast, neither anti-OVA Ab nor OVA in the presence of nonspecific rabbit serum (NSS) were retained on the FDC-reticula, confirming the importance of the IC. The number of FDC-reticula ranged between five and six in IC-immunized WT and FcγRIIB$^{-/-}$ mice compared to a total lack of labeling in Ag- or Ab-alone-injected animals (Fig. 1A4). The average reticular size was approximately 250 000 μm^2 (Fig. 1A5) whereas the average density per reticulum, which reflects the amount of IC staining, ranged between 110 and 120 pixels and did not differ between WT and knockout (KO) mice.

IC-mediated up-regulation of FDC-FcγRIIB expression

We hypothesized that direct interaction between IC and FDC-FcγRIIB up-regulates FcγRIIB expression in an auto-regulated or self-induced manner. To begin testing, we analyzed FcγRIIB labeling in FDC-reticula of 3 days passively immunized animals (Fig. 1B1-B5). Whereas the number of FcγRIIB labeling FDC-reticula in passively immunized WT animals ranged between five and six, the number in control non-immune mice with Ag in NSS or Ab alone averaged <1 per midsagittal draining axillary LN section (p <0.001). No labeling was detected on sections from FcγRIIB$^{-/-}$ mice (Fig. 1B3). The reticular size in passively immunized WT animals measured 144 200 μm^2 compared to 8200, 6153 and 6131 μm^2 in the non-immunized WT, Ag-alone- and Ab-alone-injected controls, respectively (p <0.001). The average density per reticulum, which indicates the intensity of FcγRIIB labeling, was highly variable in the control groups which include reticula induced by environmental Ag that were in various stages of decline. Moreover, the density of labeling was almost homogenous in the 3-day reticula in passively immunized animals, and this contrasted with the variability in the controls where the initial time of stimulation could not be determined.

IC increase FcγRIIB mRNA levels in FDC but not in B lymphocytes or macrophages

The immunohistochemical results support the concept that FcγRIIB is important in up-regulating FDC-FcγRIIB. However, many other cells, including

Figure 1: ***Analysis of light micrographs illustrating trapping of IgG-OVA IC (A1-A5) and labeling with anti-FcγRIIB Ab (B1-B5) in the FDC-reticula of draining axillary LN.*** Mice were passively immunized with rabbit anti-OVA Ab, followed by OVA to produce IC. After 3 days, draining axillary LN were harvested, sectioned, and midsagittal sections were labeled. IC-retaining reticula were labeled in (A1-A5) using anti-rabbit IgG. (A1) Representative passively immunized and OVA-challenged WT mouse ×50; (A2) representative no-IC (Ab alone or NSS + Ag) WT mouse ×80; (A3) representative passively immunized and challenged FcγRIIB$^{-/-}$ mouse ×50. (A4) Number and (A5) size of FDC-reticula per midsagittal axillary LN section. FDC-reticula were labeled for FcγRIIB in (B1-B5). (B1) Representative passively immunized and challenged WT mouse ×50; (B2) no-IC WT mouse with a GC ×50; (B3) representative passively immunized and challenged FcγRIIB$^{-/-}$ mouse ×50. (B4) Number and (B5) size of FDC-reticula per draining midsagittal axillary LN section. The averages were calculated using data from three mice, and results illustrate the means ± SEM. [Normal View 59K | Magnified View 95K]

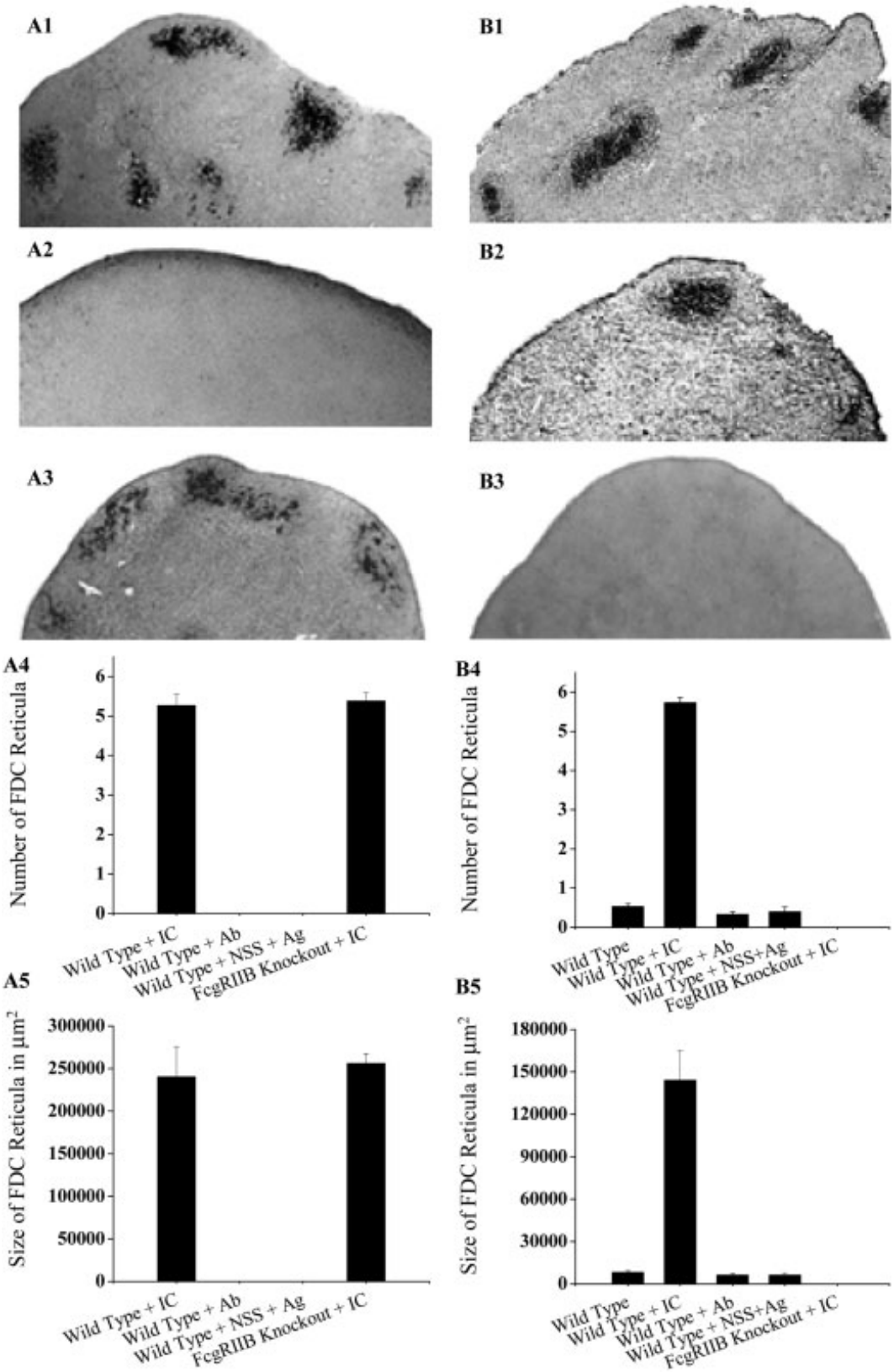
A1
B1
A2
B2
A3
B3
A4
Number of FDC Reticula
0
1
2
3
4
5
6
Wild Type + IC
Wild Type + Ab
Wild Type + NSS + Ag
FcgRIIB Knockout + IC
B4
Number of FDC Reticula
0
1
2
3
4
5
6
Wild Type
Wild Type + IC
Wild Type + Ab
Wild Type + NSS+Ag
FcgRIIB Knockout + IC
A5
Size of FDC Reticula in µm²
0
50000
100000
150000
200000
250000
300000
Wild Type + IC
Wild Type + Ab
Wild Type + NSS + Ag
FcgRIIB Knockout + IC
B5
Size of FDC Reticula in µm²
0
30000
60000
90000
120000
150000
180000
Wild Type
Wild Type + IC
Wild Type + Ab
Wild Type + NSS+Ag
FcgRIIB Knockout + IC

mast cells and macrophages, can interact with IC *in vivo* and could play a role in regulating expression of FDC-FcγRIIB. However, if direct interaction between IC and FcγRIIB induces FDC-FcγRIIB, then addition of complement-free IC to purified FDC should result in increased FcγRIIB mRNA. To examine this, we determined the effect of IC on FcγRIIB mRNA levels in purified FDC using quantitative reverse transcriptase PCR (qRT-PCR). The fold change in FcγRIIB mRNA in IC-treated FDC, as compared to untreated FDC, was calculated. IC treatment resulted in an approximately 2000-fold increase in FcγRIIB mRNA in 12 h, whereas treatment with Ab alone or Ag alone was without effect (Fig. 2A). This response appeared to be FDC specific because B cells, which bear FcγRIIB, and macrophages treated with the IC for the same period of time did not show any change in FcγRIIB expression (Fig. 2B). This result minimizes the probability that contaminating B cells or macrophages in the FDC preparations contribute to the dramatic increase in FcγRIIB mRNA levels. Furthermore, this result is consistent with histochemistry where the increase in FcγRIIB on FDC was dramatic, but was not apparent on adjacent B cells (Fig. 1B1).

Anti-FcγRIIB Ab blocks the IC-mediated increase in FcγRIIB mRNA levels

WT FDC treated with rat anti-mouse CD16/32 Ab (clone 2.4G2) for 30 min prior to IC addition showed no change in FcγRIIB mRNA levels (Fig. 2C). Since 2.4G2 blocks FcγRIIB, this result further supported a crucial role of FcγRIIB in mediating the IC-induced FcγRIIB expression on FDC.

Kinetics of IC-induced increases in FcγRIIB mRNA

The IC-induced increase in FDC-FcγRIIB mRNA levels was determined at 1, 3, 12 and 24 h. Increased FcγRIIB mRNA levels were apparent within 3 h and increased over the entire 24-h period (Fig. 2D).

IC-mediated up-regulation of FDC-ICAM-1 and -VCAM-1 expression

Murine ICAM-1 and VCAM-1 are inducible on FDC and high levels coincide with GC formation (132,133). Furthermore, these adhesion molecules are critical to the ability of FDC to stimulate B cells (69). In the present study, we sought to determine the impact of IC on FDC-ICAM-1 and -VCAM-1 expression. Three days after passive immunization and Ag challenge, FDC-ICAM-1 and -VCAM-1 were analyzed with immunohistochemistry (Fig. 3). The number of ICAM-1- and VCAM-1-labeled FDC-reticula 3 days after IC formation in passively immunized WT animals ranged between five and six per midsagittal draining axillary LN section and corresponded with IC trapping and FcγRIIB expression. In contrast, the number in non-immune WT, Ag-alone-, Ab-alone-, and passively immunized FcγRIIB KO mice was approximately one per midsagittal draining axillary LN section ($p < 0.01$). The same difference between IC *vs.* Ag or Ab alone existed with cumulative reticular size for FDC-ICAM-1 and -VCAM-1 in passively immunized WT animals. In contrast, neither ICAM-1 nor VCAM-1 labeling in FDC-reticula of passively immunized FcγRIIB$^{-/-}$ mice was significantly changed after IC treatment (Fig. 3).

Figure 2: ***RT-PCR quantification of IC-mediated FcγRIIB mRNA induction in FDC.*** (A) FDC (1×10^6) were isolated from LN and cultured for 12 h in the presence of 50 ng/mL OVA (Ag), 300 ng/mL anti-OVA Ab (Ab) or the combination of OVA + anti-OVA Ab to form IC. (B) IC-mediated FcγRIIB mRNA induction was not observed in B cells or macrophages. FDC, B cells, and peritoneal macrophages (1×10^6) were cultured in the presence of 50 ng/mL OVA (Ag), 300 ng/mL anti-OVA Ab (Ab) for 12 h. (C) Induction of FcγRIIB mRNA production in FDC by IC was blocked by anti-FcR Ab (2.4G2). FDC (1×10^6) were cultured for 12 h in the presence of 50 ng/mL OVA (Ag), 300 ng/mL anti-OVA Ab (Ab), directly or after being treated with 2.4G2 (2 μg in a final volume of 200 μL) for 30 min on ice. (D) Kinetics of IC-induced FcγRIIB mRNA production in FDC. FDC were cultured in the presence of 50 ng/mL OVA (Ag), 300 ng/mL anti-OVA Ab (Ab), and maintained for 1, 3, 12 and 24 h at 37°C in a CO_2 incubator. Data are expressed as fold increase in mRNA. These results are representative of three separate experiments of this type, and results are depicted as the means ± SEM for replicate cultures. [Normal View 26K | Magnified View 39K]

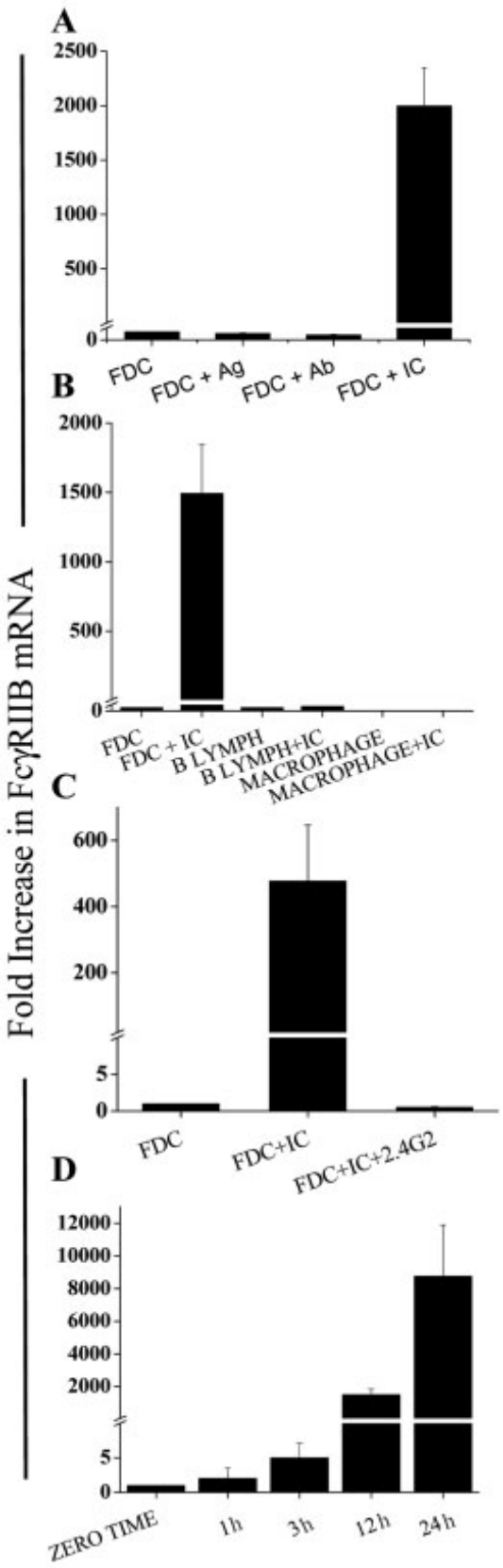
A
2500
2000
1500
1000
500
0
FDC
FDC + Ag
FDC + Ab
FDC + IC
B
2000
1500
1000
500
0
FDC
FDC + IC
B LYMPH
B LYMPH+IC
MACROPHAGE
MACROPHAGE+IC
C
600
400
200
5
0
FDC
FDC+IC
FDC+IC+2.4G2
D
12000
10000
8000
6000
4000
2000
5
0
ZERO TIME
1h
3h
12h
24h
Fold Increase in FcγRIIB mRNA

Figure 3: ***Analysis of light micrographs of draining axillary LN illustrating immunohistochemical labeling of FDC-reticula with anti-VCAM-1 (A1-A5) and anti-ICAM-1 Ab (B1-B5).*** LNs were harvested 3 days after passive immunization and challenge with OVA to form ICs. VCAM-1 labeling of FDC-reticula is analyzed in (A1-A5). (A1) Representative, passively immunized and challenged WT mouse ×50; (A2) no-IC WT mouse with a GC ×50; (A3) a passively immunized and challenged FcγRIIB$^{-/-}$ mouse with a labeled GC ×80. (A4) Number and (A5) size of FDC-reticula per draining midsagittal axillary LN section. ICAM-1 labeling of FDC-reticula is shown in (B1-B5). (B1) Representative passively immunized and challenged WT mouse ×50; (B2) no-IC WT mouse with a labeled GC ×50, (B3) passively immunized and challenged FcγRIIB$^{-/-}$ mouse with a labeled GC ×80. (B4) Number and (B5) size of FDC-reticula per draining midsagittal axillary LN section. The averages were calculated using data from three mice, and results illustrate the means ± SEM. [Normal View 61K | Magnified View 96K]

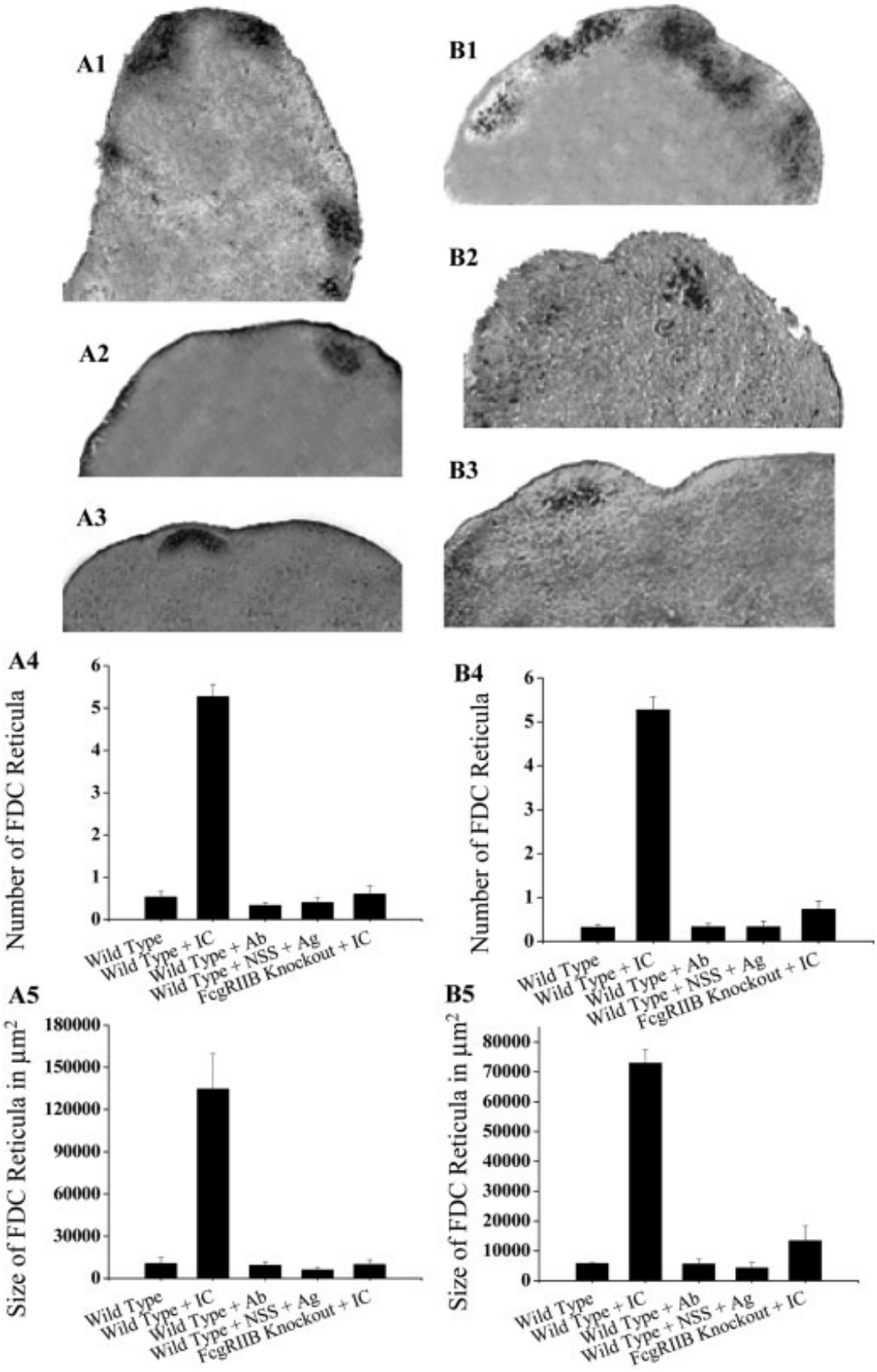
A1
B1
A2
B2
A3
B3
A4
Number of FDC Reticula
0
1
2
3
4
5
6
Wild Type
Wild Type + IC
Wild Type + Ab
Wild Type + NSS + Ag
FcgRIIB Knockout + IC
B4
Number of FDC Reticula
0
1
2
3
4
5
6
Wild Type
Wild Type + IC
Wild Type + Ab
Wild Type + NSS + Ag
FcgRIIB Knockout + IC
A5
Size of FDC Reticula in µm2
0
30000
60000
90000
120000
150000
180000
Wild Type
Wild Type + IC
Wild Type + Ab
Wild Type + NSS + Ag
FcgRIIB Knockout + IC
B5
Size of FDC Reticula in µm2
0
10000
20000
30000
40000
50000
60000
70000
80000
Wild Type
Wild Type + IC
Wild Type + Ab
Wild Type + NSS + Ag
FcgRIIB Knockout + IC

Up-regulation of surface expression of FcγRIIB, ICAM-1 and VCAM-1 on IC-stimulated FDC confirmed by flow cytometry

Flow cytometric analysis of FcγRIIB, ICAM-1 and VCAM-1 on FDC purified from WT mice showed significantly increased labeling 3 days after IC stimulation (Fig. 4A-C). Whereas 39% of FDC were FcγRIIB positive from unstimulated WT mice, 70% were FcγRIIB positive after IC activation (Fig. 4A). Labeling with anti-ICAM-1 Ab indicated that 30% of unstimulated WT FDCs were CD54/ICAM-1 positive, whereas 65% were positive after IC stimulation (Fig. 4B). Similarly, CD106/VCAM-1 was expressed on 6% of unstimulated WT FDC, rising up to 38% in IC-activated FDC (Fig. 4C). In contrast, FcγRIIB$^{-/-}$ FDC showed no change in surface expression of CD54/ICAM-1 (Fig. 4D), or CD106/VCAM-1 (Fig. 4E) after binding IC.

IC-mediated induction of FDC-ICAM-1 and -VCAM-1 mRNA in vitro

If engagement of FDC-FcγRIIB with IC initiates pathways leading to up-regulation of surface molecules that participate in interactions with GC B cells, then RNA messages for these molecules should be apparent after IC stimulation. Using qRT-PCR, mRNA levels for ICAM-1 and VCAM-1 in FDC from WT and FcγRIIB$^{-/-}$ mice were determined after culture with IC for 3, 12 and 24 h, and the fold change was calculated using mRNA levels in untreated FDC as the baseline. In WT FDC, mRNA levels for FcγRIIB, ICAM-1, and VCAM-1 were significantly elevated within 3 h and dramatically increased after 24 h (Fig. 5). In contrast, FDC from FcγRIIB KO mice did not display any changes in ICAM-

1 or VCAM-1 mRNA levels (Fig. 5). Controls included IC made in the presence of fresh complement to enhance IC binding to FDC from FcγRIIB KO and WT mice. The presence of complement fragments in the IC did not up-regulate ICAM-1 or VCAM-1 mRNA levels in KO mice or enhanced the IC-mediated up-regulation of these molecules in WT mice (data not shown).

Figure 4: ***Effect of IC stimulation on FDC-CD32/CD16, CD54/ICAM-1 and CD106/VCAM-1 surface expression.*** FDC were from WT (A-C) or FcγRIIB$^{-/-}$ (D, E) mice. Three days after subcutaneous injection of IC or saline, FDC were isolated and labeled for CD32/CD16, CD54/ICAM-1 or CD106/VCAM-1, and analyzed by flow cytometry. WT FDC exhibited increased surface expression of CD32/CD16 (A), CD54/ICAM-1 (B) and CD106/VCAM-1 (C) when stimulated with IC, whereas FcγRIIB$^{-/-}$ FDC showed no change in the surface expression of CD54/ICAM-1 (D) or CD106/VCAM-1 (E) upon IC treatment. These data are representative of three separate experiments of this type. [Normal View 41K | Magnified View 63K]

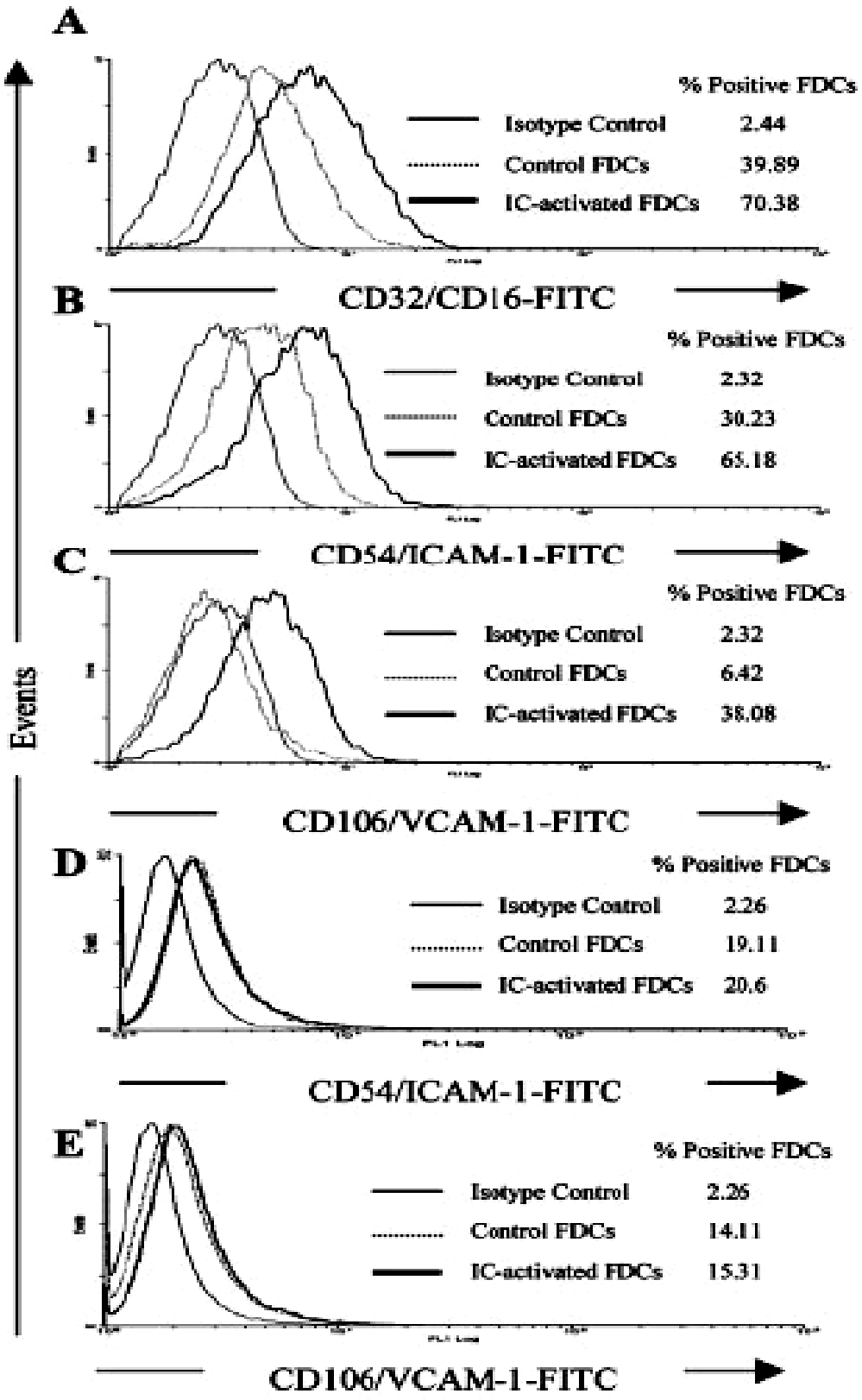
A
% Positive FDCs
Isotype Control 2.44
Control FDCs 39.89
IC-activated FDCs 70.38
B
CD32/CD16-FITC
% Positive FDCs
Isotype Control 2.32
Control FDCs 30.23
IC-activated FDCs 65.18
C
CD54/ICAM-1-FITC
% Positive FDCs
Isotype Control 2.32
Control FDCs 6.42
IC-activated FDCs 38.08
Events
CD106/VCAM-1-FITC
D
% Positive FDCs
Isotype Control 2.26
Control FDCs 19.11
IC-activated FDCs 20.6
CD54/ICAM-1-FITC
E
% Positive FDCs
Isotype Control 2.26
Control FDCs 14.11
IC-activated FDCs 15.31
CD106/VCAM-1-FITC

Figure 5: ***Effect of IC stimulation on mRNA for markers indicative of the activated FDC phenotype.*** FDC were cultured in the presence of 50 ng/mL OVA (Ag) and 300 ng/mL anti-OVA Ab (Ab) for 3, 12 and 24 h. Total RNA was isolated and FcγRIIB, VCAM-1, and ICAM-1 mRNA were quantified using qRT-PCR. Data are expressed as fold increase in mRNA of IC-activated FDC above the basal level expressed in untreated FDC. These results are representative of three separate experiments of this type, and results are depicted as the means ± SEM of replicate cultures. [Normal View 17K | Magnified View 25K]

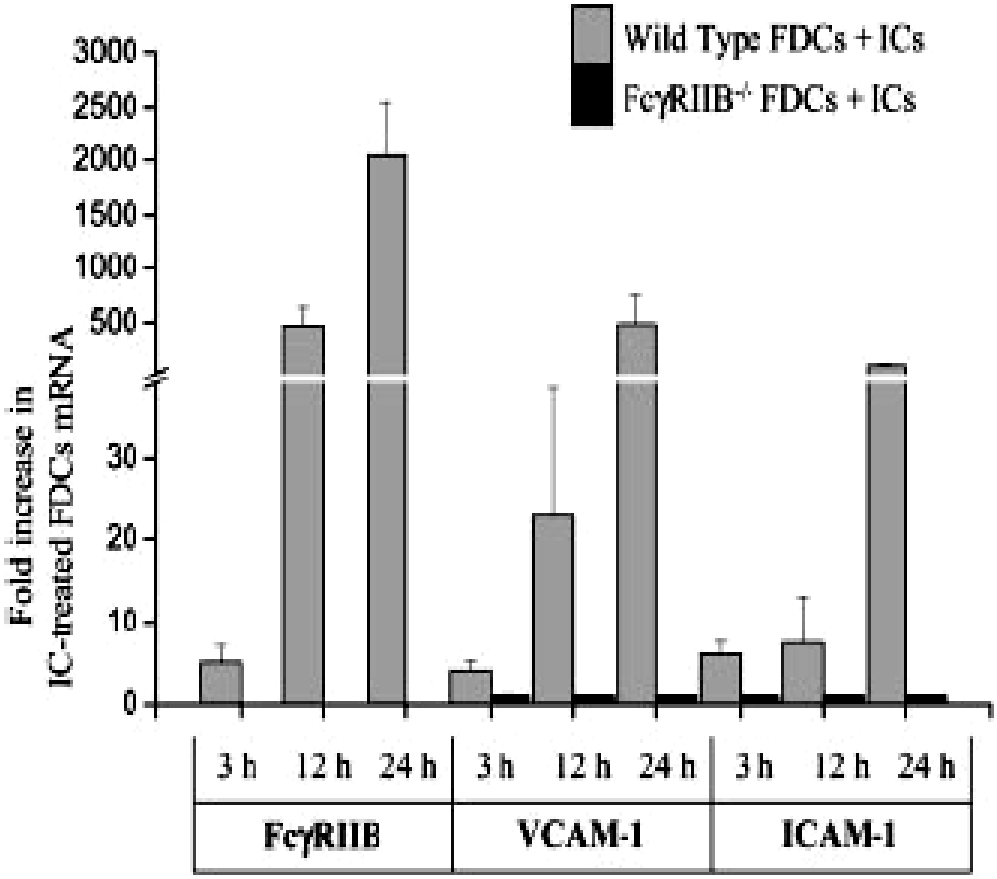
Wild Type FDCs + ICs
FcγRIIB-/- FDCs + ICs
Fold increase in IC-treated FDCs mRNA
3000
2500
2000
1500
1000
500
30
20
10
0
3 h
12 h
24 h
3 h
12 h
24 h
3 h
12 h
24 h
FcγRIIB
VCAM-1
ICAM-1

Discussion

The phenotype of FDC in primary and secondary follicles is very different. In secondary follicles, FDC bear high levels of FcγRIIB, ICAM-1 and VCAM-1, and these molecules are involved in converting poorly immunogenic IC into a highly immunogenic form for B cells and in facilitating FDC-B cell interactions required for optimal FDC accessory activity (30,57,69,132). In contrast, in primary follicles, FDC-reticula can be found by labeling with anti-CR1/2 Ab, but FcγRIIB, ICAM-1, and VCAM-1 levels are low and difficult to detect (30,132,134). These relationships prompted questions about how FDC are activated and what molecules participate in the activation process. Disruption of lymphotoxin (LT)/TNF, or their cognate receptors, disrupts LN organogenesis and interferes with FDC development (135-138). Furthermore, these molecules are important to maintain FDC with a functional phenotype, as indicated by the loss of IC and the activated phenotype when these interactions are blocked (136,139). Activated B cells are known to provide LT and TNF, suggesting that B cell activation might lead to FDC activation and that could explain why FDC associated with resting B cells exhibit a resting phenotype while those in active GC express an active phenotype (138-141). However, in recall responses, FDC activation is evident before B cell activation is apparent, suggesting that the IC itself might play a role in activating FDC (57,58). The data presented here support this concept. Encounter of FDC-FcγRIIB with Ag-Ab complexes in the absence of complement *in vitro* leads to increased mRNA for FcγRIIB in

purified FDC in 3 h. Increased levels of FDC-FcγRIIB could be detected by 24 h in passively immunized mice, and by 3 days not only was the labeling intense, but the area occupied by FcγRIIB-positive FDC-reticula on a single midsagittal draining axillary LN section had increased between 10- and 15-fold (10 000 μm^2 to nearly 150 000 μm^2). Results for ICAM-1 and VCAM-1 were similar, with mRNA being clearly elevated in isolated cells within 3 h and 10-15-fold increases in the area of FDC-reticula being occupied by labeled FDC.

The importance of FcγRIIB in initiating the signaling pathway for these molecules is supported by results indicating that IC could be trapped on FDC-reticula by FcγRIIB$^{-/-}$ mice, but there was no increase in mRNA or protein for ICAM-1, or VCAM-1. Furthermore, blocking FcγRIIB on WT FDC with anti-FcR Ab (clone 2.4G2) also blocked the mRNA response. FcγRIIB$^{-/-}$ mice exhibited ICAM-1 and VCAM-1 labeling at a frequency of approximately one FDC-reticulum per LN section, indicating that FDC in these animals could express these molecules. However, the presence of five to six IC-retaining reticula per LN section did not correspond with any increase in ICAM-1 or VCAM-1. The complement receptors are capable of trapping IC on FDC in these KO animals (30), but CR engagement did not mediate the IC-induced up-regulation of VCAM-1 or ICAM-1. Thus, the signaling pathways involved in converting resting FDC in primary follicles into activated FDC that emerge as the secondary follicles develop appears to be initiated by FDC-FcγRIIB engaging IC.

The molecules used to characterize FDC activation are known to be important in FDC-B cell interactions. The FcγRIIB binds the Ig-Fc in IC and thus minimizes ITIM activation as a consequence of coligation of B cell-FcγRIIB and BCR (57,58). The adhesion molecules, ICAM-1 and VCAM-1, are important in stabilizing FDC-B cell interactions leading to FDC-B cell clusters, and FDC accessory activity is most apparent in the clustered cells (69). Engaging FDC-FcγRIIB with IC induced a significant rise in ICAM-1 and VCAM-1 mRNA within 3 h and showed a dramatic increase after 24 h. In some experiments, we also examined mRNA for FDC-CD40 which has no known role in interactions between FDC and B cells. In this case, no increase in mRNA was found after engaging FDC-FcγRIIB with IC (data not shown). These results indicate that stimulation through FDC-FcγRIIB does not induce mRNA production generally, but does promote messages for proteins involved in B cell-FDC interactions.

In the present study, the initial trapping in FcγRIIB$^{-/-}$ mice was indistinguishable from WT after 3 days. These data are consistent with the well-established role of complement and CR in IC trapping by FDC and suggest that CR on resting FDC in primary follicles would trap IC very well. The trapped IC could engage the low level of FDC-FcγRIIB and auto-up-regulate this receptor as well as up-regulate other molecules important in FDC-B cell interactions. We reason that IC formation and binding to FDC-FcγRIIB would occur as soon as the first Ab appears in a primary response and within minutes after injecting Ag

into an immune animal for a recall response. This rapid up-regulation would facilitate GC formation, leading to class switching, somatic hypermutation, and the selection of B cells with high-affinity receptors needed to facilitate affinity maturation (39).

Phenotypic changes in FDC-reticula appear to be closely associated with the dynamics of the GC reaction. Typical GC have a lifespan of approximately 3 wk (137) and their termination begins around day 14. This corresponds with alterations in FDC morphology including termination of iccosome production, and persisting Ag becomes buried within a labyrinth of membrane, thus minimizing BCR stimulation (28). While primary FDC-reticula can be labeled with CR1/2, FDC with the activated phenotype are associated with active peanut agglutinin $(PNA)^+$ GC (30). The lack of activated FDC-reticula in the absence of PNA labeling strongly suggests that the activated FDC phenotype is lost as the GC reaction is terminated.

FcγRIIB is generally considered to be an inhibitory receptor and is known to reduce the functionality of B cells, mast cells, and conventional dendritic cells (reviewed in (122,142)). However, in FDC, this receptor appears to promote a phenotype associated with FDC accessory activity. Clearly, engaging the same FcγRIIB receptor on B cells with the same IC did not lead to an apparent up-regulation of FcγRIIB on GC B cells or an increase in mRNA on isolated B cells. Thus, the FcγRIIB signaling pathway leading to the change in FDC phenotype is likely very different in FDC *vs.* other FcγRIIB-bearing cells. A recent report by Victoratos *et al.* (128) indicates that IκB kinase (IKK)2-

dependent signals are critical for IC-driven induction of VCAM-1 and ICAM-1 expression in FDC through the canonical NF-κB pathway, whereas, p55TNFR is essential for FDC network formation and maintenance, which is independent of IKK2. The data reported here are in complete harmony with these results (128).

Critical ligand-receptor reactions involved in FDC-B cell interactions include Ag-BCR, CD21L-CD21 and FcγRIIB-Fc. These receptor-ligand interactions are not MHC restricted and murine as well as human FDC work across MHC and even species barriers (56). FcγR genes are derived from a common ancestral gene, and the FcγRII genes in humans and mice are structurally related with a single FcgRIIB gene coding for a single protein chain characterized by an extracellular ligand-binding domain together with an intracellular cytoplasmic tail (143,144). The present data support the concept that engagement of murine FDC-FcγRIIB with IC induces the activated phenotype, and we reason that ICs likely activate human FDC as well.

CHAPTER 2

Toll-like Receptor-4 on Follicular Dendritic Cells:

An Activation Pathway that Promotes Accessory Activity

Introduction

Accessory cells of the immune system tend to remain quiescent until they encounter alarm signals that promote activation. Activation involves upregulation of molecules, including co-stimulatory molecules, needed for optimal presentation of Ag to specific lymphocytes and the initiation of adaptive immune responses. Infectious agents are a major source of alarm signals that are recognized by pattern recognition receptors (PRRs) that engage conserved pathogen-associated molecular patterns (PAMPs) (145-147). The range of molecular patterns recognized by PRRs includes signals from injured or stressed host cells and tissues (148,149). Prominent PRRs include the evolutionarily conserved membrane bound Toll-like receptors (TLRs) that recognize PAMPs and initiate responses in organisms as diverse as flies and mammals (150-154). TLR4 is an especially clear example of a receptor that is known to engage LPS, an amphiphilic molecule in the outer leaflet of the outer membrane of Gram-negative bacteria, and activate accessory cells (149,155,156).

Follicular dendritic cells (FDCs) are localized to the light zones of germinal centers (GCs), where their dendritic processes interdigitate and form three-dimensional FDC-networks or -reticula (44,46,157) that help these non-circulating cells remain fixed while attracting specific lymphocytes (47,67). FDC functions include the capture and retention of ICs (22,30,158), promotion of B cell survival (111-115,115) and promotion of high affinity Ab production (39,116). The phenotype of FDCs in primary and secondary follicles is very

different. In secondary follicles, FDCs bear high levels of FcγRIIB, ICAM-1, and VCAM-1 and these molecules are involved in converting poorly immunogenic ICs into a highly immunogenic form for B cells and in facilitating FDC-B cell interactions (30,57,69,132). In contrast, FcγRIIB, ICAM-1, and VCAM-1 levels are low and difficult to detect in FDC-reticula of primary follicles (30,132,134). The presence of these resting and activated FDCs prompted the hypothesis that FDCs, like other accessory immune cells, may express PRRs capable of recognizing PAMPs leading to the acquisition of an activated phenotype required for optimal FDC accessory activity.

To begin hypothesis testing, we sought to determine if FDCs express TLR4 and if LPS can activate FDCs via TLR4. Activation was indicated by increased expression of FDC function-associated molecules FcγRIIB, ICAM-1 and VCAM-1 by flow cytometry. TLR4 expression on FDCs *in situ* was studied with immunohistochemistry followed by flow cytometric and RT-PCR analyses on purified FDCs. The role of FDC-TLR4 engagement with LPS was investigated by adoptive transfer of wild-type LPS-responsive C3H/HeN leukocytes into TLR4-mutated LPS-hyporesponsive C3H/HeJ mice with host FDCs. The TLR4 activation pathway involves NF-κB activation and the involvement of this pathway was examined by flow cytometric analysis of intracellular phospho-IκB-α in FDCs. Finally, we sought to determine if activated FDCs have increased accessory activity as indicated by the enhanced ability to promote specific IgG responses *in vitro*.

The results indicated for the first time that FDCs express TLR4 on their surfaces and that TLR4 engagement mediates activation as indicated by a marked increase of FDC function-associated molecules and that activation involves the NF-κB pathway. Moreover, like other accessory cells, activated FDCs have increased accessory activity as indicated by increased anti-OVA production in comparison with non-activated FDCs. An important implication of these studies is that TLR agonists may promote immune responses not only by stimulating dendritic cells (DCs) and enhancing T cell function but also by stimulating FDCs and promoting B cell function. An understanding of how TLR agonists influence FDC activation may give insight into how adjuvants should be formulated to give optimal humoral immune responses when administering vaccines.

Materials and Methods

Animals

Six to eight weeks old BALB/c mice were obtained from the National Cancer Institute (Bethesda, MD). The C3H/HeNTac mice were from Taconic Farms (Hudson, NY), and the C3H/HeJ mice were from the Jackson Laboratory (Bar Harbor, ME). All mice were housed in standard plastic shoebox cages with filter tops and maintained under specific pathogen-free conditions in accordance with guidelines established by Virginia Commonwealth University Institutional Animal Care and Use Committee.

Antibodies and other reagents

Sigma (L-7895) cell culture tested, gel-filtration purified, γ-irradiated LPS from *Salmonella typhosa* was used in this study with more than 99% purity. FITC conjugated rat anti-mouse CD106 (mVCAM-1, catalog # 553332), CD54 (mICAM-1, catalog # 553252), CD16/CD32 (FcγRII/III, catalog # 553144), Fc blocker (2.4G2, catalog # 553142), rat anti-mouse FDC-M1 (catalog # 551320), biotinylated anti-rat κ light chain (catalog # 553871), rat IgG2bκ (catalog # 553988), Rat IgG2aκ (catalog # 554688), hamster IgG1κ (catalog # 553971) isotype controls, streptavidin-HRP (catalog # 550946) and the DAB substrate kit (catalog # 550880) were from BD PharMingen (San Diego, CA). FITC conjugated rat anti mouse TLR4 was from Imgenex (San Diego, CA, catalog # IMG-428C). Anti-biotin microbeads, CD45R (B220) MicroBeads (130-049-501), and MACS LS columns were purchased from Miltenyi Biotec GmbH

(Auburn, CA). Rabbit anti-mouse TLR4 (ab47093) and biotinylated goat anti rabbit IgG (ab6720-1) were purchased from Abcam (Cambridge, MA). Biotin labeled goat anti-rat IgG was from Southern Biotech (Birmingham, AL, catalog # 3050-08) and the Universal Block was from KPL (Gaithersburg, MD, catalog # 71-00-61). Antibodies used in flow cytometry were used at a concentration of 1 μg/10^6 cells while antibodies used in immunohistochemistry were used at a concentration of 5 μg/ml.

Immunohistochemical labeling of TLR4, FDC-M1, and GL-7 in situ

Popliteal LNs were collected from normal BALB/c mice and frozen in CryoForm embedding medium (IEC, Needham Heights, MA). Frozen sections of 10 μm thickness were cut on a Leica (Jung Frigocut 2800E) cryostat and air-dried. Following absolute acetone fixation, the sections were dehydrated and the endogenous peroxidase activity was quenched with the Universal Block. The sections were washed and saturated with 10% BSA. Serial sections were incubated with unlabeled rabbit anti-mouse TLR4 or rat anti-mouse FDC-M1. Sections were washed and then incubated with biotin-conjugated goat anti-rabbit or anti-rat IgG followed by streptavidin-HRP. The sections were developed using a DAB substrate kit. For germinal center B cell labeling, 10 μm cryostat sections of axillary lymph nodes from OVA-immunized BALB/c mice were labeled with IgM rat anti-mouse T- and B-cell activation antigen (GL-7, Ly-77) (eBioscience 14-5902-85), followed by biotinylated goat anti-rat IgM (Southern Biotech 3020-08) and phosphatase-labeled streptavidin (KPL 15-30-00). The

sections were developed with SIGMA*FAST*™ BCIP/NBT alkaline phosphatase substrate (Sigma, B5655). Rabbit polyclonal IgG (Abcam ab27478), rat IgG2c (BD Biosciences 553982) rat IgM (eBioscience 14-4341) isotype controls were similarly treated. Images were captured with Optronics digital camera and analyzed with Bioquant Nova software.

DC, FDC, and B cell isolation

DCs were isolated from splenic leukocytes using the CD11c micro-bead kit from Miltenyi Biotec GmbH (Auburn, CA). FDCs were isolated by positive selection from LNs (axillary, lateral axillary, inguinal, popliteal, and mesenteric) of irradiated adult mice as previously described (130). One day before isolation mice were irradiated with 1000 rad to eliminate most lymphocytes, then mice were killed, LNs were collected, opened and treated with 1.5 ml collagenase D (22 mg/mL, C-1088882; Roche), 0.5 mL of DNase I (5000 U/mL, D-4527; Sigma), and 2 mL DMEM with 20 mM HEPES. After 45 min at 37°C in a CO_2 incubator, released cells were washed in 5 mL DMEM with 10% FCS. Cells were then sequentially incubated with FDC-specific Ab (FDC-M1) for 45 min, 1 μg of biotinylated anti-rat κ light chain for 45 min, and with 20 μl anti-biotin microbeads (Miltenyi Biotec GmbH (Auburn, CA) for 15-20 min on ice. The cells were layered on a MACS LS column and washed with 10 ml ice-cold MACS buffer. The column was removed from the VarioMACS and the bound FDCs were released with 5 ml MACS buffer. $B220^+$ B cells were isolated from

BALB/c lymph nodes using CD45R (B220) MicroBeads from Miltenyi Biotec GmbH (Auburn, CA).

Labeling of purified FDCs and B220$^+$ B cells with anti-TLR4

FDCs and B220$^+$ B cells isolated from BALB/c mice were incubated with mouse Fc-Block (BD PharMingen) for 15 min on ice, followed by FITC conjugated rat anti mouse TLR4 or isotype control for 60 min in the dark at 4°C. After washing, the cells were analyzed using an FC500 flow cytometer and Cytomics RXP analysis software. Histograms were gated for FDCs based on their forward and side scatter properties established with FDC phenotypic markers including FDC-M1, CD21/35, and CD32 (130). The figures were plotted using WinMDI software (Scripps Research Institute).

Detection of TLR4 mRNA in purified FDCs by RT-PCR

Total cellular RNA was extracted from 2x10^6 FDCs purified from lymph nodes or spleens as well as control splenic dendritic cells of BALB/c mice using TRIzol reagent (Invitrogen Life Technologies, Carlsbad, CA) according to the manufacturer's instructions, and a 100 ng was reverse transcribed into cDNA using GeneAmp Gold RNA PCR Core Kit. One tenth of cDNA was primed with TLR4 specific primers 5'-GCTTTCACCTCTGCCTTCAC-3' and 3'-CGAGGCTTTTCCATCCAATA-5' and amplified by PCR. PCR products were electrophoresed in 1.5 % agarose, stained with ethidium bromide, and visualized by UV trans-illuminator.

Analysis of FcγRIIB, VCAM-1, and ICAM-1 on LPS-treated FDCs in vivo and in vitro

FDCs were positively selected with FDC-M1 from the draining lymph nodes of irradiated BALB/c mice three days after injecting 25 μg of LPS in the four limbs. Control FDCs were isolated from saline injected mice. In addition, 1 x 10^6 purified FDCs were treated *in vitro* with 10 μg LPS in 1 ml media for three days and the surface expression of FcγRIIB, VCAM-1, and ICAM-1 was compared with 1 x 10^6 control FDCs cultured in media without LPS. Analysis was done by incubating FDCs with mouse Fc-Block (BD PharMingen) for 15 min on ice, followed by FITC conjugated rat antibodies against FcγRIIB, ICAM-1, and VCAM-1 or isotype control for 60 min in the dark at 4°C. After washing, the cells were analyzed by flow cytometry.

Adoptive transfer

C3H/HeJ and C3H/HeN recipients were exposed to 600 rad of irradiation and one day later they were reconstituted with 2 x 10^7 LPS-responsive C3H/HeN total splenic leukocytes injected behind the neck. The mice were challenged with LPS in the legs and the FDCs were isolated after 3 days.

Analysis of FcγRIIB, VCAM-1, and ICAM-1 on LPS-treated C3H/HeN and C3H/HeJ FDCs

FDCs were positively selected from the lymph nodes of C3H/HeN or C3H/HeJ mice three days after injecting 25 μg of LPS in each limb and control FDCs were isolated from saline injected mice. FDCs were first incubated with

mouse Fc-Block for 15 min on ice, followed by FITC conjugated rat antibodies against FcγRIIB, ICAM-1, and VCAM-1 or isotype control for 60 min in the dark at 4°C. After washing, the cells were analyzed by flow cytometry.

Intracellular labeling of phospho-IκB–α in Purified FDCs treated with LPS in vitro

Purified FDCs were serum-starved for 24 hours then treated with 10 μg/ml LPS overnight in DMEM with 10% FCS. Control groups of unstimulated FDCs as well as macrophage cell line J774 were similarly treated. Cells were washed then fixed and permeabilized using Fix & Perm cell permeabilization kit (Caltag, Burlingame, CA). Intracellular phospho-IκB-α was labeled with rabbit anti-phospho-IκB-α (Cell Signaling Technology, Danvers, MA) followed by PE conjugated goat anti-rabbit IgG and cells were analyzed with flow cytometry.

Cell culture and ELISA assessment of OVA specific IgG

Lymph nodes cells from OVA-immunized BALB/c mice were cultured, in the presence of 100 ng/ml OVA-anti-OVA ICs, with FDCs isolated from LPS-treated mice and compared with control FDCs at ratios of 64, 128 and 256 lymphocytes per FDC. The media was changed after one week and OVA specific IgG was assessed by ELISA 7 days later as previously described (29).

Results

Immunohistochemical labeling of TLR4 on FDCs but not on GC B cells in situ

As shown in panel A of Fig. 1, adjacent sections of lymph nodes were labeled with FDC specific marker FDC-M1 (Fig. 1*A-a*) and anti-TLR4 (Fig. 1*A-c*). TLR4 co-localized with the FDC-M1 as indicated by the labeling in the area between the arrows. The characteristic labeled FDC-network or reticulum made up by interactive dendrites of FDCs can be seen. Germinal center B cells intermingle with FDCs and we sought to determine if they label with anti-TLR4 and contribute to the labeling in Fig. 1*A-c*. Germinal center B cells are activated and labeled with anti-mouse T- and B-cell activation antigen GL-7 (Fig. 1*B-a*), but in contrast with FDCs, they did not label with TLR4 in adjacent lymph node sections (Fig. 1*B-c*). Thus TLR4 labeling in GCs appeared to be attributable to FDCs and not B cells. Isotype controls (Fig. 1*A-b, A-d, B-b, B-d*) were included and shown to the right of the corresponding labeled sections.

TLR4 labeling of purified FDCs

To confirm expression of TLR4, FDCs were purified by positive selection using the monoclonal Ab FDC-M1, and labeled with anti-TLR4-FITC. As illustrated in panel C of Fig. 1, flow cytometric analysis revealed that virtually the entire FDC population shifted to the right when labeled with anti-TLR4 with more than a two fold increase in mean fluorescent intensity (MFI) over the background control. Analysis was restricted to viable cells indicating

that TLR4 is expressed on the surface of FDC membranes. B cells positively selected with B220, an antigen expressed on B lineage cells throughout their development but not on plasma cells, also appeared to shift to the right as a consequence of anti-TLR4 labeling (Fig. 1*D*). However, in contrast with FDCs where the MFI more than doubled upon labeling with anti-TLR4, the increased MFI for the B cells was only 0.2 above the isotype control. In short, murine B cells may express some TLR4 but it is unlikely that they are making a significant contribution to the strong TLR4 labeling in GC areas where the FDC-reticulum identified by FDC-M1 is present.

TLR4 mRNA in purified FDCs

RNA extracted from purified FDCs from murine lymph nodes (Fig. 2*A*) and spleen (Fig. 2*B*) was reverse transcribed into cDNA. TLR4 specific primers were used to amplify the relevant DNA and the results were compared with similarly treated purified splenic dendritic cells (DCs) as a positive control (Fig. 2*C*). Gel electrophoresis of amplified PCR products revealed a single 361 bp band shared between dendritic and follicular dendritic cells indicating TLR4 expression by FDCs.

LPS-mediated upregulation of FDC-FcγRIIB, -ICAM-1, and -VCAM-1

Injecting LPS increased the levels of FcγRIIB, ICAM-1, and VCAM-1 on FDCs from the draining lymph nodes (Fig. 3*A-a, b, c*) where virtually the entire FDC population shifted to the right when labeled with antibodies reactive with these markers and the MFI approximately doubled in each case. Similarly,

Figure 1: ***Labeling of FDCs with anti-TLR4.*** *A*, Illustrates TLR4 labeling on FDCs in situ using immunohistochemistry. Adjacent sections from popliteal LNs were labeled for TLR4 and the FDC-specific marker FDC-M1. As indicated by arrowheads, FDC-M1 labeling (*Aa*) colocalized with TLR4 expression (*Ac*), and the characteristic labeling of FDC network or reticulum made up by interactive FDC dendrites can be seen. *B*, Lack of TLR4 labeling on GC B cells. Adjacent sections from axillary LNs of OVA-immune animals were labeled with GL-7, anti-mouse T and B cell activation Ag (*Ba*), and anti-TLR4 (*Bc*). As shown between arrowheads, GL-7^+ B cells did not label with anti-TLR4. Isotype controls (*Ab*, *Ad*, *Bb*, and *Bd*) are shown to the *right* of the appropriate adjacent section. *C*, Flow cytometry was used to assess TLR4 labeling of purified FDCs in vitro. Purified FDC preparations were labeled with anti-TLR4-FITC and compared with an isotype control. The MFI of TLR4-FITC-labeled FDCs was double the isotype control. *D*, TLR4 labeling of purified $B220^+$ B cells. Purified $B220^+$ B cell preparations were labeled with anti-TLR4-FITC and compared with an isotype control. $B220^+$ B cells were hardly labeled with TLR4-FITC, and the MFI of TLR4-FITC-labeled B cells was 0.2 above the MFI of the isotype control. These data are representative of three separate experiments of this type.

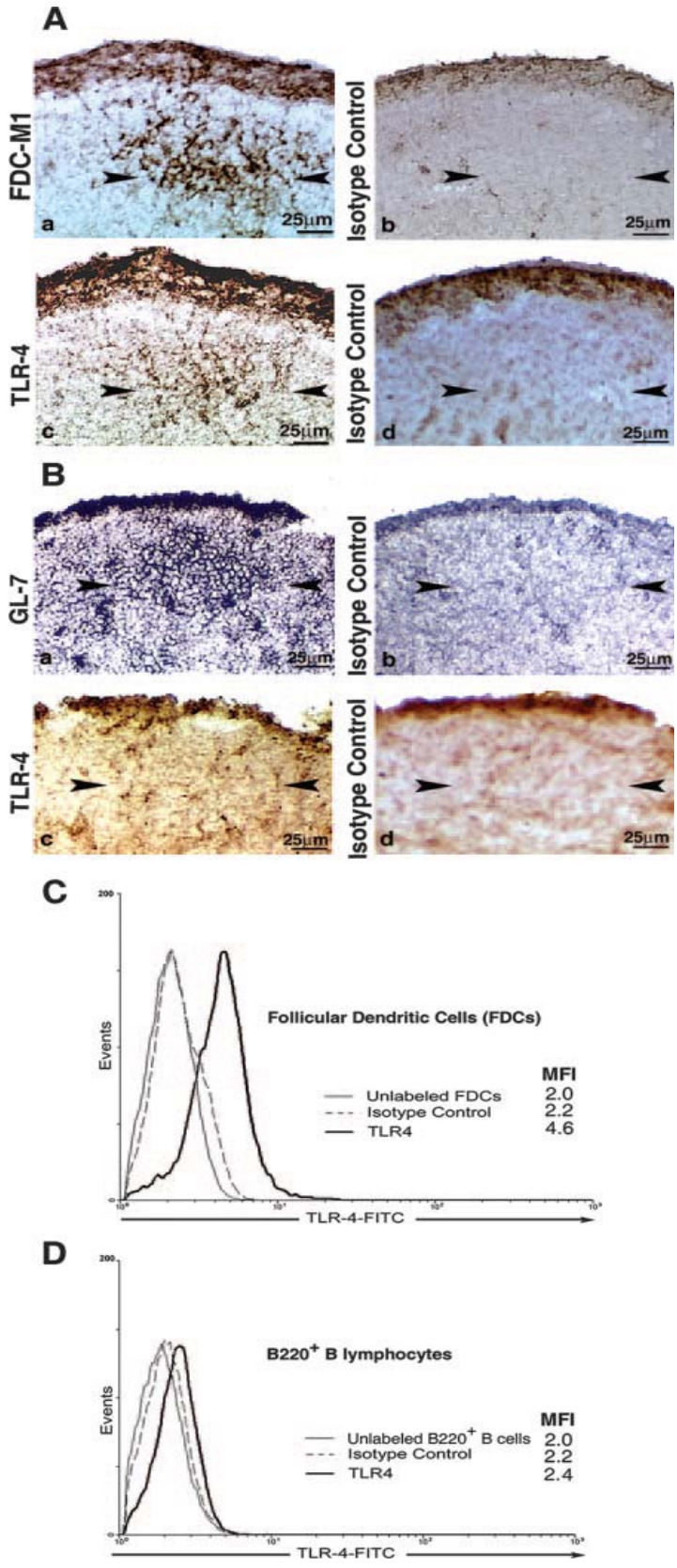
A
FDC-M1
a
25μm
Isotype Control
b
25μm
TLR-4
c
25μm
Isotype Control
d
25μm
B
GL-7
a
25μm
Isotype Control
b
25μm
TLR-4
c
25μm
Isotype Control
d
25μm
C
Events
Follicular Dendritic Cells (FDCs)
MFI
Unlabeled FDCs 2.0
Isotype Control 2.2
TLR4 4.6
TLR-4-FITC
D
Events
B220+ B lymphocytes
MFI
Unlabeled B220+ B cells 2.0
Isotype Control 2.2
TLR4 2.4
TLR-4-FITC

Figure 2: ***RT-PCR analysis of TLR4 mRNA in purified FDCs.*** Total RNA extracted from purified FDCs of mouse LNs (*A*) and spleen (*B*) were primed with TLR4-specific primers and compared with purified DCs isolated from mouse spleen (*C*). A single 361-bp band shared between DCs and FDCs is seen, providing evidence for TLR4 expression in FDCs.

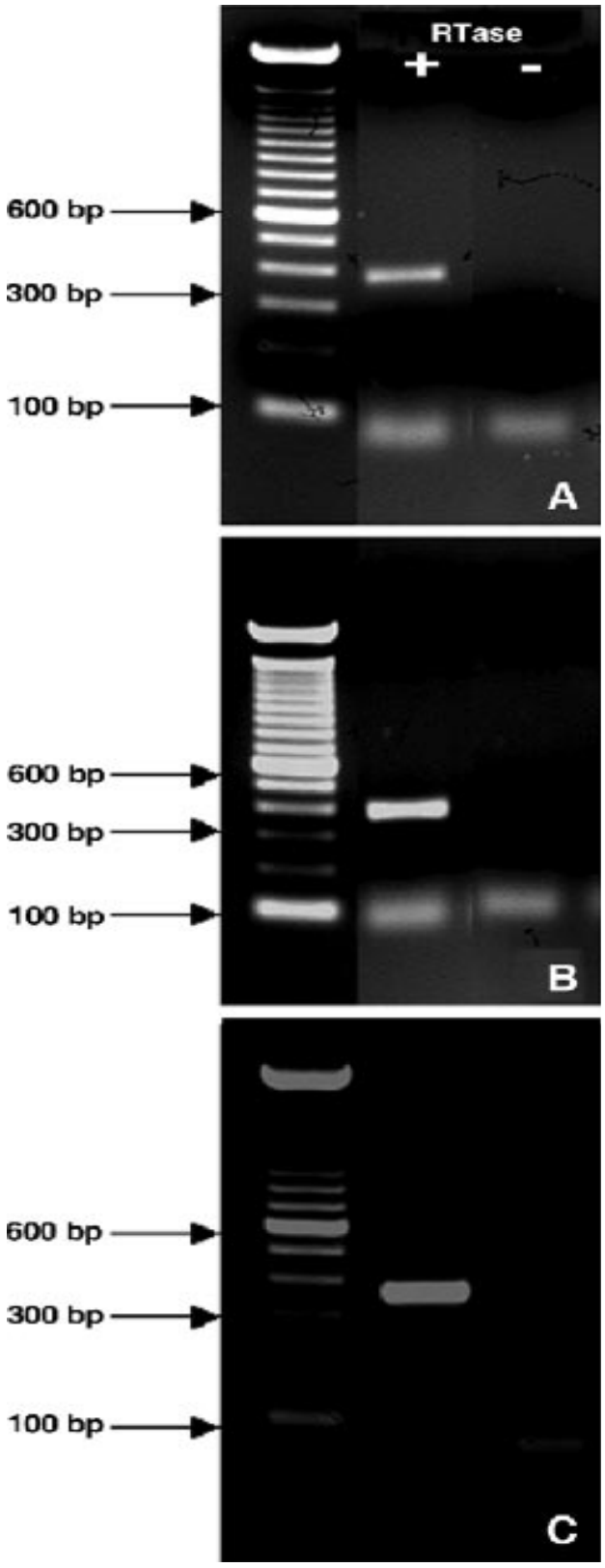
RTase
+
-
600 bp
300 bp
100 bp
A
600 bp
300 bp
100 bp
B
600 bp
300 bp
100 bp
C

Figure 3: ***Up-regulation of FcγRIIB, ICAM-1, and VCAM-1 on LPS-treated FDCs in vivo (A) and in vitro (B).*** FDCs were purified from the LNs of LPS-treated BALB/c mice and compared with control FDCs isolated from saline-injected mice (*A*). Likewise, purified FDC preparations treated in vitro with LPS for 3 days were compared with control FDCs cultured in medium without LPS (*B*). FDCs were labeled with FITC-conjugated rat Abs against FcγRIIB (*a*), ICAM-1 (*b*), and VCAM-1 (*c*) or isotype control. The MFI of FITC-labeled FDCs were almost double the corresponding isotype controls in vivo and in vitro, although the intensity of VCAM-1 up-regulation on FDCs stimulated in vitro was comparatively less. These data are representative of three separate experiments of this type.

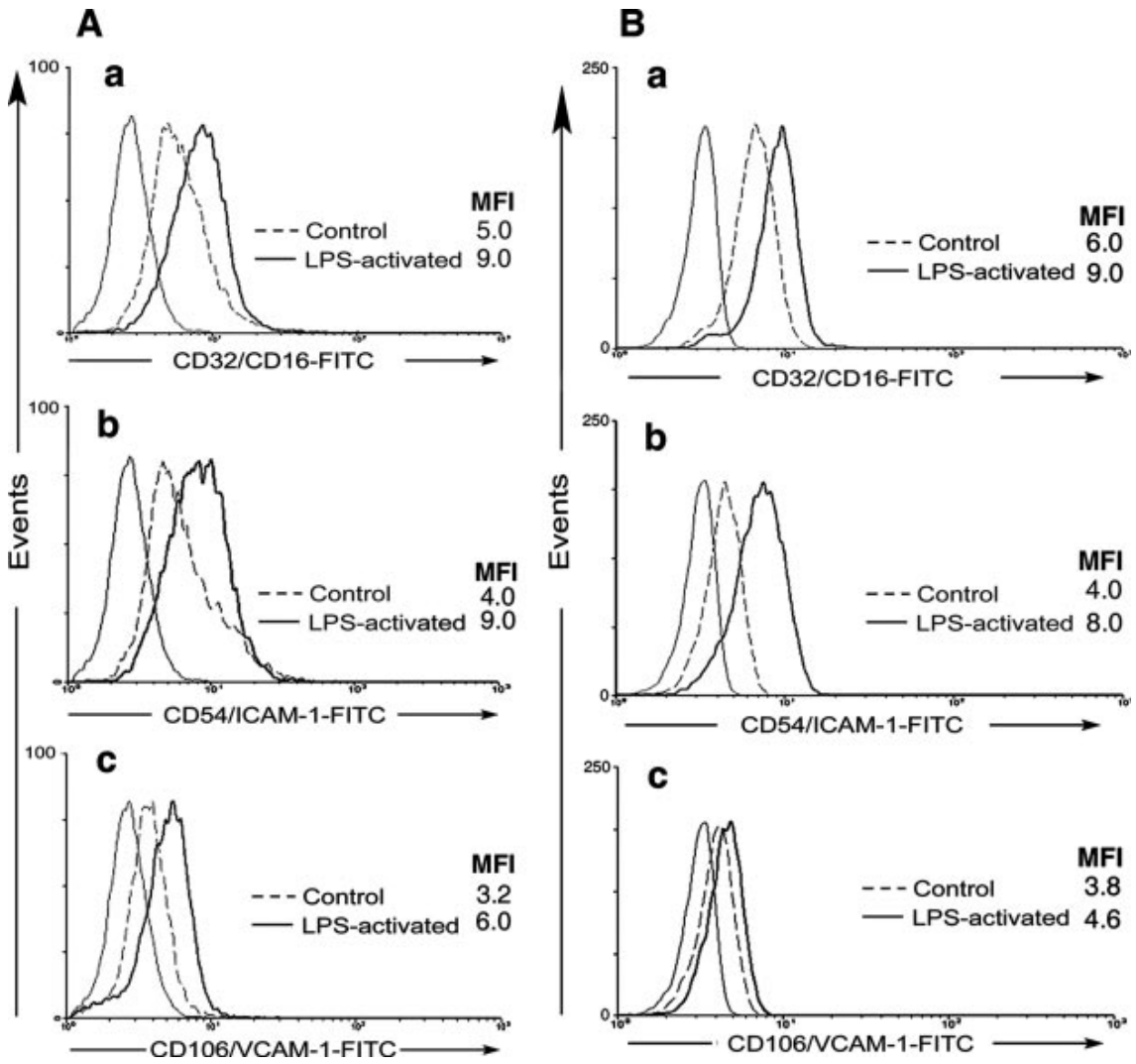
A
B
a
b
c
Events
100
250
0
MFI
Control
LPS-activated
5.0
9.0
6.0
9.0
4.0
9.0
4.0
8.0
3.2
6.0
3.8
4.6
CD32/CD16-FITC
CD54/ICAM-1-FITC
CD106/VCAM-1-FITC

treating purified FDCs *in vitro* (Fig. 3*B-a, b, c*) with LPS for three days increased the levels of FcγRIIB, ICAM-1, and VCAM-1 expression on FDCs although the intensity of VCAM-1 upregulation was comparatively less.

FDCs purified from TLR4-mutated C3H/HeJ mice did not respond to LPS even when reconstituted with leukocytes from TLR4 wild-type mice

FDCs from wild-type LPS-responsive C3H/HeN mice upregulated FDC-FcγRIIB, ICAM-1, and VCAM-1 when injected with LPS (Fig. 4A) much like the BALB/c mice shown in Fig. 3. Moreover this response persisted after irradiation and reconstitution with LPS-responsive C3H/HeN total splenic leukocytes (Fig. 4B). In marked contrast, FDCs from TLR4-mutated C3H/HeJ mice failed to upregulate FDC-FcγRIIB, -ICAM-1, and -VCAM-1 after LPS injection (Fig. 4C) even after reconstitution with wild-type TLR4 LPS-responsive C3H/HeN leukocytes (Fig. 4D). This suggests that LPS engagement of TLR4 on the FDC is important, and that FDC activation is not simply a response to cytokines being produced by other TLR4 responsive leukocytes.

LPS mediated upregulation of intracellular phospho-IκB-α in FDCs indicative of NF-κB activation

Signaling through TLR4 typically involves the NF-κB pathway prompting the hypothesis that stimulation of FDCs with LPS would upregulate intracellular phospho-IκB-α in FDCs. Purified FDCs were incubated with 10 μg/ml LPS overnight. Control groups included unstimulated FDCs and murine macrophage cell line J774 that were similarly treated. Flow cytometric analysis

revealed that the MFI of intracellular phospho-IκB-α in the control macrophage cell line about doubled after exposure to LPS (Fig. 5*A*). The FDC response to LPS was very similar and the increase in MFI was even higher (Fig. 5*B*). Similar results were obtained with 0.1 and 1μg of LPS but the results were most apparent with the 10 μg dose illustrated in Fig. 5.

LPS activated FDCs exhibited enhanced accessory activity in promoting recall responses in vitro.

FDCs from normal mice are known to enhance recall responses optimally at ratios between 1 FDC to 4 - 16 lymphocytes although detectable accessory activity may be apparent with more lymphocytes (159). We reasoned that LPS activated FDCs would have enhanced accessory activity and that might be most apparent in IgG recall responses at low FDC to lymphocyte ratios. When cultured at a ratio of 1 FDC to 64 lymphocytes, the IgG anti-OVA produced in cultures containing activated FDCs was about 4 times higher than the production with FDCs from normal mice which in turn produced anti-OVA IgG comparable to 1 activated FDC to 256 lymphocytes (Fig. 6). In marked contrast, FDCs from normal mice were without detectable activity at 1 FDC to 256 or even 128 lymphocytes (Fig. 6).

Figure 4: ***Lack of up-regulation of FcγRIIB, ICAM-1, and VCAM-1 on FDCs purified from TLR4-mutated C3H/HeJ mice even when reconstituted with leukocytes from TLR4 wild-type mice.*** The levels of expression of FcγRIIB, ICAM-1, and VCAM-1 in TLR4-intact LPS-responsive C3H/HeN were assessed using flow cytometry 3 days after LPS injection (*A*) or after irradiation, reconstitution with C3H/HeN leukocytes, and LPS injection (*B*). Similarly, FcγRIIB, ICAM-1, and VCAM-1 in TLR4-mutated C3H/HeJ mice were analyzed 3 days after LPS injection (*C*) or after irradiation, reconstitution with C3H/HeN leukocytes, and LPS injection (*D*). FDCs from TLR4-intact LPS-responsive C3H/HeN mice demonstrated up-regulation of FcγRIIB, ICAM-1, and VCAM-1 when injected with LPS, and that persisted after irradiation and reconstitution. On the contrary, FDCs purified from TLR4-mutated C3H/HeJ mice failed to up-regulate their FcγRIIB, ICAM-1, and VCAM-1 upon encountering LPS, and that persisted even after reconstitution with TLR4-intact LPS-responsive C3H/HeN leukocytes. These data are representative of three separate experiments of this type.

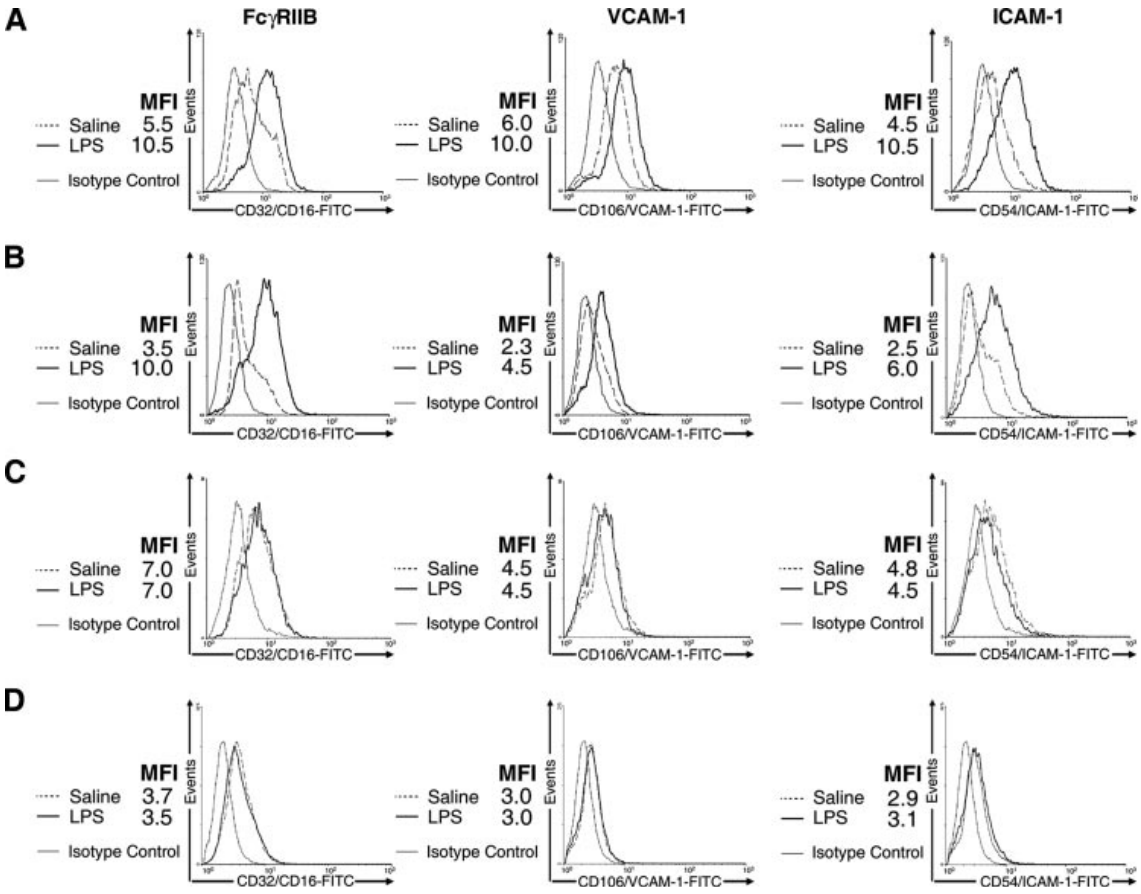
A
FcγRIIB
VCAM-1
ICAM-1
MFI
Saline 5.5
LPS 10.5
Isotype Control
Events
CD32/CD16-FITC
MFI
Saline 6.0
LPS 10.0
Isotype Control
Events
CD106/VCAM-1-FITC
MFI
Saline 4.5
LPS 10.5
Isotype Control
Events
CD54/ICAM-1-FITC
B
MFI
Saline 3.5
LPS 10.0
Isotype Control
Events
CD32/CD16-FITC
MFI
Saline 2.3
LPS 4.5
Isotype Control
Events
CD106/VCAM-1-FITC
MFI
Saline 2.5
LPS 6.0
Isotype Control
Events
CD54/ICAM-1-FITC
C
MFI
Saline 7.0
LPS 7.0
Isotype Control
Events
CD32/CD16-FITC
MFI
Saline 4.5
LPS 4.5
Isotype Control
Events
CD106/VCAM-1-FITC
MFI
Saline 4.8
LPS 4.5
Isotype Control
Events
CD54/ICAM-1-FITC
D
MFI
Saline 3.7
LPS 3.5
Isotype Control
Events
CD32/CD16-FITC
MFI
Saline 3.0
LPS 3.0
Isotype Control
Events
CD106/VCAM-1-FITC
MFI
Saline 2.9
LPS 3.1
Isotype Control
Events
CD54/ICAM-1-FITC

Figure 5: ***Up-regulation of intracellular phospho-IκB-α in purified FDCs treated with LPS in vitro.*** Purified FDC preparations were treated with 10 μg/ml LPS overnight, and control groups of unstimulated FDCs as well as macrophage cell line J774 were included. FDC intracellular phospho-IκB-α rose after LPS treatment to levels comparable to those seen in the control macrophage cell line. These data are representative of three separate experiments of this type.

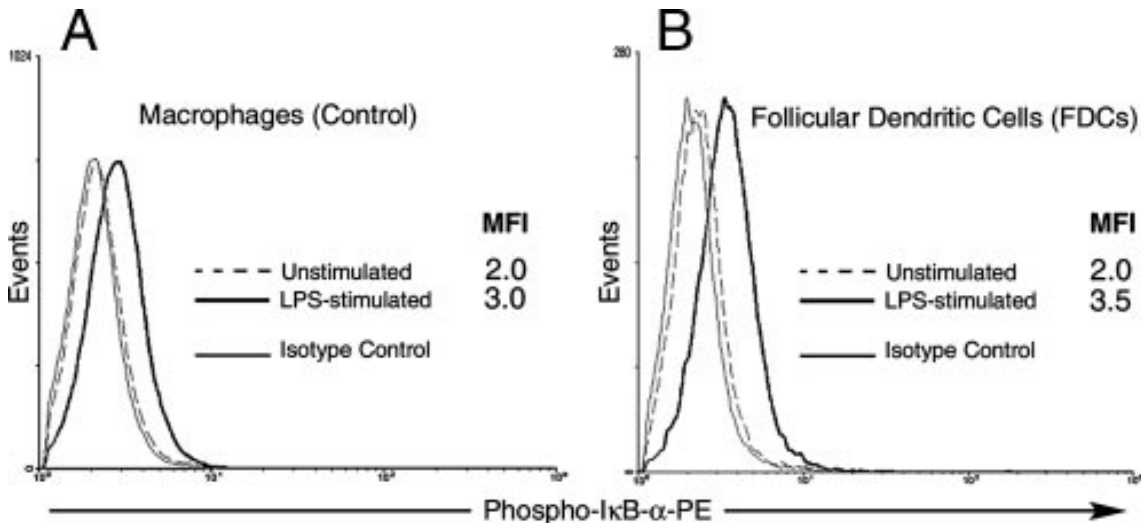
A
Macrophages (Control)
Events
MFI
Unstimulated
LPS-stimulated
Isotype Control
2.0
3.0
B
Follicular Dendritic Cells (FDCs)
Events
MFI
Unstimulated
LPS-stimulated
Isotype Control
2.0
3.5
Phospho-IκB-α-PE

Figure 6: ***Activated FDCs have enhanced accessory cell activity in OVA-specific recall responses.*** OVA-specific lymphocytes were cultured, in the presence of OVA-anti-OVA ICs, with FDCs isolated from LPS-treated mice and compared with control FDCs at ratios of 64, 128, and 256 lymphocytes to 1 FDC. Two weeks later, OVA-specific IgG was assessed by ELISA. At all tested ratios, cultures containing activated FDCs promoted significantly higher anti-OVA IgG levels than cultures with control FDCs, ($p < 0.01$; Student's *t* test). Averages were calculated using data from three cultures, and results illustrate the means ± SEM.

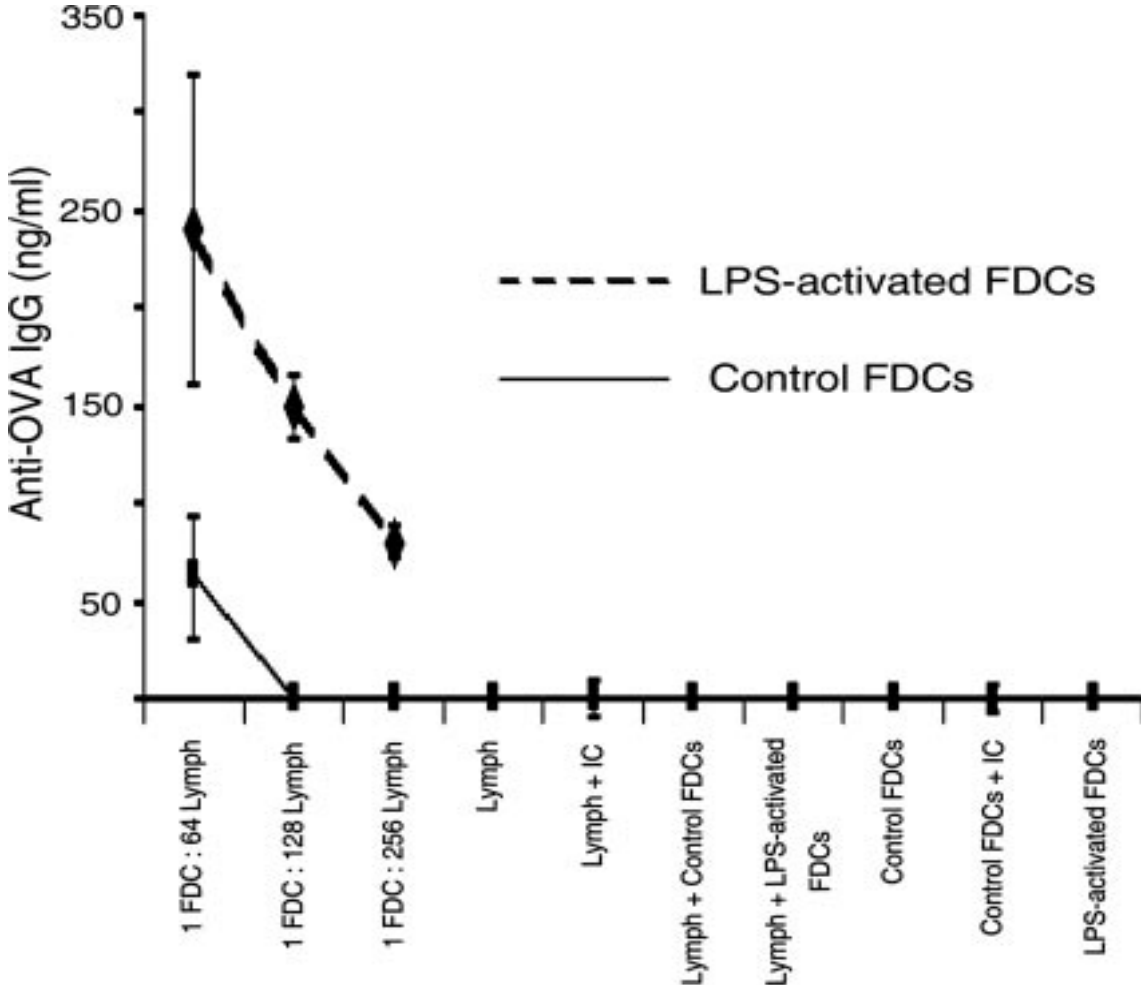
350
250
150
50
Anti-OVA IgG (ng/ml)
LPS-activated FDCs
Control FDCs
1 FDC : 64 Lymph
1 FDC : 128 Lymph
1 FDC : 256 Lymph
Lymph
Lymph + IC
Lymph + Control FDCs
Lymph + LPS-activated FDCs
Control FDCs
Control FDCs + IC
LPS-activated FDCs

Discussion

Engagement of TLRs on DCs leads to physiological and phenotypic changes that dramatically alters their ability to present Ag to T cells (145,160,161). DC alterations include changes in: survival, chemokine receptor expression, chemokine secretion, migration, cell shape and endocytic activity (162). LPS and other TLR agonists promote DCs maturation and accessory activity in priming naïve T cells, promoting clonal expansion, and stimulating differentiation of T cells into effectors (163). We reasoned that for the immune system to respond to microbial invasion as an integrated unit, microbial patterns encountered early in immune responses should activate not only the DC-T cell axis but also the FDC-B cell axis. The data reported here indicated that FDCs express surface TLR4 and that engagement of this receptor *in vivo* and *in vitro* altered their physiology and phenotype leading to FDC activation. Moreover, activated FDCs were far more effective in enhancing the production of specific IgG than FDCs from normal mice. Immune complex bearing FDCs reside in germinal centers where B cells: proliferate, isotype switch, somatically hypermutate, become memory cells, and transition from B cells into antibody forming cells (reviewed in (46,125)). Considerable data indicate that FDCs influence these B cell functions (reviewed in (44,46)). An understanding of FDC activation could facilitate our ability to manipulate the immune system such that the appropriate adjuvants could be selected to activate FDCs and optimize humoral immune responses when vaccines are administered.

Analysis of mRNA by RT-PCR in the present study suggested that TLR4 expression in DCs and FDCs is comparable. The fact that FDCs are barely endocytic and retain Ag in immune complexes on their surfaces (164) allows the surface expressed FDC-TLR4, as shown by flow cytometry, to engage LPS in an environment spatially associated with other FDCs accessory functions, including IC trapping and receptor mediated B cell-FDC clustering and interactions. The presence of TLR4 molecules inside the FDCs has not been excluded, but clearly anti-TLR4 labels FDC membranes intensely. Cytokines help activate many cell types and we reasoned that cytokines induced by LPS may play an important role in FDC activation. However, no support for this idea was found in the present study. When normal splenic leukocytes, that are fully capable of secreting cytokines upon TLR4 engagement, were injected into irradiated TLR4 mutated C3H/HeJ mice and challenged with LPS, the FDCs with mutated TLR4 still failed to activate (Fig. 4*D*). These results argue that functional TLR4 on FDCs is important. Moreover, when purified wild-type FDCs were treated with LPS *in vitro,* they responded well suggesting that FDC-TLR4 is sufficient (Fig. 3*B*).

FDC-associated germinal center B cells failed to label immunohistochemically *in situ* with anti-TLR4, and purified B cell preparations positively selected with the pan-B cell marker CD45R (B220) were barely labeled with anti-TLR4 by flow cytometry. These data are consistent with similar results reported by Akashi et al where cell surface TLR4-MD-2 was

hardly detectable on CD19-positive B cells and intracellular staining by the saponin detergent did not make a difference (165).

FcγRIIB plays an important role in FDC-B cell interactions. Both FDC and B cells express FcγRIIB (57,58), but B cell activation may be inhibited by immunoreceptor tyrosine-based inhibition motif (ITIM) signaling mediated by IC coligating the B cell receptor for Ag (BCR) and B cell-FcγRIIB (122,123). Engagement of BCR in the absence of such coligation induces rapid activation of tyrosine kinases, generation of inositol phosphates, elevation of cytoplasmic Ca^{2+} concentrations, and activation of mitogen-activated protein kinases (reviewed in (122,123)). These events promote B cell activation and lead to proliferation, differentiation, and Ab secretion (124). In marked contrast, coligation of BCR and FcγRIIB by ICs leads to inhibition of the extracellular Ca^{2+} influx, reduction of cell proliferation, blockage of blastogenesis, and inhibition of Ig synthesis (122-124). Nevertheless, ICs on FDCs provide potent activation signals for B cells that result in induction of germinal center dark zones where B cells rapidly proliferate and differentiate (reviewed in (125)). However, FDCs lacking FcγRIIB or expressing only low levels of FcγRIIB are unable to convert poorly immunogenic IC into a highly immunogenic form for B cells, although they can trap IC using CRs (complement receptors) (30). In active GC, FDCs express high levels of FcR relative to B cells, and these FDC-Fc receptors bind Fc portions of Ab in ICs and appear to minimize their binding to FcR on B cells (30,44,57). Accordingly, cross-linking of BCR and FcγRIIB

via IC is minimized, ITIM signaling is reduced, and B cell proliferation and differentiation is promoted. Thus, activating FDCs and increasing FDC-FcγRIIB levels would be expected to enhance accessory activity.

FDCs and B cells form large clusters in culture and B cells proliferate adjacent to FDCs much like they do in the dark zone of GCs *in vivo* (69). FDC-ICAM-1 and -VCAM-1 are important adhesion molecules and blocking these molecules inhibits clustering of FDCs and B cells and the ability of B cells to proliferate in GC reactions *in vitro* (69). Upregulating these adhesion molecules should promote FDC-B cell interactions, facilitate clustering and presentation of FDC-Ag to B cells, and enhance the GC reaction. The signaling pathway known to up-regulate FDC-ICAM-1 and -VCAM-1 is mediated via the NF-κB (128) and up-regulation of FDC-ICAM-1 and -VCAM-1 may be initiated by ICs engaging FDC-FcγRIIB (70). Similarly, the NF-κB pathway appeared to be activated when FDC-ICAM-1 and -VCAM-1 were upregulated by LPS engaging FDC-TLR4 in the present study.

The initial exposure to appropriate immunogen primes T cells and stimulates specific B cells to begin making Abs. Specific Abs bind the immunogen and form ICs, ICs are trapped by FDCs, B cells are stimulated by the Ag in FDC-ICs, and GC reactions are initiated. The data presented here suggest that FDCs can be activated by TLR4 agonists and such agonists can be delivered by the pathogen or with the immunogen. Thus, FDCs could be activated and ready to trap ICs and optimally stimulate B cells as soon as the

first ICs are made. The ICs themselves can activate FDCs but that requires 24 to 48 hours after encountering adequate amounts of ICs (70). The present study indicated that FDCs were activated via TLR4 engagement in 3 days, and that would precede Ab production and IC formation. Thus, ICs could be trapped by activated FDCs and that would speed up and enhance GC events including B cell proliferation, isotype switching, somatic hypermutation, memory cell formation, transition from B cells to antibody forming cells, selection, and affinity maturation. In addition to TLR4, preliminary studies using RT-PCR indicated that FDCs express TLR-2, TLR-3 and TLR-9. By use of flow cytometry with purified FDCs we were able to confirm expression of TLR-2 and TLR-3. Stimulation of FDCs with the TLR-3 ligand poly (I:C) resulted in upregulation of CR1/2, FcγRIIB and VCAM-1. However, the data suggest that TLRs may differ in their impact on FDC phenotype & function and further studies in this area are in progress. Nevertheless, an understanding of how FDCs can be optimally activated via TLR engagment could provide information needed to control and enhance the development of protective humoral immune responses.

CHAPTER 3

FOLLICULAR DENDRITIC CELLS STIMULATED BY COLLAGEN TYPE I DEVELOP DENDRITES AND NETWORKS IN VITRO

Introduction

Follicular dendritic cells (FDCs) are located in the light zone of germinal centers (GCs), where their dendritic processes interdigitate and form three-dimensional networks or FDC-reticula (42,46,157,166). Functions of FDCs include the production of chemokines that help organize lymphoid follicles (67), capture and retention of immune complexes (ICs) (30), presentation of ICs to B cells under conditions that minimize activation of the immuno tyrosine inhibitory motif in B cells (44), promotion of B cell survival (111-114,114), promotion of Ig class switching, production of high affinity Abs, B cell selection associated with affinity maturation and production of B memory cells with high affinity receptors (39,116,167).

Although description of antigen localization in lymphoid follicles dates back to 1950 (168), the nature of the antigen retaining cells remained obscure until described at the ultrastructural level in rodent spleen or lymph node sections by Szakal and Hanna (21) and Nossal et al (166) in 1968. These authors reported radiolabeled antigen associated with highly convoluted infoldings of the plasma membrane of FDCs, and antigen was associated with electron dense material found in the extracellular spaces adjacent to FDC processes (21,22). Subsequent studies indicated that these antigen retaining cells are not free to circulate and Ag remained localized to FDCs in the draining lymphatics for months to years (51). Consequently, antibody induced by the retained Ag is

restricted to draining lymph nodes and this pattern was followed for as long as one year (51).

Several cells in lymphoid tissues have dendritic processes that distinguish them from lymphocytes and typical macrophages; however, the ability of FDCs to trap and retain ICs for long periods makes them unique. Different names have been used for FDCs, e.g. antigen retaining reticular cells, follicular immune complex retaining cells, follicular antigen-binding dendritic cells, follicular reticular cells, follicular dendritic reticulum cells, and dendritic macrophages until 1982 when the name: follicular dendritic cell was accepted (23).

Morphologically, FDC are characterized by their irregularly shaped euchromatic nuclei surrounded by a narrow rim of cytoplasm from which long slender highly convoluted dendrites emanate (42). Although FDCs represent only 1–2% of GC cells, their numerous long slender dendrites intertwine and create an extensive network or reticulum that makes them a prominent GC component (42). The extensive network enables FDCs to be in intimate contact with neighboring B cells (90% of GC cells) and T cells (5–10% of GC cells) (11,42,169). FDCs use complement (119,120) and FcγRs (30,170) to capture and retain ICs and they deliver the Ag in the form of IC-coated bodies (iccosomes) to neighboring B cells for subsequent presentation to GC T cells to obtain T cell help (38).

Our understanding of FDC biology has been promoted by use of enriched FDCs *in vitro*. Twenty-one years ago we isolated and characterized FDCs from murine lymph nodes. These FDCs were identified by the ICs they retained, and descriptions were based on light microscopy using Nomarski optics, scanning electron microscopy, and transmission electron microscopy. These freshly isolated FDCs had numerous long filliform or beaded dendrites and lacked the ability to adhere to glass or plastic (42). Subsequent enrichment procedures included whole body irradiation to remove the irradiation sensitive lymphocytes, Percoll replaced BSA in the gradients, and more recently positive selection with FDC-M1 antibodies on magnetic columns (69,130). Increased handling resulted in individual FDCs that appeared almost spherical under light microscopy and short to medium length dendritic processes were only readily apparent under electron microscopy (130). Clearly, the FDC-reticulum, so characteristic of cells *in vivo,* had been destroyed and the longer FDCs were cultured the less dendritic they appeared.

Structure typically promotes function and numerous attempts were made to increase dendrite formation and reestablish FDC-reticula *in vitro* without success. Given that FDC purification requires use of collagenase and that FDCs may be found at the edges of the GCs attached to the supporting reticular fibers (171), we reasoned that isolated FDCs might reattach to collagen and form processes and reticula. To test this, positively selected FDCs were incubated on dried collagen and collagen related molecules. The results presented here

indicate that FDCs bind these molecules and that interaction with collagen type I promotes dendrite formation and the production of FDC-reticula *in vitro*. In short, FDCs placed on collagen-coated plates, attached to the matrix, regenerated processes, and formed immobile networks with numerous features in common with networks *in vivo*.

Materials and Methods

Animals

Normal 6- to 8-wk-old BALB/c mice were purchased from the National Cancer Institute. The mice were housed in standard plastic shoebox cages with filter tops and maintained under specific pathogen-free conditions in accordance with guidelines established by Virginia Commonwealth University Institutional Animal Care and Use Committee.

Antibodies and other reagents

Rat-tail collagen type I was purchased from Roche Diagnostic GmbH (Indianapolis, IN). Hyaluronic acid, Biglycan and Laminin were from Sigma (St Louis, MO). Rabbit anti-collagen Type I and biotin-conjugated goat anti-rabbit IgG were from Abcam (Cambridge, MA). FDC-M1, biotin-labeled anti-rat kappa, Streptavidin-HRP and DAB substrate kit were from BD PharMingen (San Diego, CA). Anti-Biotin MicroBeads, and MACS LS columns were purchased from Miltenyi Biotec GmbH (Auburn, CA).

FDC Isolation

FDCs were isolated by positive selection from axillary, lateral axillary, inguinal, popliteal, and mesenteric lymph nodes of adult mice as recently described (130). In brief, one day before isolation four mice were irradiated with 1000 rads to eliminate most lymphocytes. On the day of isolation, mice were killed, lymph nodes were pooled, and the capsules were opened using two 26-gauge needles. The nodes were incubated with 1.5ml of collagenase D

(22mg/ml, C-1088882, Roche), 0.5ml of DNase I (5000 units/ml, D-4527, Sigma), and 2 ml DMEM with 20 mM HEPES. After 45 min at 37^{o}C in a CO_2 incubator, the released cells were washed in 5ml DMEM with 10 % FCS. Cells were then sequentially incubated with FDC specific Ab (FDC-M1) for 45 min, 1μg of biotinylated anti-rat-κ light chain for 45 min, and with 20μl anti-biotin MicroBeads (Miltenyi Biotec) for 15-20 min on ice. The cells were layered on MACS LS column and washed with 10ml of ice-cold MACS buffer. The column was removed from the VarioMACS and the bound cells were released with 5ml of MACS buffer. Approximately 85 to 95% of these cells were FDC-M1^{+}, CD40^{+}, CR1/2^{+}, and FcγRIIB^{+}.

FDCs adhesion assessment

One million freshly purified FDCs were layered on collagen type I, laminin, biglycan or hyaluronic acid layers. Twelve hours later, cells were washed off the matrices and the released cells were counted. The percentage of attached cells was calculated. Control lymphocytes and FDCs on plastic were compared.

Collagen coating of plates

Ten mg sterile lyophilized rat tail collagen type I was dissolved in 5 ml sterile 0.2% acetic acid (v/v) to give a final concentration of 2 mg/ml, pH was adjusted to 7.4 ± 0.2 by 0.1 M NaOH and 0.1M HCl. Twenty-four-well culture plates were coated with collagen type I at a concentration of 5 μg/cm^2. Collagen was air dried on the plates for 2 hours at 25^{0}C in a laminar flow hood.

Light microscopy and FDC labeling

FDCs, $1x10^6$, were cultured in DMEM supplemented with 10% FCS on collagen type I for up to 30 days. Cultures were directly examined using a Nikon Bio-inverted microscope equipped with Nomarski optics and digital images were acquired. Thirty days old FDC cultures were labeled for FDC-M1 and ICs. Cultures were washed with PBS and incubated with FDC specific marker M-1 or OVA-rabbit-anti-OVA ICs for 2 hours. Cells were fixed in 0.9% glutraldehyde + 1% paraformaldehyde for 10 min and washed. Cells were then incubated for 45 mins with biotinylated mouse anti-rat-kappa light chain (MRK-1) followed by streptavidin-HRP, for FDC-M1 labeling, or HRP-conjugated goat anti-rabbit IgG, for IC labeling. Rat IgG isotype control for FDC-M1 and non-specific rabbit serum control for IC labeling were similarly treated. HRP was developed with DAB substrate and images were captured.

Scanning Electron Microscopy

Thirty days old FDC cultures on collagen type I were washed with PBS and fixed in 0.9% glutraldehyde + 1% paraformaldehyde (24). Small culture chips were prepared and examined with JSM-820 JEOL scanning electron microscope.

Immunohistochemical labeling of collagen type I and FDC-M1 in vivo

Popliteal LNs were collected 5 and 48 hours after footpad injection of 10 μg OVA in BALB/c mice passively immunized with rabbit anti-OVA IgG and frozen in CryoForm embedding medium (IEC, Needham Heights, MA). Frozen

sections of 10-μm thickness were cut on a Leica (Jung Frigocut 2800E) cryostat and air-dried. Following absolute acetone fixation, the sections were dehydrated and the endogenous peroxidase activity was quenched with PBS containing 0.1% phenylhydrazine-HCl (Sigma, St Louis, MO). The sections were washed and saturated with 10% BSA. Serial sections were incubated with unlabeled rabbit-anti-type I collagen or FDC specific marker M-1. Sections were washed and then incubated with biotin-conjugated goat anti-rabbit or biotinylated mouse anti-rat-kappa light chain (MRK-1) followed by streptavidin-HRP. The sections were developed with a DAB substrate kit (BD Pharmingen, CA) and images were captured using Optronics digital camera and Bioquant Nova software.

Flow Cytometry

Positively selected FDCs were incubated with purified mouse Fc-block (2.4G2) for 15 mins on ice followed by 30 mins incubation with FITC-conjugated mAb against CD29 (β_1), CD49b (α_2), CD49a (α_1), CD44 and isotype matched controls. Cells were washed thoroughly and analyzed by Beckman Coulter FC500 flow cytometer and Cytomics software.

Results

Assessment of FDC adhesion to extracellular matrices (ECM) components

After overnight incubation, 80 to 90% of FDCs on plastic and lymphocytes on collagen type I, laminin, biglycan or hyaluronic acid could be removed by washing indicating a lack of adherence (Data not shown) In marked contrast, 80% of cells in FDC preparations bound these extracellular matrices and remained fixed (Fig. 1).

Light microscopy of FDCs cultured on collagen type I

Many FDCs cultured on collagen type I started to spread out and acquired small processes within a week. Cell processes were visible within 14 days (Fig. 2a) forming occasional chains or interconnections between cells (Fig. 2b). By day 30, the cell bodies were spread out and most cells had very fine filiform processes that appeared to form networks through interdigitation of cell processes with neighboring cells (Fig. 2c).

Scanning electron microscopy of FDCs on collagen type I

To determine the nature of the FDC processes, scanning electron microscopy (SEM), was used to study thirty-day-old FDC cultures on collagen type I where numerous convolutions and branching of fine filiform dendrites were apparent (Fig. 3a, 3b, 3c). The dendrites often emanated from one pole of the cell body that was approximately 10-12 μm in diameter. Smaller dendrites appeared to help anchor the cell body to the collagen extended from the opposing parts of the cell body (Fig. 3c). Higher magnification showed dendrites

Figure 1: ***Adhesion of FDCs to extracellular substrates.*** Positively selected FDCs that expressed FDC-M1$^+$, CD40$^+$, CR1/2$^+$, and FcγRIIB$^+$ were incubated on plastic, collagen type I, laminin, biglycan, or hyaluronic acid. After 12 h, approximately 85% of FDCs on plastic could be removed by washing, whereas 85% of the FDCs bound to substrates remained attached

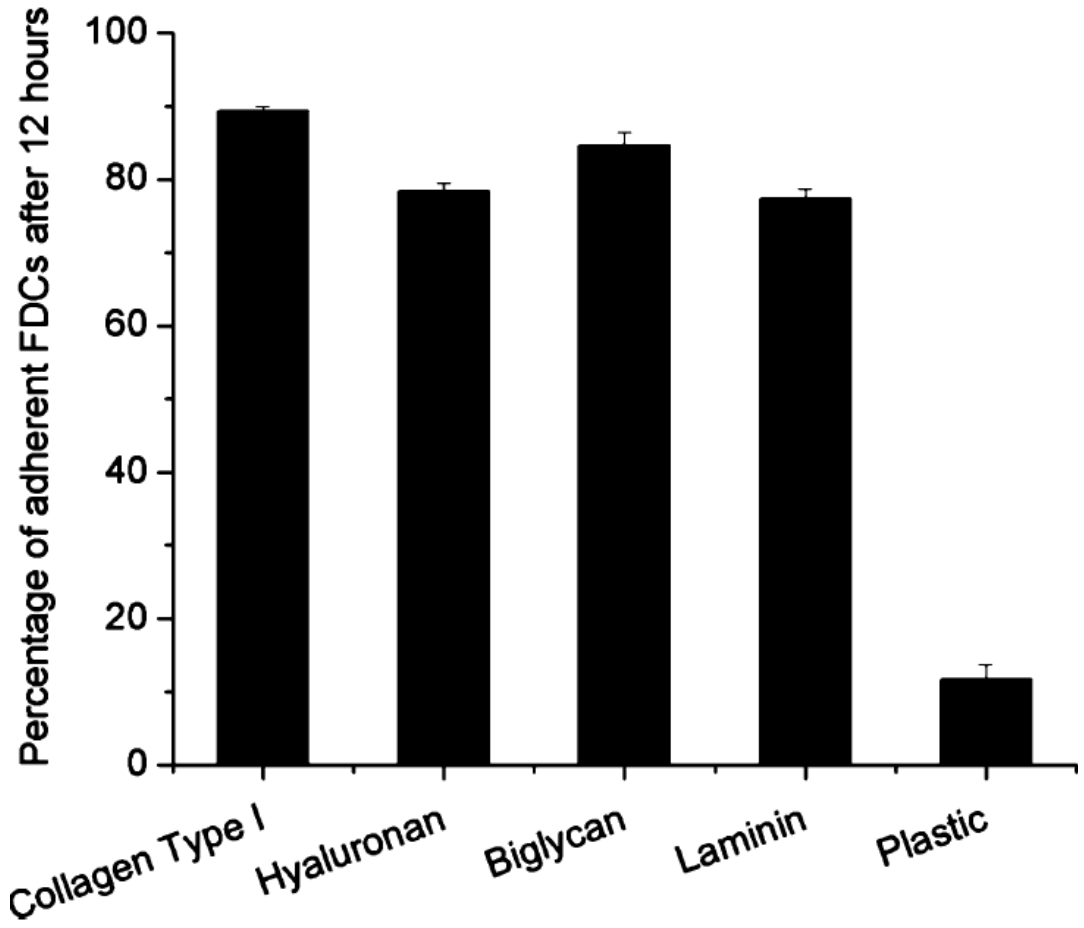
Percentage of adherent FDCs after 12 hours
100
80
60
40
20
0
Collagen Type I
Hyaluronan
Biglycan
Laminin
Plastic

Figure 2: ***Light microscopy of FDCs cultured on collagen type I.*** Purified FDC preparations were incubated on collagen type I for 30 days. Within the first 14 days, although many cells remained rounded, FDCs cultured on collagen type I started to spread out and acquire small processes (**a**) with occasional chains or interconnections (**b**). By day 30, most cells had extended long thin processes that formed networks by interdigitation with the processes from neighboring cells; the cell bodies had spread out (**c**)

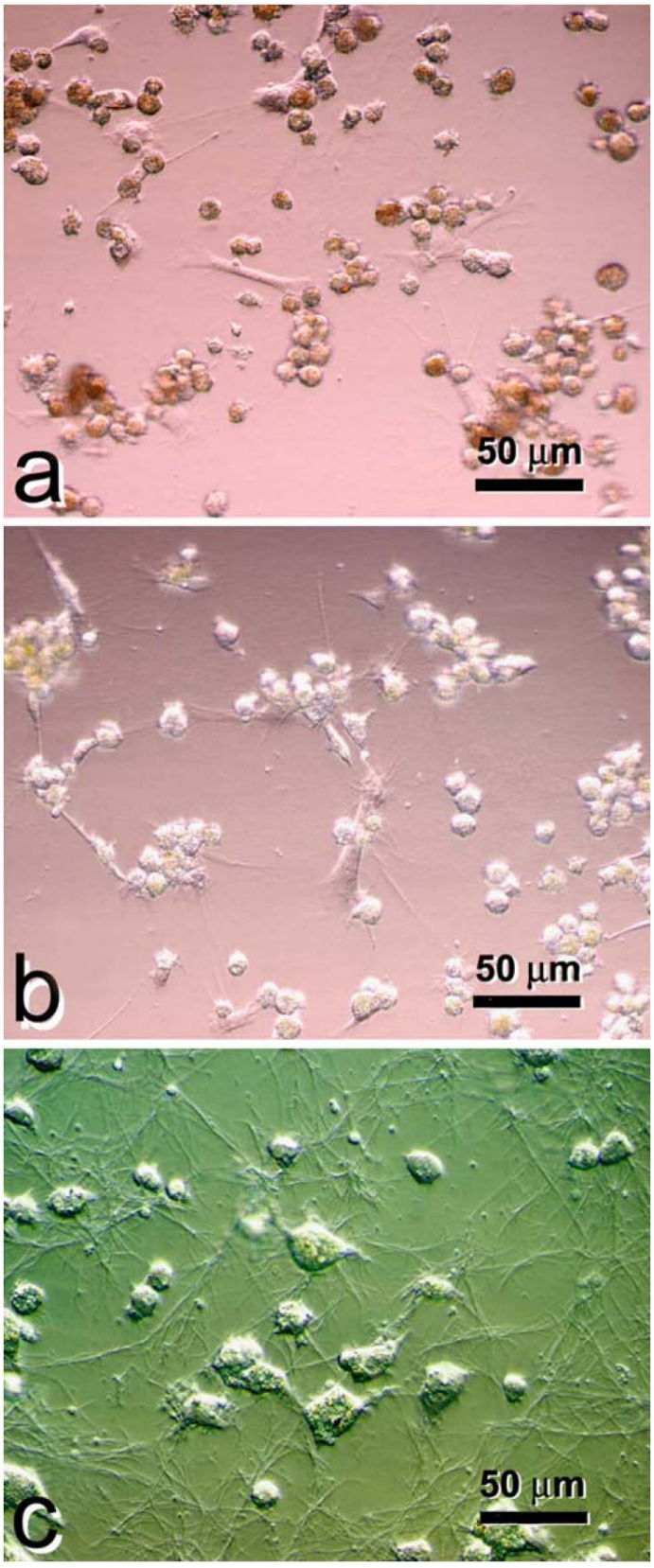
a
50 µm
b
50 µm
c
50 µm

Figure 3: ***Scanning electron microscopy (SEM) of FDCs on collagen type I showing dendritic regeneration.*** FDCs in 30-day-old cultures on collagen type I showed numerous convolutions and branchings of fine filliform dendrites (**a**–**c**). Cell processes emanated primarily from one pole of cell body (diameter of 10–12 μm) with some smaller dendrites helping to anchor the cell body to the collagen (**c**)

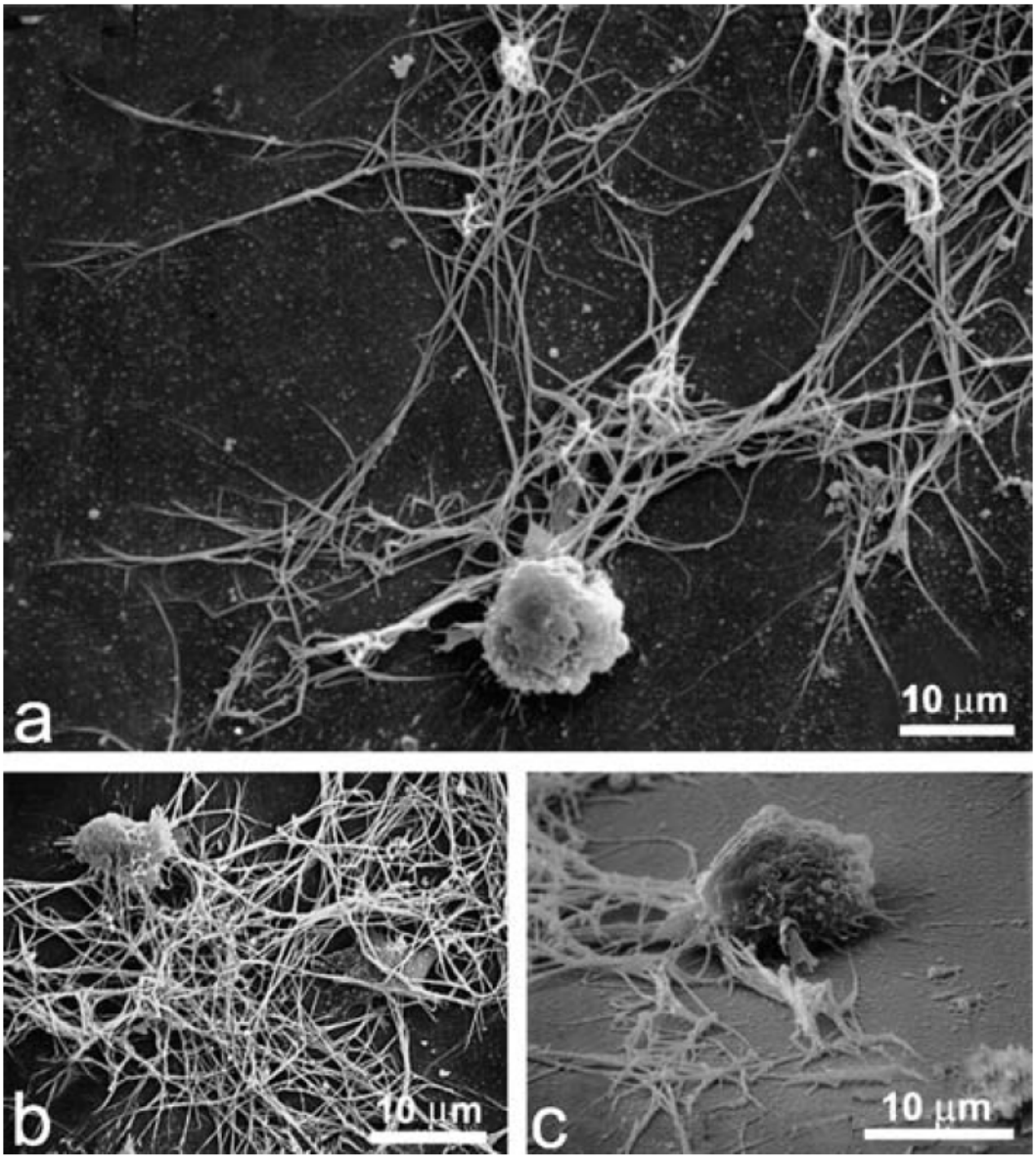
a
10 µm
b
10 µm
c
10 µm

emanating from one pole of an FDC and crossing over another cell body (Fig. 4a, 4b). Groups of 4-6 FDCs were seen forming networks much like those seen *in situ* (Fig. 5a, 5b, 5c).

Immunohistochemical labeling of FDC reticula for FDC-M1 and ICs

Functionally, active FDCs are characterized by the presence of FDC-M1 and the ability to trap ICs (130). Cultures of 30 day FDCs, with well developed dendrites and networks, labeled with the FDC-specific monoclonal Ab FDC-M1 (Fig. 6a) and were able to trap and retain OVA-anti-OVA ICs (Fig. 6c). Isotype controls for FDC-M1 (Fig. 6b) and ICs (Fig. 6d) lacked labeling.

Immunohistochemical labeling of collagen type I and FDC-M1 in vivo

The presence of reticular fibers interspersed between FDC dendrites was reported at the ultrastructural level at the periphery of the light zone (37). This prompted an examination of the localization of collagen type I in lymphoid follicles as related to germinal center FDCs. Five hours after footpad challenge with OVA in BALB/c mice passively immunized with rabbit anti OVA IgG, collagen type I abundantly co-localized with the specific FDC monoclonal antibody FDC-M1. However, two days later, collagen type I exhibited characteristic marginal distribution around the FDC-M1$^+$ area (Fig. 7).

Expression of CD29 and CD44 on FDCs

The rapid binding of FDCs to collagen prompted us to look for collagen binding receptors on FDCs. Flow cytometric analysis showed that approximately 85% of FDCs expressed CD29; the β1 integrin subunit shared by

collagen ($\alpha_{1,\ 2,\ 3,\ 9,\ 10,\ 11}\beta_1$), laminin ($\alpha_6\beta_1$) and fibronectin ($\alpha_4\beta_1$) receptors as well as the hyaluronic acid receptor CD44 (Fig. 8). CD29 and CD44 may, in part, mediate the interaction between FDCs and collagen type I and its associated molecules. However, FDCs treated with mAbs against these molecules still bound collagen type I without difficulty (Data not shown). Expression of α_1/CD49a and α_2/CD49b integrins were not detectable in significant amounts on freshly isolated FDCs (Fig. 8).

Figure 4*:* ***Origin of dendrites at higher magnification; SEM.*** The developed dendrites clearly emanate from one pole of the FDC (**b**). Some dendrites cross over other cell bodies (**a**)

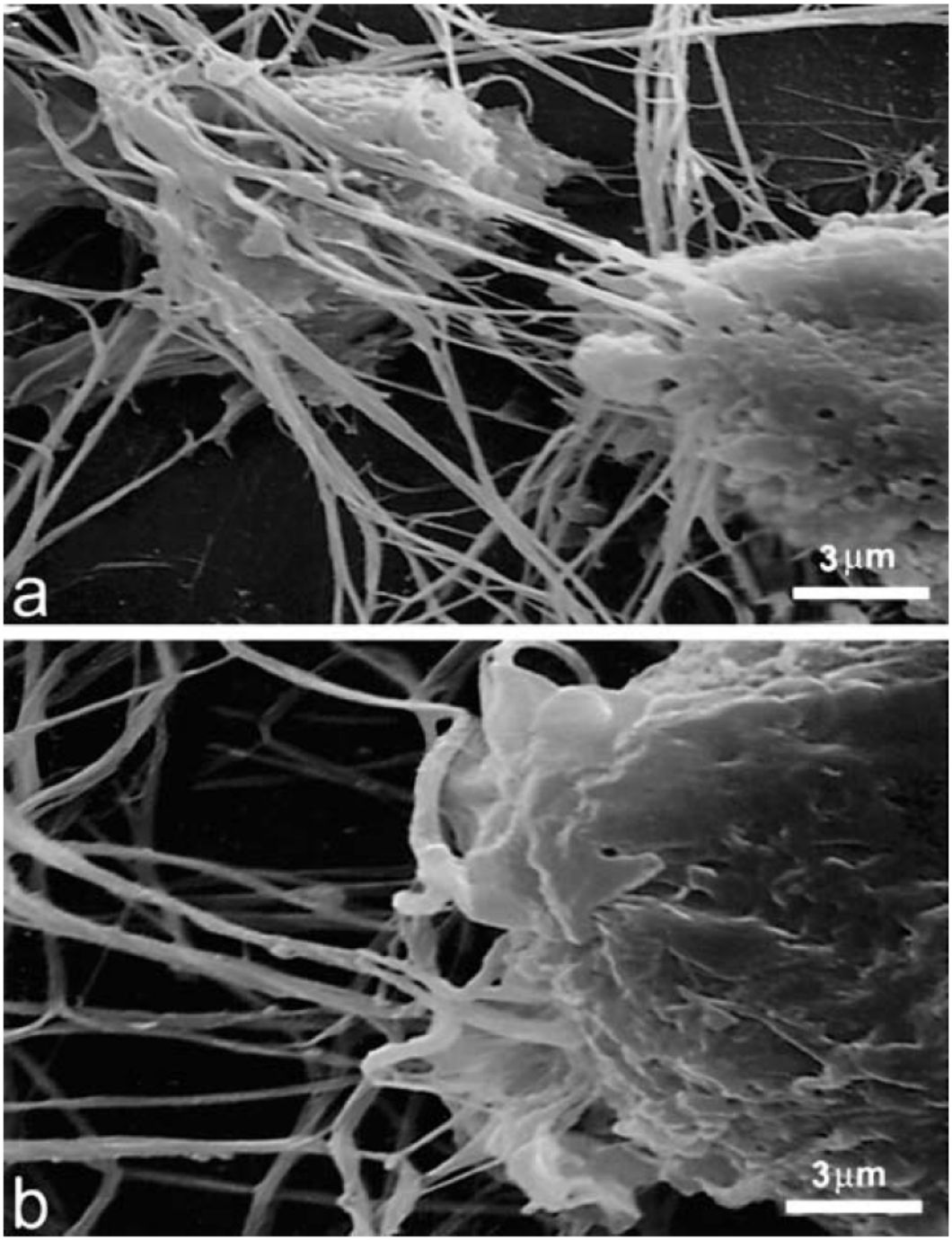
a
3μm
b
3μm

Figure 5: ***Groups of 4–6 FDCs on collagen type I showing the formation of networks (or reticula);*** SEM (**a**–**c**)

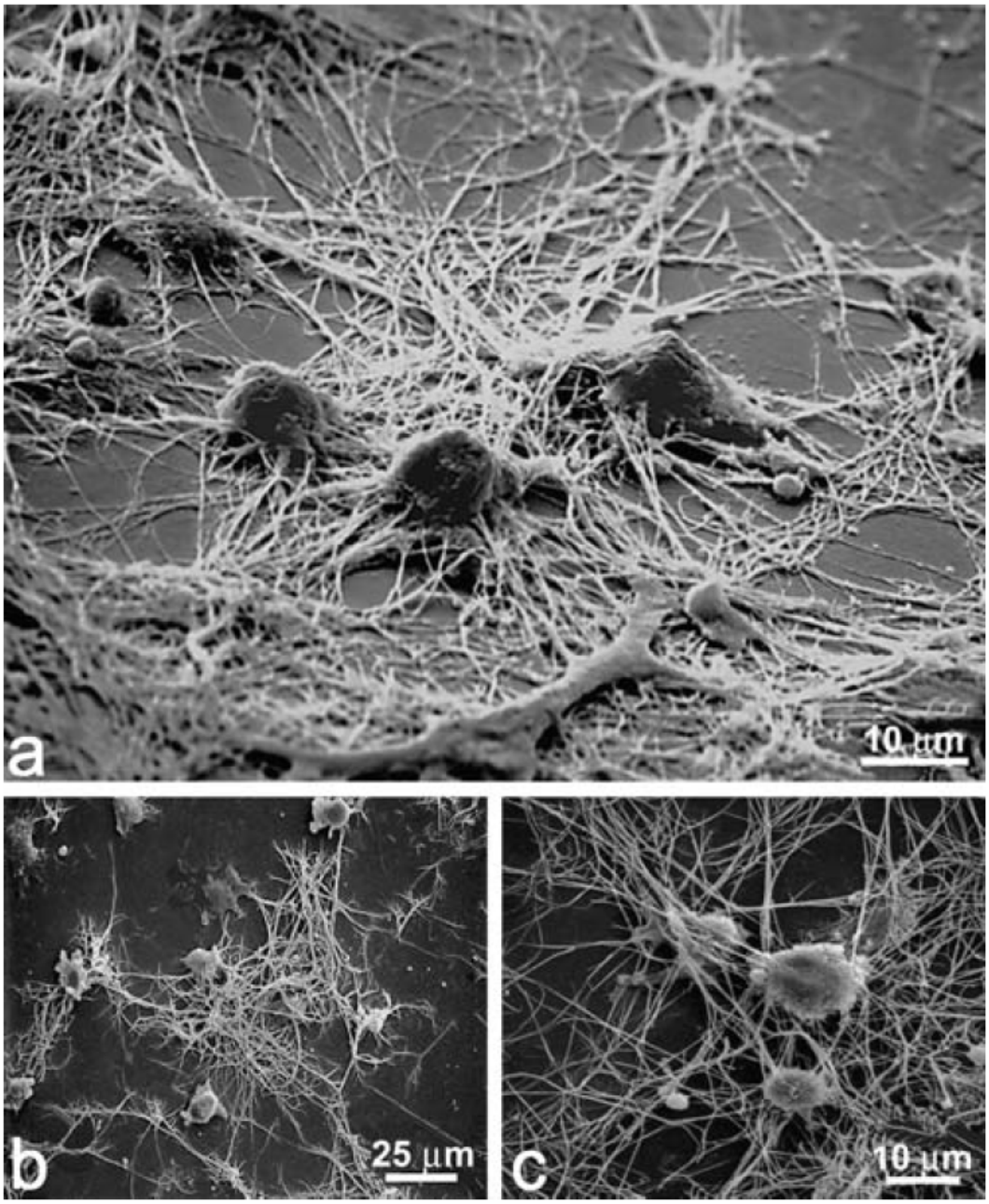
a
10 µm
b
25 µm
c
10 µm

Figure 6: ***Immunohistochemical labeling of FDC reticula with FDC-M1 and ICs.*** The FDCs in cultures maintained for 30 days on collagen type I were heavily labeled with the FDC-specific mAb FDC-M1 (**a**) and retained rabbit OVA-anti-OVA ICs as indicated by labeling with goat-anti-rabbit IgG (**c**); HRP/development with DAB. No labeling was observed in isotype controls for FDC-M1 (**b**) and ICs (**d**); Nomarski optics

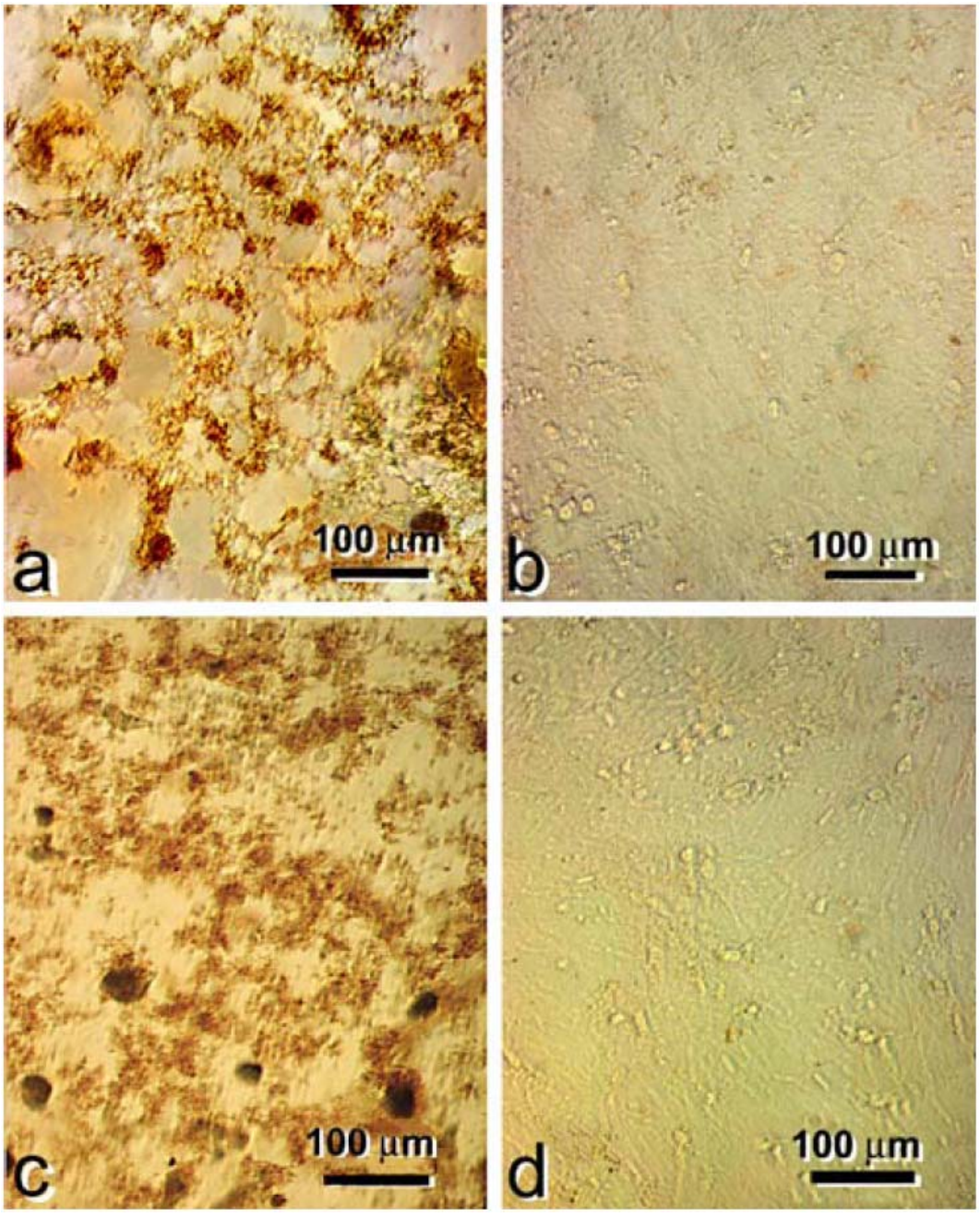
a
100 µm
b
100 µm
c
100 µm
d
100 µm

Figure 7: ***Immunohistochemical labeling for collagen type I and FDC-M1.*** Adjacent frozen sections from popliteal lymph nodes were labeled for collagen type I (**a**, **c**) and FDC-M1 (**b**, **d**) 5 h (**a**, **b**) and 2 days (**c**, **d**) after challenge with OVA in OVA immune BALB/c. Sections were incubated with unlabeled rabbit anti type I collagen or FDC-M1. Biotinylated goat anti-rabbit or biotin-mouse anti-rat-κ was applied followed by streptavidin-HRP. The sections were developed with DAB substrate. Fibers labeled with anti-collagen type I were seen co-localizing with FDC-M1 at 5 h (*arrows*). After 2 days, the distribution of collagen type I was restricted to the periphery of the follicle labeled for FDC-M1 (*arrows*)

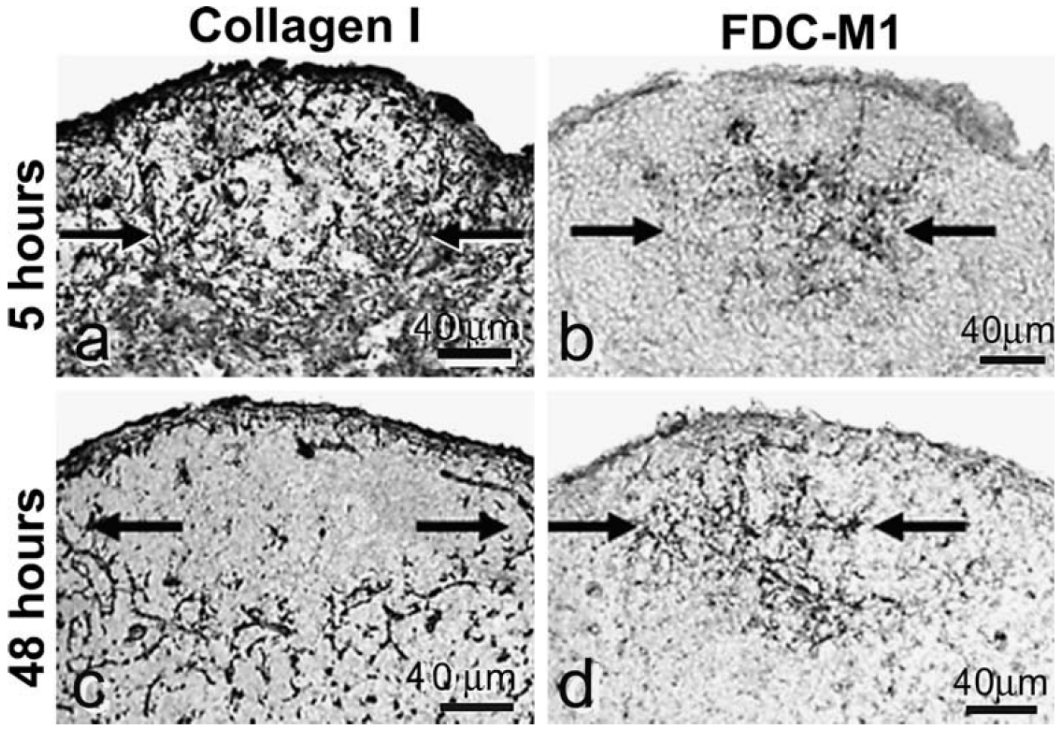
Collagen I
FDC-M1
5 hours
48 hours
a
b
c
d
40µm
40µm
40µm
40µm

Figure 8: ***Expression of CD29 and CD44 on FDCs.*** Purified FDCs preparations were incubated with FITC-conjugated mAb against CD29 (β_1; **a**), CD44 (**b**), CD49a (α_1; **c**), CD49b (α_2; **d**), and isotype-matched controls (*gray lines* unlabeled FDCs, *dotted lines* isotype controls). Flow cytometric analysis showed that approximately 85% of FDCs expressed CD29 (the β_1 integrin subunit) and the hyaluronic acid receptor, CD44

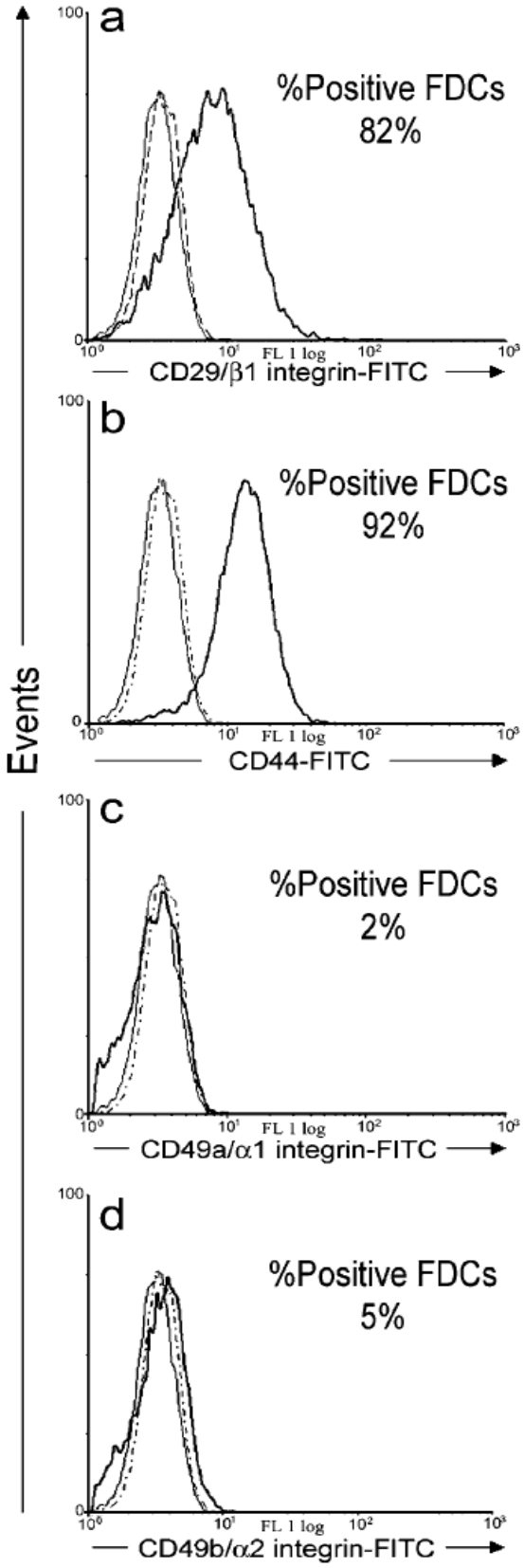
a
%Positive FDCs
82%
CD29/β1 integrin-FITC
b
%Positive FDCs
92%
CD44-FITC
c
%Positive FDCs
2%
CD49a/α1 integrin-FITC
d
%Positive FDCs
5%
CD49b/α2 integrin-FITC
Events
FL 1 log

Discussion

The move from *in vivo* to *in vitro* assessment of FDC biology is important given that cells *in vitro* are more readily amenable to manipulation. However, dendrites represent a cardinal morphological feature of FDCs and this morphology and the associated networks are largely lost when FDCs are isolated (42). Moreover, the more *in vitro* manipulations are introduced, the less the dendritic morphology is apparent (130). Nevertheless, isolated FDCs did have accessory activity *in vitro* and dendritic morphology is identifiable at the electron microscopy level but it has been impossible to regenerate the extensive processes and networks to study the importance of these structures *in vitro*. The fact that FDCs are fixed in GCs supported by reticular fibers and that enzymatic digestion with collagenase was required to release them from their *in vivo* environment prompted the hypothesis that modeling a supporting substrate *in vitro* might stimulate reattachment of isolated FDCs and promote regeneration of dendritic processes and networks. We report here that FDCs have a remarkable ability to bind to collagen type I and reestablish extensive dendrites and networks. Structure typically promotes function and the ability to regenerate extensive dendrites and FDC-networks on collagen type I offers a new opportunity to study how FDC structures relate to function.

We reasoned that if FDCs were influenced by collagen or collagen-associated molecules, then an attachment step would be necessary. To test this, positively selected FDCs were incubated on purified collagen type I, laminin,

biglycan or hyaluronic acid and left for twelve hours. The vast majority of viable FDCs adhered to these matrices. The ability to firmly bind all these matrices may help explain why these cells are fixed and do not migrate *in vivo*. Comparison of FDCs incubated on different substrates indicated that collagen type I exerted the most influence on FDC morphology. Accordingly, we incubated FDCs on type I collagen for 30 days and cultures were examined to verify formation of dendrites and reticula. FDCs survived throughout the culture period without signs of apoptosis or proliferation which is consistent with the reports of long term culture of murine FDCs up to 8 weeks (115) and human FDCs up to 150 days (172). In the first week cells started to spread out and begin to acquire processes with occasional interconnections. However, by day 30, most cells had fine processes that formed networks through interdigitation of cell processes with neighboring cells. *In vivo* FDCs trap ICs and form interconnecting networks or reticula. Studies with labeled Ag indicate that Ag-bearing ICs remain localized to FDC-networks in lymph nodes draining the site of Ag injection. For example, Donaldson et al (173) reported that antigen retaining networks remained localized to lymph nodes draining the injection site one year after Ag challenge. Similarly, FDCs *in vitro* resisted washing off the supporting matrices and on collagen type 1 they formed networks that could only be mobilized by collagenase treatment.

FDC-M1 is a marker for FDCs and IC trapping and retention is characteristic of FDCs (69,130). To confirm the identity of the cells, 30-day

cultures were labeled with FDC-M1 or ICs. Both, FDC-M1 and ICs, intensely labeled FDC processes and IC binding and surface retention established this FDC function.

We reasoned that a receptor-mediated mechanism was likely involved in attaching FDCs to collagen and in signaling formation of dendrites and reticula. Flow cytometric analysis indicated that FDCs express CD29; the β1 integrin subunit shared by collagen ($\alpha_{1,\ 2,\ 3,\ 9,\ 10,\ 11}\beta_1$), laminin ($\alpha_6\beta_1$) and fibronectin ($\alpha_4\beta_1$) receptors as well as the hyaluronic acid receptor CD44. However, blocking these molecules did not prevent FDCs from binding collagen type I suggesting there are additional receptors involved.

Scanning Electron Microscopy was used to study the ultrasturcture of dendrites and to make sure the processes emanated from cells and were not fibers formed in the collagen. SEM revealed FDCs organized in groups, ranging between 4 to 6, forming reticular structures with interconnecting dendrites. Dendrites emanated from the cell bodies and some were seen extending from one pole of an FDC over the cell body of another FDC. Characteristically, FDC dendrites exhibit numerous branches and convolutions, often there is polarity regarding the cell body, and processes *in vivo* may be found attached to collagen fibers (37,42). All of these features were apparent with FDCs on collagen type I.

Besides their structural role, collagens, especially type I collagen which is the most abundant collagen type, help define functional properties of tissues (174). Hyaluronic acid binds cells via CD44 and is widely distributed in the

body. FDC-CD44 may play a role in mechanisms leading to dendrite regeneration and network formation seen here since proteoglycan-associated hyaluronic acid is seen in rat tail collagen (175). The receptor CD44 has been implicated in a number of cellular functions such as adhesion, growth, differentiation, and apoptosis (176). Recently, it has been demonstrated that both 8D6 and CD44 expressed on FDCs mediate their antiapoptotic activity that helps maintain lymphomas *in vivo* (65).

Collagen type I has been found to enhance activation and dendrite formation in other cells. The ability of collagen type I to provoke phenotypic changes associated with activation has been described in DCs including GM-CSF-propagated liver DCs (177) and monocyte-derived DCs (178). In addition, network formation and angiogenic stimulation has been described in endothelial cells when cultured on type I collagen (179). Moreover, neurons seeded on collagen gels regenerated neurites that appear to correspond to axons and dendrites (180).

The characteristic dislocation of collagen type I fibers to the periphery of active follicles two days after antigenic challenge agrees with a similar observation in reactive human tonsils (181). However, neither the paucity of collagen type I associated with FDCs two days after antigenic challenge *in vivo*, nor the ultrastructure of FDC dendrites and networks on the collagenous matrix *in vitro*, support the concept that FDCs produce type I collagen in their processes favoring a fibroblastic origin (182). In short, the data presented here

indicate that purified FDCs express CD29 and CD44 and are able to regenerate their dendritic networks *in vitro* when cultured on collagen type I. We are looking forward to functional studies comparing the activity of free-floating FDCs with FDCs in networks with interest.

CHAPTER 4

IL-6 produced by immune complex-activated follicular dendritic cells promotes germinal center reactions, IgG responses, and somatic hypermutation

Introduction

Follicular dendritic cells (FDCs) are prominent in GCs because their numerous long slender dendrites intertwine and create extensive FDC-networks or -reticula. These FDC-networks are fixed in the follicles while T and B cells are free to circulate. Nevertheless, FDCs release chemokines that attract recirculating lymphocytes that help organize the follicle and participate in the GC reaction (66,183). FDCs, bearing specific Ag in the form of ICs, are requisite for full development of GCs (38,46,69) and interaction of FDCs with ICs leads to activation and the expression of high levels of FDC-FcγRIIB, -ICAM-1 and -VCAM-1 (70). FDC-ICs also deliver a late antigenic signal that promotes SHM (35). Important events include: 1) induction of specific Ab that binds immunogen and forms ICs, 2) IC trapping by FDCs, 3) GC B cell stimulation by Ag in these FDC-ICs, and 4) promotion of SHM by this late second Ag signal delivered by IC-bearing FDCs (35). However, FDCs provide signals, beyond specific Ag, that promote B cell maturation and we sought to determine if FDC-IL-6 promotes SHM.

Interleukin-6, known in the early literature as B-cell stimulatory factor (BSF-2), is recognized for its role in regulating terminal B cell differentiation (Reviewed in (184)). Somatic hypermutation (SHM) is a major events in terminal B cell differentiation that occurs in germinal centers (GCs) in the second wk after primary immunization (Reviewed in (185-188)). It has also been reported that murine FDCs are the source of IL-6 in GCs (68) and that ICs

activate FDCs (70). This prompted the hypothesis that IC-activated FDCs produce elevated levels of IL-6 and that FDC-derived IL-6 is important not only for optimal Ab responses but also for GC reactions and SHM. We postulated that elevated production of IL-6 by IC activated FDCs, one to two wks after primary immunization, would correlate with enhanced GC reactions, IgG responses, and SHM.

While there are numerous reports supporting the hypothesis that FDCs produce IL-6 (189-192), there are also studies reporting the inability to detect IL-6 in FDCs (193-195). To further test the hypothesis that FDCs produce IL-6 and that IC-activated FDCs produce elevated levels of IL-6, ICs were added to purified FDCs and 2 to 6 days later IL-6 production had clearly increased. Specific Ab is induced 4-7 days after primary immunization and IC formation would follow soon thereafter. Thus, 6 to 13 days after immunization a burst in FDC-IL-6 production would be expected in developing GCs. To test the postulate that IL-6 promotes GC reactions, specific IgG responses, and SHM; these responses were studied in IL-6 KO mice and in GC reactions *in vitro* where IL-6 was specifically inhibited by anti-IL-6. The present study, including both *in vivo* and *in vitro* experiments, confirms earlier results indicating, that optimal GC reactions and IgG anti-NIP responses require IL-6 and that FDCs are the only cells in GC reactions making IL-6 (68). In addition, we found that IL-6 was not detectable in *in vitro* GC reactions with IL-6 KO FDCs with T & B cells from WT mice. In contrast, IL-6 production was normal in GC reactions

with WT FDCs with T and B cells from IL-6 KO mice. The absence of IL-6 in cultures lacking WT FDCs resulted in marked reduction in the rate of SHM that coincided with the reduction in specific anti-NIP. Moreover, GCs were abundant in irradiated WT mice reconstituted with spleen cells from IL-6 KO mice while GCs were virtually undetectable in irradiated IL-6 KO mice reconstituted with normal spleen cells. These data provide strong support for the physiological relevance of FDC-IL-6 in GC reactions *in vitro* and *in vivo* and report for the first time that FDC-IL-6 is inducible by ICs and is involved not only in influencing the amount but also the mutations that are known to enhance the affinity of specific IgG produced.

Material and Methods

Mice, Ag and immunization

Six to 8 wk old C57BL/6 mice were purchased from the National Cancer Institute and female IL-6 KO mice (B6.129S2-116tm1Kopf/J) of the same age were obtained from the Jackson Laboratory. The mice were housed in standard shoebox cages and given food and water *ad libitum*. Animals were handled in compliance with Virginia Commonwealth University Institutional Animal Care and Use Committee guidelines. Mice were immunized by injecting 0.25 or 25 μg of alum precipitated $(NP)_{36}$-CGG with ~1.5 x 10^7 heat killed *Bordetella pertussis* s.c. in each front leg and hind foot in a 50 μl volume to give a total of 1 μg or 100 μg of $(NP)_{36}$-CGG /animal. Fourteen days later these mice were bled, serum collected, and draining lymph nodes from each group were pooled to isolate λ^+ B cells for extracting RNA. The serum was used to determine NIP-specific Ab levels and the RNA was used to determine mutations per 1000 bases in the VH186.2 gene segment. *In vitro* GC reactions were set up using memory T cells specific for CGG [$T_{(CGG)}$ cells] isolated from mice one month after immunization with 100 μg CGG as described above. To get NP specific λ B cells, WT or IL-6 KO mice were immunized with 100 μg $(NP)_{36}$-CGG plus heat killed *Bordetella Pertusis* as explained above and the λ B cells were isolated 6 days later.

Establishment of IL-6 KO / WT chimeras, immunization, and immunohistochemistry

Two days after irradiation with 600 rads, IL-6 KO (B6.129S2-116tm1Kopf/J) mice were reconstituted with 10^8 WT or IL-6 KO splenocytes injected SC behind the neck. Similarly, WT C57B/6 mice were reconstituted with 10^8 IL-6 KO or WT splenocytes and 48 hrs later, mice were immunized with 1 μg $(NP)_{36}$-CGG /animal. Fourteen days later these mice were bled, sacrificed, and the spleens were frozen in OCT medium. Sera were used for determination of the anti-NIP levels, and 10 μm cryostat spleen sections were prepared and fixed in absolute acetone. The midsaggital spleen sections were labeled for GC B cells with FITC-conjugated anti-B cell activation marker GL-7, and for the FDC-ICs with Rhodamine-Red-X anti-mouse IgG. Resting B cells were labeled with PerCP-Cy5.5 anti mouse B220 and the number of GL-7^+ GCs were counted in the midsaggital spleen sections.

Antibodies and Reagents

Functional grade, Azide free, sterile-filtered, purified anti-mouse Interleukin-6 (Cat# 16-7061, Clone MP5-20F3) and rat IgG isotype control Ab were obtained from eBioscience. Rat anti-mouse FDC (FDC-M1), biotin mouse anti-rat kappa (MRK-1), anti-mouse CD21/CD35 (Clone 7G6) and anti mouse CD32/CD16 (Clone 2.4G2) were purchased from Pharmingen (San Diego, CA). Mouse CD45R (B220) MicroBeads, mouse CD90 (Thy1.2) MicroBeads, anti-Biotin MicroBeads, and MACS LS columns were purchased from Miltenyi

Biotec GmbH (Auburn, CA). Biotin labeled rat anti-mouse kappa was purchased from Zymed (San Francisco, CA). Alkaline phosphatase labeled goat anti-mouse IgG (H+L) and P-Nitrophenylphosphate substrate were obtained from Kirkegaard & Perry Laboratories (Gaithersburg, MD). NIP-OVA (4-hydroxy-3-ioda-5-nitrophenylacetyl conjugated to ovalbumin) and $(NP)_{36}$-CGG were obtained from Biosearch Technologies (Novata, CA). Anti-CGG was obtained from hyperimmunized mice with serum anti-CGG IgG levels in excess of 1 mg/ml.

FDCs isolation, activation with ICs in vitro, and assessment of IL-6 production

FDCs were isolated as described previously (130). Briefly, lymph nodes from lethally irradiated mice were gently digested and the cell suspension incubated with rat anti-mouse FDC-M1, biotin-mouse anti-rat kappa (Clone MRK-1) and anti-biotin magnetic microbeads sequentially. Finally the FDCs were positively selected using a magnetic column (MACS). Approximately 85 to 95% of these cells expressed the FDC phenotype, FDC-$M1^+$, $CD32^+$, $CD21/35^+$, $CD40^+$ and $ICAM^+$ (130). Purified FDCs were activated by incubating $1x10^6$ cells with 100 ng/ml OVA-ICs made of OVA/rabbit-anti-OVA at a ratio of 1:6. Four independent experiments with triplicates of IC-stimulated FDCs were set up and culture supernatant fluids were sampled after 2, 4, and 6 days. In some experiments, culture supernatant fluids were collected after 3, 6, and 10 days. Controls of B220 purified B cells, Thy1.2 purified T cells, IL-6 KO

FDCs, WT B and T cells, WT B and T cells with IL-6 KO FDCs with or without ICs, WT FDCs incubated with IL-6 KO B and T cells with or without ICs, WT FDCs incubated with soluble 100 ng/ml OVA, WT FDCs pretreated with 10 μg/ml azide-free FcγR or CR blockers (mAb 2.4G2, and 7G6 respectively) or their isotype controls prior to IC loading and low Tox complement were included. IL-6 levels in the fluids were assessed using a Bio-Plex Mouse IL-6 assay (Bio-Rad, Hercules, CA, 171-G10738), data were collected on a Bio-Plex array reader (# LX10004042104), and analyzed using Bio-Plex Manager Software 4.1.

Isolation of lambda light chain positive B cells (λ^+ B cells) and memory $T_{(CGG)}$ cells

Single cell suspensions were prepared from draining lymph nodes after priming with $(NP)_{36}$-CGG or CGG as explained above. After depleting kappa light chain positive B cells with biotin-anti-κ and anti-biotin microbeads with a MACS column, the persisting λ^+ B cells were isolated with anti-B220 microbeads using a MACS column. The isolated λ^+ B cells were more than 98% pure. Memory $T_{(CGG)}$ cells from CGG primed mice were incubated with 40μl of anti-CD90.2 microbeads and the T cells were positively selected using a MACS column.

In vitro GC reactions and the anti-NIP Ab Response

GC reactions were initiated *in vitro* by culturing 1 x 10^6 unmutated but 6 day primed λ B cells, 0.5 x 10^6 T cells, and 0.5 x 10^6 FDCs in the presence of 100ng of $(NP)_{36}$-CGG as free Ag or in ICs. The ICs were made by incubating

NP-CGG with anti-CGG at a ratio of 6 ngs/ml anti-CGG to 1 ng of NP-CGG for two h and then adding IC containing 100 ng NP-CGG to appropriate wells in 24-well culture plates. Supernatant fluids were harvested 7 days later and were assayed for NIP-specific IgG Ab by ELISA using NIP-OVA to coat the plate.

Analysis of mutations in the V region

Anti-NP Igs predominantly use the VH186.2 gene (14,196) and it was analyzed in this study. Cells were collected on Day 7 of culture and RNA was isolated using Trizol (Invitrogen, Carlsbad, CA). The RNA was then reverse transcribed to cDNA with GeneAmp gold RNA PCR Core kit (PE Biosystems, Foster city, CA) using oligo dt. The VH186.2 gene followed by D and J regions and a proximal segment of the C gamma gene segment was amplified by two rounds of nested PCR with high fidelity Pfu-Ultra DNA polymerase (Stratagene, La Jolla, CA). The forward and reverse primers for the first round PCR, were 5'-catgctcttcttggcagcaacagc-3' and 5'-gtgcacaccgctggacagggatcc-3', for second round PCR, 5'- caggtccaactgcagccag-3' and 5'-agtttgggcagcaga-3. The PCR reaction was carried out as follows: 95°C 1 min, 56°C 1 min, 72°C 1 min for 30 cycles followed by 72°C for 10 min. The expected 400bp PCR product was then electrophoresed on 1.2% agarose gel, purified by gel extraction using QIAQuick kit (Qiagen, Valencia, CA) and cloned using Zero Blunt® TOPO PCR Cloning Kit (Invitrogen, Carlsbad, CA). The plasmids were transformed into one shot TOP10 chemically competent cells (Invitrogen, Carlsbad, CA) and plated onto LB media containing 50μg/ml ampicillin. Multiple discrete colonies were

picked the following day and grown for 24 hours in LB broth containing 50μg/ml ampicilin in a 37°C shaker. The plasmids were isolated using a QIAprep Spin miniprep kit (Qiagen, Valencia, CA) and the insert was sequenced using an ABI sequencer. The sequences were analyzed using GCG Wisconsin Package (Accelrys, San Diego, CA), clustalW (197,198) and BioEDIT (http://www.mbio.ncsu.edu/BioEdit/bioedit.html) software packages. Redundant sequences were excluded from our calculation of mutations per 1000 bases to avoid multiplying the effect of a single mutation. To avoid including N terminal additions, changes within 5 bases of the V-D junction were also excluded from our calculations of mutations per 1000 bases.

Immunofluorescence and confocal microscopy

Draining lymph nodes (popliteal brachial and axillary) were harvested from WT or IL-6 KO mice 14 days after immunizing with 1 ug of $(NP)_{36}$-CGG and frozen on dry ice in Optimum Temperature Compound (Tissue-Tec, Torrance, CA). Serial 10μ thin sections were cut from the frozen blocks using a Jung Frigocut 2800E Cryostat, fixed in absolute acetone, and air-dried. The sections were blocked with 10% BSA in PBS and then washed and incubated for 1 h with 2 μg/ml FITC-conjugated anti-GL7 and Cy5.5-conjugated anti-B220 (BD Pharmingen, San Diego, CA). Sections were washed, mounted with anti-fade mounting medium, Vectashield, cover-slipped, and examined with a Leica TCS-SP2 AOBS confocal laser scanning microscope fitted with an oil plan-Apochromat 40X objective. Two lasers were used, Argon (488 nm) for FITC,

and HeNe (633nm) for Cy5.5 (shown as pseudo-color magenta). Parameters were adjusted to scan at 512 X 512 pixel density and 8-bit pixel depth. Emissions were recorded in 2 separate channels. Digital images were captured, overlaid and processed with Leica Confocal and LCS Lite softwares. BIOQUANT NOVA Advanced Image Analysis software (R&M Biometrics, Nashville, TN) was used to analyze the immunohistochemistry as described previously (58). After setting an arbitrary threshold, the system allowed us to determine number, position, area, and density of labeling that best defined FDC-reticula. This predefined threshold was used throughout to enable reliable comparisons.

Statistical Analysis

The number of mutations per sequence was compared using a Poisson regression analysis (SAS Proc Genmod version 9.1, SAS Institute Inc.) An offset of log(306) was used to normalize the fitted group means to the number of nucleotides. Significant chi-square values for SHM data were determined at $p < 0.05$. Analysis of IL-6 production, GC numbers, area, and IgG production were done using a two tailed Student's T test and significance was accepted at $p < 0.05$.

Results

FDC derived IL-6 and activation via IC-FcR interaction enhanced FDC-IL-6

To begin testing the hypothesis that FDCs produce IL-6 and that IC-activated FDCs produce elevated levels of IL-6, ICs were added to purified FDCs or to purified FDCs with T and B cells. As shown in figure 1, all cultures containing WT FDCs produced IL-6 at all time points, 3, 6, and 10 days. Moreover, IL-6 production was enhanced by IC-mediated FDC activation. In marked contrast, cultures of WT B cells and T cells, separately or in combination with IL-6 KO FDCs, did not produce detectable levels of IL-6 even when ICs were added. FDCs isolated from normal mice with FDC-M1 have detectable levels of ICs on their surfaces but are capable of trapping more IC (130) and of being further activated *in vitro* via engagement of FcγRIIB (71). To further examine the need for ICs and FcγRs, FDCs were isolated from normal animals, ICs were added as an *in vitro* activation signal, and supernatant fluids were collected on days 2, 4, and 6 (Figure 2). IL-6 was apparent in the control lacking added ICs and it continued to accumulate over the 6-day period. FDCs may constitutively express IL-6 or this background IL-6 response may occur as a consequence of FDCs encountering ICs *in vivo*. In any case, addition of ICs enhanced FDC-IL-6 production within 48 hrs ($p<0.0001$) and IL-6 production continued to increase over the 6 day period. Inhibition of IC trapping *via* FcγR with the FcR blocker (mAb clone 2.4G2) significantly inhibited FDC-IL-6 production whereas the isotype control had no inhibitory effect. Moreover, addition of soluble Ag (OVA) to the FDCs, rather than OVA in ICs did not stimulate IL-6 production above background. We did not see enhancement of FDC-IL-6 production by the

Figure 1: ***FDCs but not B or T cells produce IL-6 and its production is enhanced by ICs.*** WT FDCs incubated with IL-6 KO B and T cells with or without ICs together with controls of WT B cells, T cells, IL-6 KO FDCs, WT B and T cells, WT B and T cells with IL-6 KO FDCs with or without ICs were set up and culture supernatant fluids were sampled after 3, 6, and 10 days. IL-6 levels were assessed with Bioplex. All cultures containing WT FDCs produced IL-6 at all time points, 3, 6, and 10 days, and IL-6 production was enhanced by activating FDCs with ICs. In marked contrast, cultures of WT B cells and T cells, separately or in addition to IL-6 KO FDCs, in the presence or absence of ICs did not produce detectable levels of IL-6 at any time point. Data are representative of the mean of one of four independent experiments with triplicates + SD.

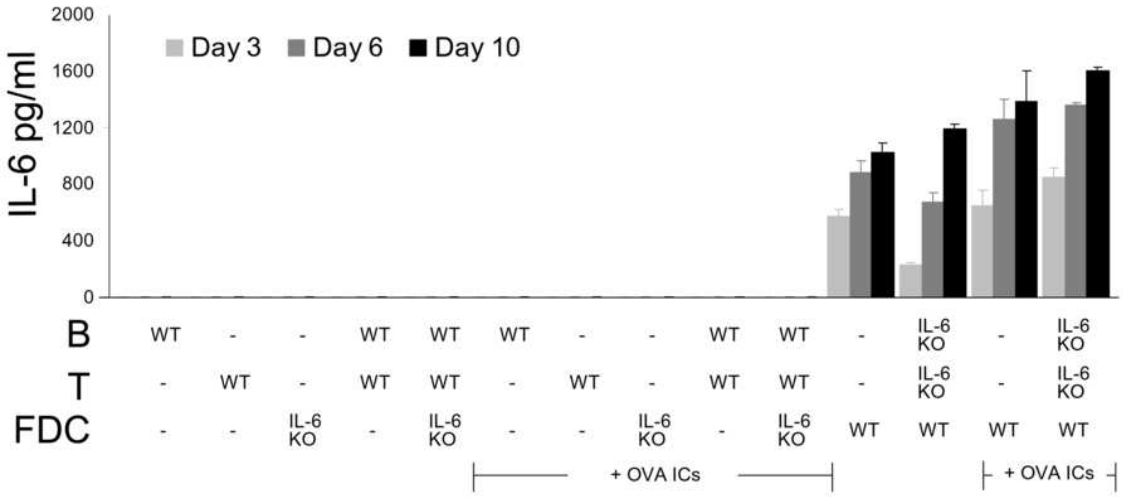
IL-6 pg/ml
2000
1600
1200
800
400
0
Day 3
Day 6
Day 10
B
T
FDC
WT
-
IL-6 KO
+ OVA ICs
+ OVA ICs

Figure 2: ***ICs induce FDC-IL-6 production by engaging FDC-FcγRs. Purified WT FDCs were activated by incubating 1x106 FDCs with 100 ng/ml OVA-ICs made of OVA/rabbit-anti- OVA at a ratio of 1:6.*** Controls of WT FDCs incubated with soluble 100 ng/ml OVA, and WT FDCs pretreated with 10 μg/ml azide-free FcγR (mAb 2.4G2) or its isotype control prior to IC loading were included. IL-6 levels in the fluids were assessed using a Bio-Plex Mouse IL-6 assay after 2, 4, and 6 days. As shown, ICs enhanced FDC-IL-6 production within 48 hrs ($p<0.0001$). The IL-6 surge apparent at day 6 after IC loading, precedes the late phases of the GC reaction (starting day 9-10 after primary challenge) when the presence of IL-6 appears to promote somatic hypermutation. Inhibiting IC trapping via FcγRs with the FcR blocker (mAb clone 2.4G2) significantly inhibited FDC-IL-6 production whereas the isotype control had no inhibitory effect. Moreover, addition of soluble Ag (OVA) to the FDCs did not stimulate IL-6 production above background. We did not see enhanced FDC-IL-6 production by the addition of low Tox complement and complement receptors do not activate FDCs whereas engagement of FcγRIIB does (6). Data represent the mean of triplicate cultures + SD and the results are representative of four independent experiments of this type

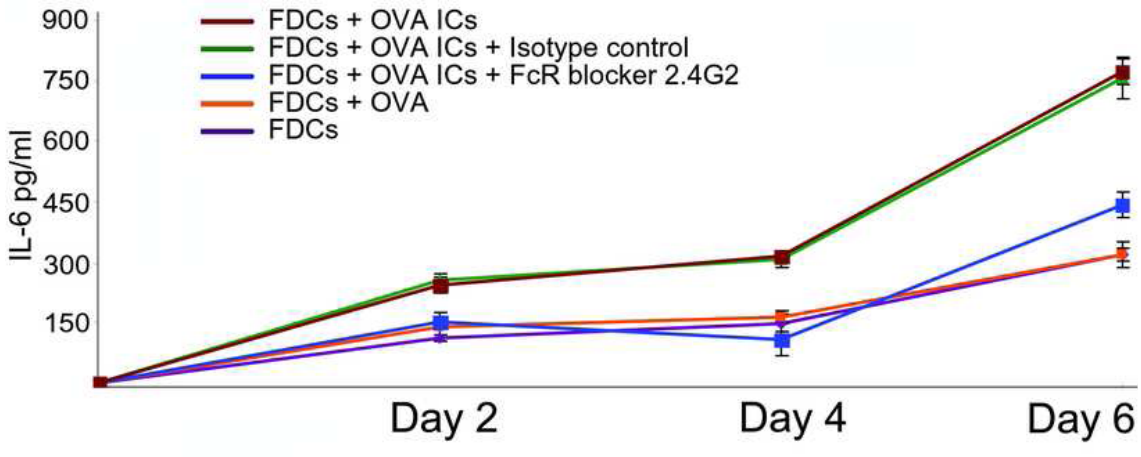
900
750
600
450
300
150
IL-6 pg/ml
FDCs + OVA ICs
FDCs + OVA ICs + Isotype control
FDCs + OVA ICs + FcR blocker 2.4G2
FDCs + OVA
FDCs
Day 2
Day 4
Day 6

including low Tox complement and complement receptors do not activate FDCs whereas engagement of FDC-FcγRIIB does (70).

Anti-IL-6 inhibited specific Ab production in vitro

Germinal center reactions were set up using purified FDCs, CGG-primed memory T cells, and lambda light chain positive B cells (λ^+ B cells) isolated from WT mice. The λ^+ B cells were obtained 6 days after immunization with 100 ug of NP-CGG per mouse. The 6 days allowed NP specific λ^+ B cells to begin clonal expansion and begin producing IgG anti-NIP *in vivo*. However, as previously shown (196,199,200) and confirmed in our studies (35), λ^+ B cells taken 6 days after primary immunization have begun class switching, IgG production is increasing rapidly, but SHM has not occurred. The amount of NIP specific Ab in the supernatant fluids after 7 days of culture was consistent with previous results with cells from WT mice (Fig. 3) (35). Without FDCs the anti-NIP IgG levels were low (Fig. 3 columns 1 & 2). B cells do not survive well in the absence of FDCs and without FDCs only about 20% of our B cells survive for a wk compared with 80 - 90% in the presence of FDCs (115). Low Ab levels in cultures lacking FDCs are, at least in part, a reflection of a loss in B cells. Addition of FDCs to the B & T cells resulted in a dramatic increase in anti-NIP production (Fig. 3 column 3). To test the importance of IL-6 in promoting this IgG response, neutralizing anti–IL-6 (10 ug/ml) or isotype control were added to the B cell, T cells and FDC cultures where optimal anti-NIP responses are obtained (35). Column 4 of Fig. 3 illustrates that anti-IL-6 reduced the anti-NIP response by nearly 80%. To determine if the IL-6 served as a survival signal, trypan blue exclusion data indicated that 91.7$\pm$3 % of the cells at the start of the culture were recovered from

cultures containing FDCs and isotype control after 7 days (1.8±0.06 x 10^6 viable cells recovered). Flow cytometry after double labeling with B220-FITC and propidium iodide (PI), revealed that 45.7±1.6 % of these cells were $B220^+/PI^-$. In cultures containing FDCs and anti-IL-6 there were 1.7±0.06 x 10^6 total viable cells persisting or 88.3±3 % of the cells at the start of the culture. Flow cytometry of these cultures revealed that 45.0±1 % of these cells were $B220^+/PI^-$ (p >0.05). These results suggest that IL-6 is promoting B cell maturation rather than survival.

Specific Ab responses and GC development impaired in IL-6 KO mice

To establish the impact of IL-6 on specific Ab and GC development, WT and IL-6 KO mice were immunized with NP-CGG. At 100 ug of NP-CGG /mouse, the IgG anti-NIP levels were not significantly depressed in IL-6 KO mice 14 days after immunization (Data not shown). However, when immunogen was limited to 1 ug NP-CGG/mouse, the IgG anti-NIP response 14 days after primary immunization was clearly suppressed in IL-6 KO mice (Fig. 4A). We reasoned that ICs would not form as rapidly in IL-6 KO animals with reduced specific Ab levels and that FDC trapping and activation be delayed and reduced. Consequently, B cells would not respond as vigorously resulting in fewer and less robust GCs in IL-6 KO mice. To test this, the number and sizes of GCs were determined 14 days after primary immunization with 1 ug of NP-CGG. As illustrated in Fig. 4B & C, GCs were apparent in both WT and IL-6 KO mice. However, GCs in IL-6 KO mice appeared to be scattered and smaller and this was confirmed using morphometric analysis which indicated that the number

and size of GCs in IL-6 KO mice were about half the WT level (Fig. 4D & E). Thus, the reduced anti-NP response correlated with a reduced GC response in IL-6 KO mice (Fig. 4A). In addition, the total splenic leukocytes in the IL-6 KO mice were about half the number of spleen leukocytes in the WT (94.6×10^6 + 11.5 Vs 61.7×10^6 + 12.6 $p<0.01$), and the GL-7^+ cells represented 3 + 0.2 % and 0.6 + 0.3 % of the splenic leukocytes in the WT and the IL-6 KO groups respectively ($p < 0.003$).

Irradiated wild type mice reconstituted with IL-6 KO splenocytes but not IL-6 KO mice reconstituted with WT splenocytes developed GCs and anti-NIP IgG in response to 1 ug NP-CGG.

FDCs are irradiation resistant and to determine if FDC derived IL-6 is important under physiological conditions *in vivo*, we set up irradiation chimeras reasoning that WT FDCs would provide IL-6 and induce GCs and IgG responses with IL-6 KO splenocytes. As illustrated in figure 5A, anti-NIP levels were significantly lower in the IL-6 KO mice ($p < 0.02$) as compared to the WT mice regardless of the source of donor splenocytes. GCs in the WT mice reconstituted with IL-6 KO splenocytes were readily apparent and labeled intensely with GL-7 (Fig. 5B) and, as expected, these GCs developed in association with the IC-retaining FDC-network (Fig 5.B2). In marked contrast, GC in IL-6 KO mice were poorly developed and very difficult to find even with WT splenocytes which could serve as a source of IL-6 (Data Not shown). Moreover, the number of GCs per midsaggital splenic section from IL-6 KO mice reconstituted with

Figure 3. ***Anti-IL-6 mediated inhibition of anti-NIP IgG production in GC reactions in vitro.*** GC reactions were set up using cells isolated from WT mice. Culture contents are indicated beneath each column (BTAg: B cells, T cells, & Ag; BTIC: B cells, T cells, & ICs; BTFDCIC ISO: B cells, T cells, FDCs, & isotype control Ab; BTFDCIC α-IL-6: B cells, T cells, FDCs, & anti-IL-6). After 7 days of culture, supernatant fluids were collected and assayed for NIP-specific IgG by ELISA. The values represent the mean ± SEM from triplicate independent experiments. Either isotype control or anti-IL-6 Ab (at 10 ug /ml) were added to B, T and FDC cultures and the difference between isotype control and anti-IL-6 was statistically significant ($p<0.05$).

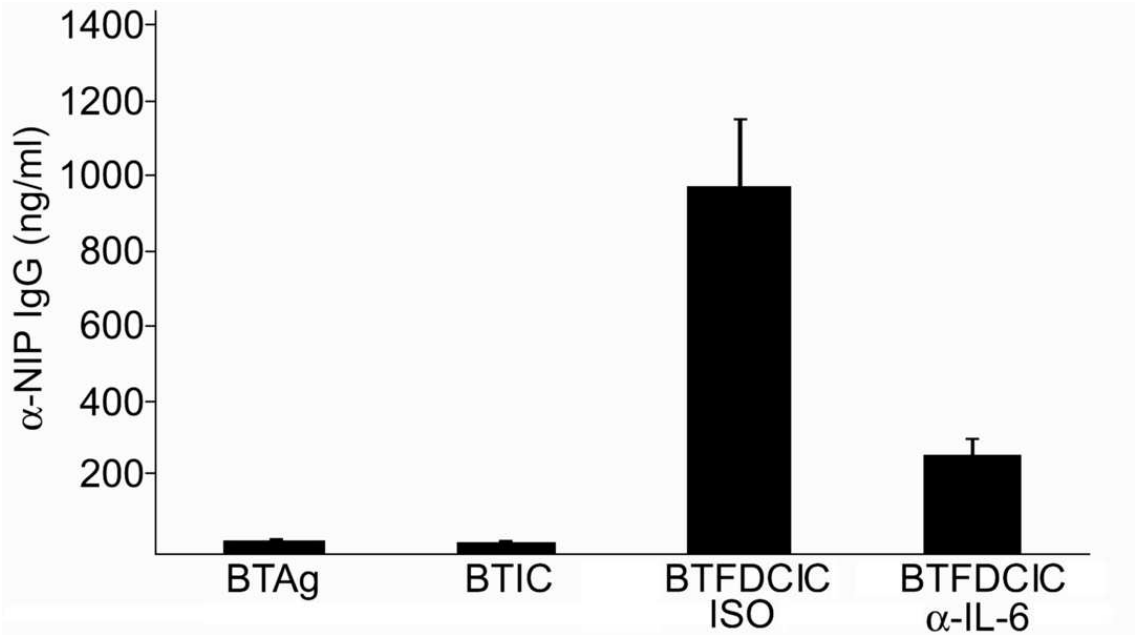
1400
1200
1000
800
600
400
200
α-NIP IgG (ng/ml)
BTAg
BTIC
BTFDCIC ISO
BTFDCIC α-IL-6

Figure 4: ***Reduced NIP specific serum IgG and a similar reduction in GCs in draining axillary lymph nodes from IL-6 KO mice 14 days after primary immunization.*** Panel A, Wild type (WT) or IL-6 KO mice were injected s.c. with 1 ug of alum precipitated (NP)36–CGG using heat–inactivated Bordetella pertussis as adjuvant. Two wk after primary immunization, serum was collected and assayed for IgG anti NIP. The data are representative of two independent experiments with 6 mice in each group. Panel B, Illustrates labeling with FITCconjugated anti-GL7 (B1) that labels GC B cells and defines a GC within the cortex of a lymph node from a WT mouse. B2 illustrates labeling of the same follicle with Cy5.5-conjugated anti- B220 that labels all B cells. B3 is an overlay of panels B1 and B2 indicating the extent of GC B cells relative to B cells generally. Panels C1, C2, & C3 are the same reagents with an IL-6 KO mouse. Panel D, illustrate the number and panel E, size of GL7+ GCs per midsagittal axillary lymph node section.

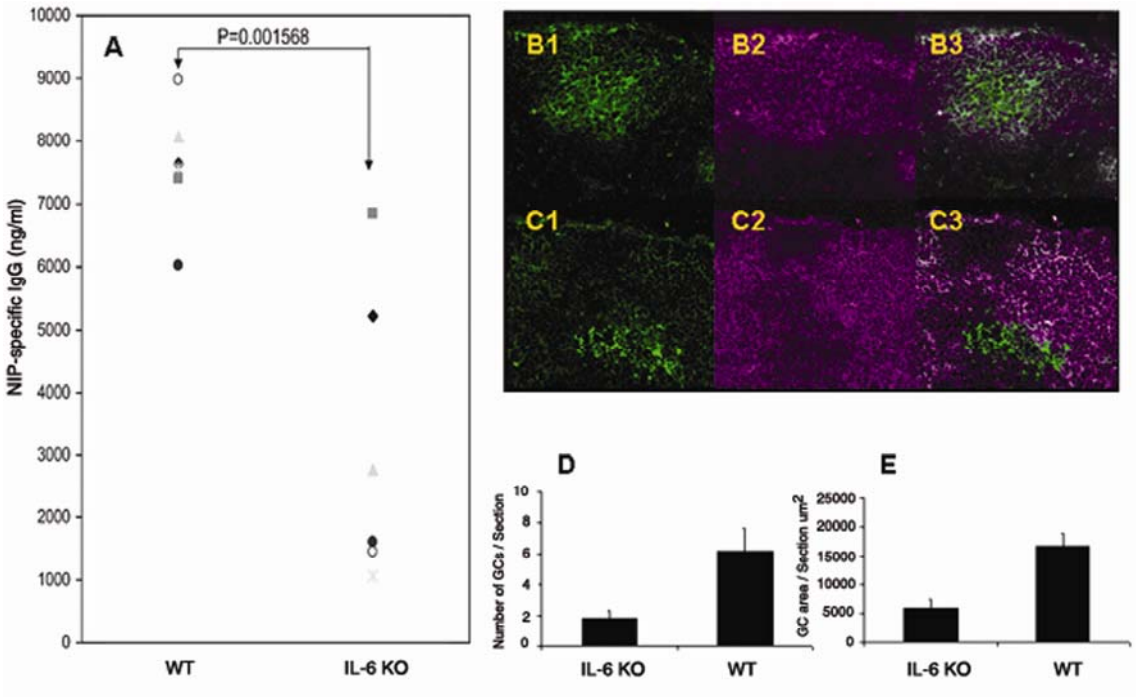
A
P=0.001568
NIP-specific IgG (ng/ml)
10000
9000
8000
7000
6000
5000
4000
3000
2000
1000
0
WT
IL-6 KO
B1
B2
B3
C1
C2
C3
D
Number of GCs / Section
10
8
6
4
2
0
IL-6 KO
WT
E
GC area / Section um2
25000
20000
15000
10000
5000
0
IL-6 KO
WT

Figure 5: ***WT mice reconstituted with IL-6 KO splenocytes, but not IL-6 KO mice reconstituted with WT splenocytes, developed GCs and anti-NIP IgG.*** Chimeras were generated by reconstituting irradiated WT C57B/6 mice with 108 IL-6 KO splenocytes and vice versa. One day later, these mice with irradiation resistant FDCs and splenocytes were challenged with 1 μg NP-CGG and the NIP-specific IgG was assessed after 14 days when the mice were sacrificed. Cryosections were prepared from each spleden, and GCs in the midsaggital sections were labeled with GL-7 and counted. As shown in figure 5, the anti-NIP levels were significantly lower in the IL-6 KO mice ($p < 0.02$) as compared to the WT mice. Germinal center development in the irradiated IL-6 KO mice was markedly impaired (averaged less than 2 as compared with 16 GL-7+ GCs counted in the reconstituted WT mice) and GC development was not rescued by reconstitution with WT splenocytes capable of producing IL-6.

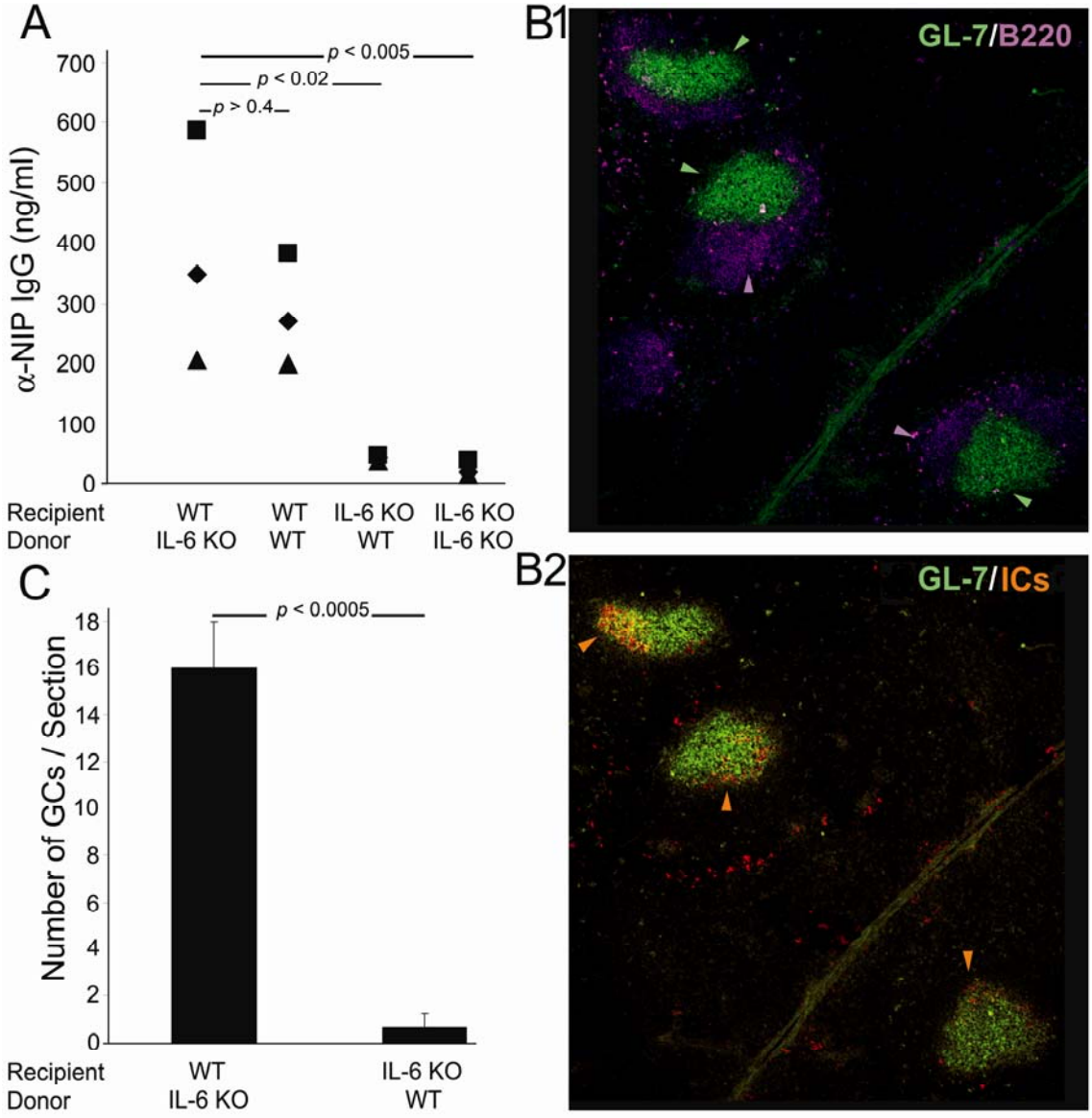
A
p < 0.005
p < 0.02
p > 0.4
α-NIP IgG (ng/ml)
700
600
500
400
300
200
100
0
Recipient
Donor
WT
IL-6 KO
WT
WT
IL-6 KO
WT
IL-6 KO
IL-6 KO
B1
GL-7/B220
B2
GL-7/ICs
C
p < 0.0005
Number of GCs / Section
18
16
14
12
10
8
6
4
2
0
Recipient
Donor
WT
IL-6 KO
IL-6 KO
WT

WT splenocytes averaged less than 2 as compared with 16 GL-7^+ GCs/section in WT mice reconstituted with IL-6 KO splenocytes ($p<0.0005$).

SHM impaired in IL-6 KO mice

IL-6 helps regulate late events in B cell differentiation and we reasoned that IL-6 may influence SHM, which occurs after the initial induction of IgG anti-NIP late in the first wk after primary immunization (35). The antibody response to the hapten 4-hydroxy-3-nitrophenylacetyl (NP) coupled to the T cell-dependent carrier CGG is dominated in C57BL/6 mice by lambda light chain bearing antibodies (201-204) expressing the VH186.2 gene (205). This response has been well characterized and consequently was adopted in the current study. To examine SHM, the draining lymph nodes from the mice immunized with 1 ug of NP-CGG and studied in Fig. 4 were collected at day 14, the λ^+ B cells were harvested and SHM was determined. Consistent with the IgG response and GC reaction data in Fig. 4, mutations were also apparent but reduced in the IL-6 KO mice. The rate of mutation in the VH186.2 gene segment switched to Ig-gamma decreased from 18 to 8.9 mutations/1000bp ($P <0.001$) in WT vs IL-6 KO mice. The mutations are illustrated in Table 1 which shows the DNA sequence alignment of the VH186.2 gene. The corresponding amino acid sequence alignments were done and as expected, most mutations were in the CDR1& 2 regions (Table 2).

Anti-IL-6 inhibited SHM in GC reactions in vitro

Provided that FDCs bearing the appropriate ICs are present (35), SHM can be studied in GC reactions *in vitro.* This prompted experiments to determine if anti-IL-6 will inhibit SHM under controlled conditions in culture to confirm the results *in vivo*. Germinal center reactions were set up *in vitro* using purified FDCs, CGG-primed memory T cells, and λ^+ B cells isolated from WT mice. The λ^+ B cells were obtained 6 days after immunization with 100 ug of NP-CGG per mouse. The 6 days allowed NP specific λ^+ B cells to clonally expand and begin producing IgG anti-NIP *in vivo*. However, as previously shown (196,199,200) and confirmed in our studies (35), λ^+ B cells taken 6 days after primary immunization are not mutated. However, SHM would be one of the next events in a GC reaction. These 6 day B cells were cultured for 7 additional days *in vitro* and the production of specific anti-NIP Ab and mutations in the VH186.2 gene segment were determined. The anti-NIP response of these mice is illustrated in Fig. 3 where anti-IL-6 reduced the IgG response by nearly 80%. Similarly, the mutation rate in these anti-IL-6 treated cultures was reduced (3.50 vs 0.65 mutations per 1000 bases in control vs anti-IL-6 treated cultures; $P< 0.02$). The data in Table 3 illustrate the DNA sequence alignment of VH186.2 gene obtained in cultures with the isotype control and cultures treated with anti-IL-6. Note that most sequences from cultures treated with the isotype control contained mutations whereas only two sequences from the anti-IL-6 treated cultures contained mutations. Of the 12 sequences analyzed from isotype control

cultures there were a total of 13 mutations. Eight of these were replacement mutations and five were silent. Six of the eight replacement mutations were in the CDR2 region. These data from cultures with the isotype control are compatible with the much larger published data sets (35) where mutations *in vitro* with IC loaded FDCs ranged from 3 to 12 mutations/1000 bases with over 60% of these mutations in CDR1 or CDR2. Results from the anti-IL-6 treated cultures were similar in that two of the three mutations were replacement mutations.

Table 1: Vh186.2 sequence alignments from 1μg $(NP)_{36}$-CGG immunized WT vs IL6 KO

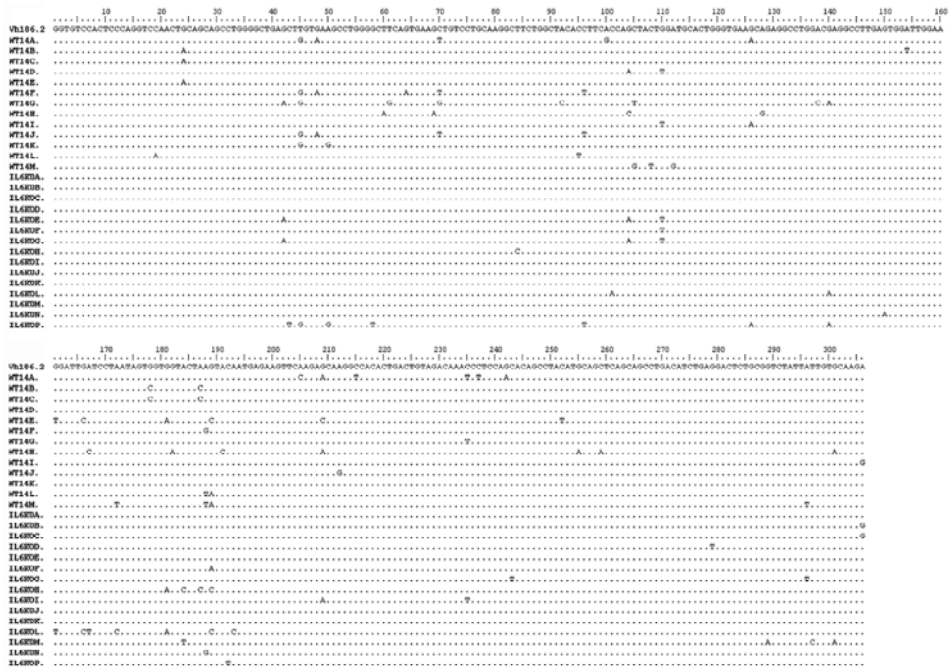

Footnote: The sequences shown in table 1 are for lambda B cells obtained from WT or IL-6 KO mice whose anti-NIP levels are shown in figure 4 part A. The anti-NIP levels as well as sequence analysis were performed 14 days after challenge of these mice with 1 μg of NP-CGG.

Table 2: Vh186.2 Amino acid sequence alignment from 1 μg (NP)36-CGG immunized WT vs IL-6 KO mice

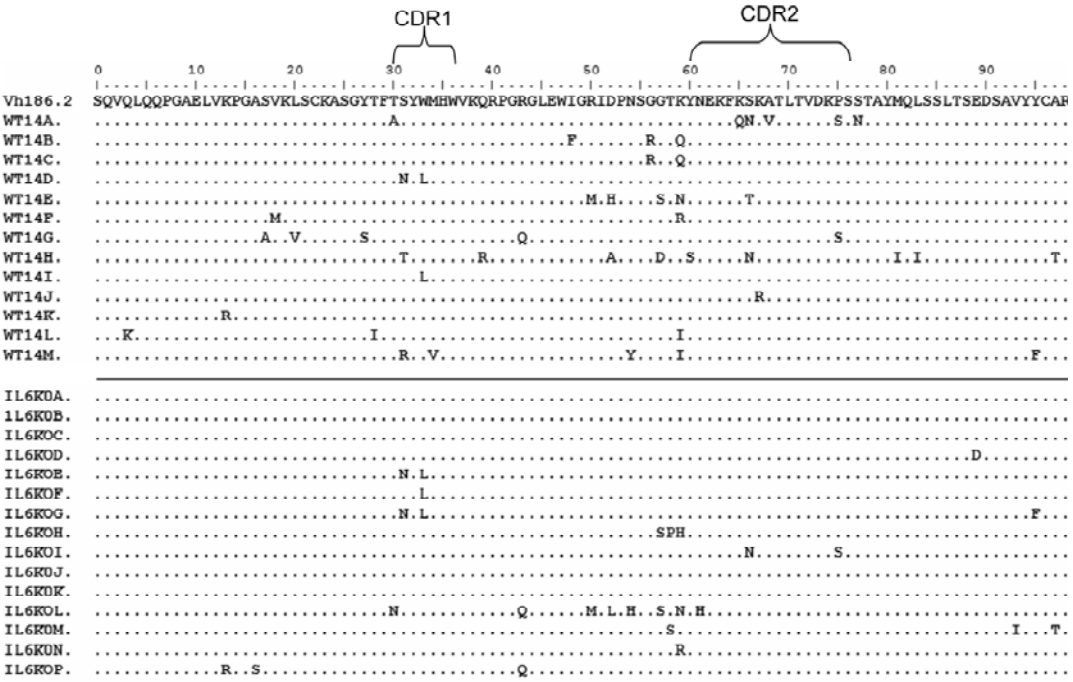

Footnote: Data represent Amino acid translation of DNA sequences shown in table 1, for lambda B cells obtained from WT or IL-6 KO mice whose anti-NIP levels are shown in figure 4 part A.

Table 3: Comparison of Vh186.2 sequence alignments from isotype and anti-IL-6 treated cultures

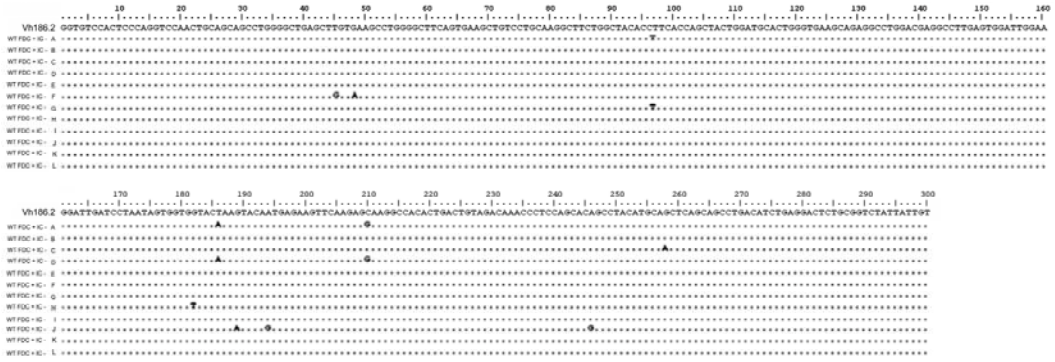

Anti-IL-6

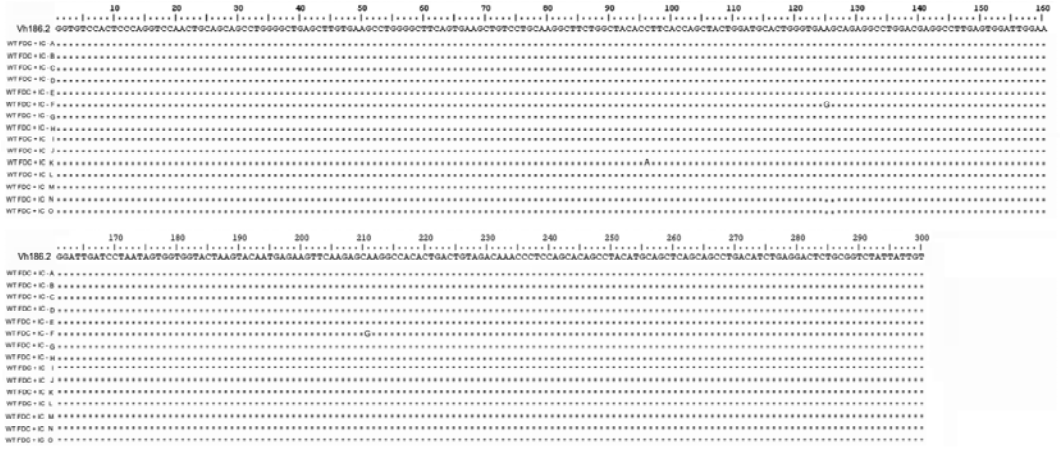

Discussion

The contribution of IL-6 to terminal B cell differentiation has long been recognized (184). However, the physiological relevance of FDC-IL-6 to GC B cell differentiation is unclear given that IL-6 can be produced by many cells and IL-6 production by FDCs has not been consistently found (193-195). In the present study, we confirmed that murine FDCs produce IL-6 and provide strong support for the physiological relevance of FDC-IL-6 in GC reactions. IL-6 was not detectable in *in vitro* GC reactions with IL-6 KO FDCs even with T & B cells from WT mice that could serve as a source of IL-6. In contrast, IL-6 production was normal in GC reactions with WT FDCs with T and B cells from IL-6 KO mice. Moreover, FDCs are irradiation resistant and GC reactions were abundant in irradiated WT mice reconstituted with spleen cells from IL-6 KO mice while GCs were virtually undetectable in irradiated IL-6 KO mice reconstituted with normal spleen cells. Moreover, like ICAM-1, VCAM-1 and FcγRIIB (70), activating FDCs with ICs upregulated FDC-IL-6 production. Immune complexes would be generated *in vivo* ~3-7 days after primary immunization suggesting that a burst in FDC-IL-6 production would occur in the follicles ~5 days after immunization and continue for a week or more. Although, class switching and low affinity Ab production may occur before a GC reaction (19,206), the IgG response is amplified as GCs develop over the next week. Moreover, SHM is a late event apparent in GCs after the first wk (35,196,199,200). Thus, SHM would coincide with optimal production of IL-6

by IC-activated FDCs. Both *in vivo* and *in vitro* data indicated that anti-NIP responses and SHM can take place in the absence of IL-6, but IL-6 clearly promoted both responses. The novel findings reported here are that FDC-IL-6 levels are upregulated by ICs and that FDC-IL-6 is high in the second week after immunization concurrent with SHM, and that IL-6 is required for optimal SHM. Thus, FDC-IL-6 appears to influence not only GC development and the level of IgG produced, but also the mutations that promote enhanced IgG affinity.

Results presented here confirm and extend the report of Kopf, et al. (68) who first demonstrated that IL-6 mRNA is produced by cells within murine GC clusters and determined it was the FDC-enriched populations (> 80 % pure) rather than the lymphocytes that produced the IL-6 mRNA. Immunohistochemistry performed by these authors on cryosections from immune WT mice further supported their results revealing that cells with dendritic morphology within FDC-network produced the IL-6. This production was limited to active GCs and not detected in primary follicles, which may help explain why some studies have failed to detect IL-6 in FDCs. By use of an IL-6 bioassay, Kopf et al found that IL-6 was present only in cultures containing either FDC-lymphocyte clusters or the FDC irradiated population but not in the sorted T or B lymphocytes. However, IL-6 was not quantified and our data extend this report by quantification of IL-6 production in highly purified FDCs *in vitro* and demonstrated IC mediated induction.

The extent of *in vivo* suppression of the immune response in the IL-6 KO mice in the present study appears to be less than that observed by Kopf and colleagues (68). Our use of *Bordetella pertussis* as adjuvant may have helped compensate for the lack of IL-6 *in vivo*. Alternatively, CGG may be more stimulatory in the absence of IL-6 than the OVA they used.

A previous study of GC reactions *in vitro* indicated that FDCs promote IgG production by B cells taken 6 days after primary immunization. However, in the absence of a second late exposure to Ag, SHM was not detected (35). This model was used in the present study which suggests that optimal SHM also requires IL-6. Typically SHM occurs in the second wk after primary immunization, however, if memory T cells are given along with immunogen in the form of IgG-ICs, extensive GC development and high levels of SHM can be obtained in the first wk *in vivo* (35). The importance of ICs is indicated by the observation that replacing ICs with Ag, which will not load on FDCs, does not induce SHM in the first wk even though memory T cells are present (35). Moreover, it is important for the ICs be made with IgG to promote SHM (207) and IgG-ICs are arranged on FDCs with a periodicity known to optimally engage BCRs and stimulate B cells (34,35). In short, the combined data provide support for the concept that the unique ability of FDCs to trap and retain IgG-ICs for months provides them with the Ag necessary to deliver late specific and non-specific signals like IL-6 needed to promote SHM. Moreover, FDCs bearing

the appropriate ICs promote activation-induced cytidine deaminase production, and affinity maturation by NP specific B cells (39).

In the present study, the *in vivo* reductions in specific Ab and SHM in IL-6 KO mice were most apparent at low Ag dose. At our usual immunization dose of 100 ug of NP-CGG /mouse, neither the reductions in IgG anti-NIP levels nor SHM were statistically significant 14 days after immunization (Data not shown). However, defects in Ab production and SHM were readily apparent when the dose was reduced to 1 ug of NP-CGG/mouse. A similar Ag dose-effect relationship has been reported in lymphotoxin alpha KO mice. Mature FDC-reticula and GCs do not develop in these mice, nevertheless, if the Ag dose is high enough, SHM is apparent in these FDC-reticula defective animals (208). Most infections start with only a few organisms, and if specific Ab is significant in immunity, it is important that immunity develops before the infection gets widespread. The results reported here indicate that under low immunogen dose conditions FDC-IL-6 is likely to be important in generating rapid production of high affinity specific IgG. We look forward to studies testing the relationship between FDC-IL-6, selection of high affinity clones with SHM, and affinity maturation both *in vivo* and *in vitro*.

CHAPTER 5

T-Independent Antibody Responses to T-dependent Antigens: A Novel Follicular Dendritic Cell-Dependent Activity

Introduction

Antigens are classified as T cell dependent (TD)[4] or T cell independent (TI) depending on whether T cell help is needed to induce an Ab response. TI Ags are further classified into TI type 1 and 2. The TI-1 Ags, such as LPS, are B cell mitogens, which function by non-specifically or polyclonally activating most B cells (209). The TI-2 Ags, such as polysaccharides, are large molecules with repeating epitopes that are typically able to activate complement, but lack the ability to induce MHC-dependent T cell help (95). In ideal form, TI-2 Ags are flexible, non-degradable, and hydrophilic molecules capable of simultaneously engaging multiple B cell receptors (BCRs) (98). The molecular structure of classical TI-2 Ags consists of a non-immunogenic backbone exhibiting recurring immunogenic epitopes 95-675 Å apart. This periodicity appears to be optimal for simultaneously engaging and cross-linking multiple BCRs and rapidly inducing IgM responses (within 48 hrs) (98,210).

Follicular dendritic cells (FDCs) reside in the light zones of germinal centers (GC) and retain Ags in the form of immune complexes (ICs). FDC-ICs resist degradation and persist for months to years on numerous intertwining dendrites. The non-mobile FDCs remain in the GCs where their intertwining dendrites create extensive Ag retaining reticula (ARR) intimately in contact with numerous mobile B cells (37,42). In GCs, which are typically involved in refining humoral immunity to TD Ags, FDCs promote: B cell survival, Ig class switching, somatic hypermutation, selection of somatically mutated B cells with

high affinity receptors, affinity maturation, B memory production, and induction of secondary IgG and IgE responses (29,35,38,46,69,112,114,185,186,211,212).

FDCs trap Ag in the form of ICs via Fc and C receptors although FcRs are adequate to periodically arrange the ICs (34,44,70). In addition to Ag, FDCs provide costimulatory signals to B cells. Both C3 (C3b) and C4 (C4b) engage C4 binding protein (C4BP) which co-localizes with ICs on FDCs (59). C4BP in ICs trapped on FDCs has been shown to signal B cells via CD40 independent of T-cell derived CD40L (CD154) (59). Notably, injection of mice with FDC-M2, which recognizes an epitope on C4 bound within ICs, inhibits TI GC development (59). Moreover, C3- and C4-deficient mice showed impaired TI Ab responses consistent with the concept that ICs on FDCs provide Ag-specific, complement-derived, and CD40-mediated signals to B cells in TI GCs (59). In addition, FDCs produce BAFF (B-cell activation factor of the TNF family) (60-62) that also promotes TI B cell activation (213,214). The functional outcome of BAFF signaling is multifaceted and different receptors mediate different functions. Peripheral B cell survival, plasma cell survival, MZ B cell integrity, GC maintenance, CD21 & CD23 expression, TI B cell responses and Ig class switching all appear to be influenced by BAFF (64).

The Ags trapped in ICs on FDCs are typically TD and these Ags are arranged periodically with characteristic 200-500 Å spacing on the cell surface (24,34). The periodicity of ICs on FDCs was reported initially with ICs trapped *in vivo* (24) followed by similar results *in vitro* (34). This periodicity of TD Ags

in ICs on the surfaces of flexible FDC dendrites with 200-500 Å spacing corresponds with recurring immunogenic epitopes 95-675 Å apart on a flexible backbone of ideal TI-2 Ags (98,210). We reasoned that the periodically arranged FDC-ICs would promote extensive BCR cross-linking and would induce rapid TI IgM production when delivered in conjunction with cosignals mediated by FDC-C4BP and/or FDC-BAFF.

To test the above hypothesis, ICs were used to load FDCs and B cells were stimulated *in vivo* and *in vitro* in the absence of T cells or T cell factors. Our data indicated that OVA-IC challenged nude mice produced OVA-specific IgM within 48 hrs after IC challenge and the response was maintained for weeks. In marked contrast, OVA in adjuvant induced no OVA specific IgM at any time. The draining lymph nodes of these IC challenged mice exhibited well developed GL-7^+ GCs associated with FDC-ARR and B lymphocyte-induced maturation protein-1^+ (Blimp-1^+) plasmablasts within 48 hrs of IC administration and the GCs persisted for at least 7 days. Moreover, purified FDCs loaded with OVA-IC induced purified human and murine B cells to produce OVA-specific IgM *in vitro* in 48 hrs. We also tested the postulate that anti-IgD mAb, which can not signal alone, will signal the vast majority of B cells as a consequence of engaging multiple BCRs when loaded on FDCs in the form of ICs. Evidences of *in vitro* B cell activation included increased levels and redistribution of intracellular phosphotyrosine, expression of the B cell activation marker GL-7, Blimp-1^+ plasmablast differentiation, B

cell proliferation and polyclonal IgM production within 48 hrs. This TI but FDC-dependent IgM response was inhibited when FDC-FcγRIIB was blocked to interfere with the ability to periodically arrange ICs. Similarly, neutralizing FDC-C4BP or BAFF also inhibited this TI response. In short, this study is the first to report the ability of FDCs to convert TD Ags into TI Ags capable of inducing B cell activation and Ig production in the absence of T cells or T cell factors.

Materials and Methods

Mice

Homozygous athymic NCr-*nu/nu* and heterozygous NCr-*nu*/+ mice were purchased from The National Cancer Institute at Frederick, MD (NCI-Frederick). FDC networks develop in the presence of B cells but much faster in normal mice with both T and B cells (215). Accordingly, the *nu/nu* mice used were 9 months of age to be sure the time was adequate for FDC-networks to fully develop. Mice were housed in standard plastic shoebox cages with filter tops and maintained under specific pathogen-free conditions in accordance with guidelines established by Virginia Commonwealth University Institutional Animal Care and Use Committee.

Immunization

Homozygous nude (*nu/nu*) and heterozygous (*nu*/+) mice were injected with 20 μg OVA, in each limb, in the form of (1) alum precipitated OVA (Sigma-Aldrich, St. Louis, MO, A5503) with *Bordetella pertussis*, or (2) OVA immune complexes (ICs) made of NIP (4-Hydroxy-3-iodo-5-nitrophenylacetyl)-OVA (Biosearch Technologies, Novato, CA, N-5041-10) + goat polyclonal anti-tri-nitro-phenol Abs (Anti-TNP, Biomeda corp., Foster City, CA, J05) or (3) OVA ICs made of alum precipitated NIP-OVA with *Bordetella pertussis* + anti-TNP. Anti-TNP Abs effectively binds NIP forming ICs with the NIP-OVA. Fifty μg azide-free functional grade purified anti-mouse CD90 (Thy-1, eBioscience, 16-0901) were given IP per nude mouse 12 hrs

before Ag challenge to inhibit residual T cell activity, especially γδ T cells, that may be present in these animals. Animals were bled 48 hrs, 1 week and 2 weeks after Ag challenge. Homozygous *nu/nu* mice were also bled after 7 weeks. OVA-specific IgM and IgG were assessed in the collected sera and levels were recorded after subtracting the pre-immunization background levels.

Confocal microscopy for GCs, FDC-reticula, and plasmablasts

Confocal microscopy was used to assess GC development and plasmablast differentiation in association with FDC-ARR at 48 hrs and 7 days after IC administration. To this end, groups of *nu/nu* mice were challenged with: a) OVA-specific rabbit serum (Meridian Life Science Inc, Cincinnati, OH, W59413R) + alum-precipitated OVA and *B. pertussis* or b) normal (non-specific) rabbit serum (Gibco, Grand Islands, NY) + alum-precipitated OVA and *B. pertussis*. Two and 7 days later, axillary lymph nodes (LNs) were collected and frozen in CryoForm embedding medium (IEC). Frozen sections of 10-μm thickness were cut on a Leica (Jung Frigocut 2800E) cryostat then air dried. Following fixation in absolute acetone, the sections were blocked with 10% horse serum and washed in phosphate buffered saline. Mid-saggital sections were triple labeled with GL-7-FITC (BD Pharmingen, San Jose, CA, 553666) (for GC B cells), B220-Cy5.5 (Pharmingen, San Jose, CA, 552771) (general B cell marker), and Rhodamine Red-X-affinipure goat anti-rabbit IgG (Jackson ImmunoResearch Laboratories, West Grove, PA, 111-295-144) multiple adsorbed to minimize any cross reactivity with mouse, rat and human serum

proteins (to label the OVA ICs retained in the FDC reticulum). To label GC-associated plasmablasts, the Rhodamine Red-X-affinipure goat anti-rabbit IgG was replaced with Blimp-1-PE (Santa Cruz Biotechnology Inc, Santa Cruz, CA. sc-13203 PE). Sections were mounted with anti-fade mounting medium, Vectashield (Vectashield, Vector Laboratories, Burlingame, Calif.), cover-slipped, and examined with a Leica TCS-SP2 AOBS confocal laser scanning microscope fitted with an oil plan-apochromat 40X objective. Three lasers were used, Argon (488 nm) for FITC, HeNe (543 nm) for Rhodamine-Red X or PE, and HeNe (633nm) for Cy5.5 (shown as pseudo-color magenta). Parameters were adjusted to scan at 512X512 pixel density and 8-bit pixel depth. Emissions were recorded in 3 separate channels and digital images were captured and processed with Leica Confocal and LCS Lite softwares.

In vitro stimulation of purified B cells with purified IC-bearing FDCs

Naïve "untouched" human B cells were purified by negative selection on LS MACS separation columns using The Naive B Cell Isolation Kit II (Miltenyi Biotec, Auburn, CA, 130-091-150). Murine B cells were purified by positive selection using CD45R (B220) on LS MACS separation columns MicroBeads (Miltenyi Biotec, Auburn, CA, 130-049-501).

FDCs were isolated by positive selection from LNs (axillary, lateral axillary, inguinal, popliteal, and mesenteric) of irradiated adult mice, as previously described (130). In brief, one day before isolation, mice were irradiated with 1000 rad to eliminate most lymphocytes, then sacrificed, and

LNs were collected, opened, and treated with 1.5 ml of collagenase D (22 mg/ml, C-1088882; Roche), 0.5 ml of DNase I (5000 U/ml, D-4527; Sigma-Aldrich), and 2 ml of DMEM with 20 mM HEPES. After 45 min at 37°C in a CO_2 incubator, released cells were washed in 5 ml of DMEM with 10% FCS. Cells were then sequentially incubated with FDC-specific Ab (FDC-M1) (BD Pharmingen, San Jose, CA, 551320) for 45 min, 1 μg of biotinylated anti-rat κL chain (BD Pharmingen, San Jose, CA, 553871), for 45 min, and 20 μl of anti-biotin microbeads (Miltenyi Biotec, Auburn, CA, 130-090-485) for 15–20 min on ice. The cells were layered on a MACS LS column and washed with 10 ml of ice-cold MACS buffer. The column was removed from the VarioMACS, and the bound FDCs were released with 5 ml of MACS buffer.

Purified FDCs were loaded with 100 ng/ml OVA ICs made of OVA/rabbit anti-OVA at a ratio of 1:6. IC-loaded FDCs were used to stimulate $20x10^6$ purified B cells at a ratio of 1FDC:2B cells. Cells were cultures in 10 ml culture medium and OVA-specific Abs were assessed after 48 hrs.

The rat anti-mouse IgD mAb clone 11-26 (SouthernBiotech, Birmingham, Alabama, 1120-14) was selected because this mAb *per se* does not induce proliferation of mature B cells *in vitro*, nor does it activate B cells *in vivo* (216). Consequently, any ability of this mAb to activate B cells would be attributable to the influence of FDCs. To load this mAb on FDCs it was complexed with Fc-specific rabbit anti-rat IgG (Jackson ImmunoResearch Laboratories, West Grove, PA, 312-005-046) at a ratio of 1:4 and the ICs were

incubated with purified FDCs. Anti-IgD ICs at doses of 0.1, 1.0, and 10 μg/ml were used to load FDCs and used to stimulate 10^4, 10^5, and 10^6 purified murine B cells in 1 ml cDMEM. Controls included B cells in the absence of FDCs with free and complexed anti-IgD in the presence or absence of 10% Low Tox Complement (Cedarlane Laboratories Ltd. Ontario, Canada) to provide complement-mediated co-stimulation as well as conditions where the B cell FcγRIIB was blocked with azide-free anti-CD16/CD32 (mAb clone 2.4G2, 553140, BD Pharmingen, San Jose, CA) to minimize ITIM signaling. To assess the role of FDC-FcγRIIB in IgM production by FDC-IC-stimulated B cells, $0.5x10^5$ FDCs were treated with 1 μg/ml azide-free anti-CD16/CD32, prior to loading with anti-IgD ICs. ICs were trapped with the complement receptors and 10^5 B cells were cultured with the IC-bearing FDCs. Culture supernatant fluids were assessed after 48 hrs for polyclonal mouse IgM production by ELISA.

ELISA

Total and OVA-specific IgM were assessed in sera and culture supernatant fluids 48 hrs after stimulation of B cells with OVA or anti-IgD-IC-bearing FDCs *in vivo* and *in vitro*. Samples were loaded on ninety-six well plates coated with 100 μg/ml OVA (for OVA-specific Abs) or goat anti-mouse IgM (for total IgM). Samples were left overnight, washed, and captured mouse IgM was detected with biotinylated goat anti-mouse IgM followed by streptavidin-alkaline phosphatase. Alkaline phosphatase was developed with

pNPP alkaline phosphatase substrate system (KPL, Gaithersburg, Maryland, 50-80-00) and read on ELISA reader at 405 nm.

Assessment of FDC-BAFF production and the effect of neutralizing BAFF and C4BP on IgM production by IC-stimulated B cells

One million purified FDCs were cultured *in vitro* for 48 hrs alone or with 100 ng/ml soluble OVA, OVA-ICs, or OVA-ICs, in the presence of 10 μg/ml FcR blocker (2.4G2), or rat IgG2b isotype control. Culture supernatant fluids were collected and BAFF production was assessed by ELISA using Quantikine Mouse BAFF/BLyS/TNFSF13B Immunoassay (R&D Systems, Inc., Minneapolis, MN, MBLYS0). To assess the effect of FDC-BAFF blockade on IgM production by IC-stimulated B cells, B220 purified B cells were cultured with anti-IgD IC-bearing FDCs at a ratio of 1 FDC:2 B cells in the presence of 1 μg/ml decoy recombinant mouse BAFF R/TNFRSF13C/Fc chimera, (R&D Systems, Inc., Minneapolis, MN, 1357-BR). Control conditions included B cells alone, B cells + anti-IgD mAb, B cells + anti-IgD ICs, and B cells + anti-IgD mAb + FDCs. FDC-M2 is a rat anti-mouse mAb that detects an epitope of C4 localized to the ICs trapped on FDCs (59,217). This anti-C4 appears to block C4-bBP which is capable of interacting with CD40 on B cells (59). In mice immunized with TNP-Ficoll, a TI-2 Ag, injection of FDC-M2 blocks the FDC-IC-mediated CD40-dependent activation of follicular B cells and reduces TI GC development by 90% (59). To test the effect of FDC-M2 on IgM production by FDC-IC-stimulated B cells, $0.5x10^6$ B220 purified B cells were stimulated with

$0.25x10^6$ anti-IgD IC-bearing FDCs in the presence or absence of 1 μg/ml C4BP-blocking FDC-M2 (from hybridoma cell line generously provided by Dr. M. Kosco-Vilbois, NovImmune SA, Switzerland). Forty-eight hrs later culture supernatants were collected and assessed for mouse IgM with ELISA.

Visualization and quantification of intracellular phosphotyrosine in stimulated B cells using confocal microscopy and flow cytometry

Purified B cells were stimulated with anti-IgD-IC-bearing FDCs for 45 minutes. Cells were washed, fixed, and permibilized using Fix & Perm cell permeabilization kit (Caltag Laboratories). Intracellular phosphotyrosine was detected with FITC-conjugated anti-phosphotyrosine, clone 4G10, (Upstate Biotechnology, Lake Placid, NY, 16045). Cells were washed and analyzed with flow cytometry or deposited onto polylysine-coated glass slides for visualization with confocal microscopy using argon beam emitting 488 nm laser.

Flow cytometric analysis of GL-7, Blimp-1, and CFSE labeling of B cells stimulated with anti-IgD IC-bearing FDCs in vitro

Purified B cells were stimulated with anti-IgD IC-bearing FDCs for 48 hrs then assessed for GL-7 and Blimp-1 expression as well as B cell proliferation using carboxyfluorescein diacetate, succinimidyl ester (CFSE) dilution assay. To assess GL-7 expression, cells were washed, blocked with Fc-blocker to reduce non-specific binding of GL-7 to the Fcγ receptors, labeled with FITC-conjugated anti-B-cell activation antigen (GL-7), or isotype control rat IgM-FITC (BD Pharmingen, San Jose, CA, 553942). An unstimulated B cell

control was similarly treated and GL-7 expression was assessed by flow cytometry. For intracellular Blimp-1 assessment, purified B cells stimulated with anti-IgD-IC-bearing FDCs for 48 hrs, were washed, fixed, and permibilized using Fix & Perm cell permeabilization kit (Caltag Laboratories). Intracellular Blimp-1 was labeled with PE-conjugated anti-Blimp-1(Santa Cruz Biotechnology Inc, Santa Cruz, CA. sc-13203 PE) then cells were washed and analyzed with flow cytometry. B cell proliferation was assessed by The CellTrace™ CFSE Cell Proliferation Kit (C34554, Invitrogen) following the protocol of the manufacturer. The working range of CFSE is 0.5-25 μM/ml, however, 1 μM CFSE/10^6 cells/ml was satisfactory and avoided toxicity that occasionally occurs with high concentrations of DMSO that was used as a CFSE solvent. After labeling, data were collected using FC500 Flow Cytometer Beckman Coulter, analyzed using Cytomics RXP analysis software, and plotted using WinMDI software (Scripps Research Institute).

Results

Nude mice challenged with OVA-ICs but not OVA mounted OVA-specific IgM responses

If periodically arranged FDC-ICs can induce specific IgM in the absence of T cells, then nude mice should rapidly produce specific IgM when challenged with a TD Ag in the form of ICs but not with free Ag. This hypothesis was tested in *nu/nu* mice given 50 μg of α-Thy-1, to block any residual T cell activity, and challenged with OVA in adjuvant or OVA in ICs with or without adjuvant. As expected, anti-OVA was not detectible in animals immunized with OVA over a 7 week period even with adjuvant (Fig. 1-A). In marked contrast, OVA-specific IgM was present in the sera of all ICs injected animals with or without adjuvant in just 48 hrs. The highest OVA-IgM levels were induced using OVA-ICs in adjuvant and these IgM levels were maintained over a 7 week assessment period. The adjuvant effect was expected, given that LPS activates FDCs and promote their accessory activity (71). Phenotypically normal heterozygous *nu/+* mice also responded to ICs by producing OVA-specific IgM within 48 hrs (Fig. 1-B), although, these IgM levels declined as the isotype switched from OVA specific IgM to IgG, in the presence of T cell help (Fig. 1-C).

GCs in nude mice are associated with well-developed ARR and plasmablasts

Rapid induction of OVA-specific IgM responses in *nu/nu* mice challenged with OVA-ICs prompted study of GC development and plasmablast

differentiation in their draining lymph nodes. As expected for a TD protein Ag, GCs were not detected at day 2 or at day 7 in *nu/nu* mice challenged with OVA + adjuvant in the presence of non-specific rabbit serum where ICs would not form (Fig. 2-A). The B cell follicles labeled with B220 (magenta) but not with the GC B cell marker GL-7 (green). In marked contrast, the follicles in *nu/nu* mice challenged with OVA-ICs developed large GCs within 48 hrs and these persisted for at least one week (Fig. 2-B). The overlay of B220 and GL-7 illustrated a GL-7 bright GC B cell zone surrounded by a zone of resting B220 bright B cells. Note the activation marker GL-7 corresponds with an area of dim B220 labeling since activated B cells tend to down regulate B220 upon acquisition of the GL-7^{+} phenotype (218). In Fig. 2-C, labeling with anti-rabbit IgG (binds rabbit IgG in OVA + rabbit-anti-OVA IgG ICs) revealed well-developed crescent-shaped FDC-ARR at day 2 and day 7. A funnel-shaped Ag transport site extending from the sub-capsular sinus into the lymph node cortex was seen in association with the ARR illustrated at day 7 (37). As shown in the overlay, the green GC is capped with the ARR in red and this overlapping orange-yellow interface represents the GC light zone.

The vigorous OVA specific IgM responses in *nu/nu* mice suggested that challenge with OVA ICs would induce plasmablasts and plasma cells, which label with Blimp-1. As shown in Fig. 2-D, Blimp-1 positive cells were found at the paracortical borders of multiple GCs (red) with a group migrated toward the medullary cords deeper in the node. These cells were also GL-7^{+} and the overlay

of Blimp-1 (red) and GL-7 (green) resulted in orange-colored cells suggesting that these cells are plamablasts. We reason that these cells are migrating toward the medullary cords and bone marrow where they would be expected to mature into plasma cells that would no longer label with GL-7.

Purified OVA IC-bearing FDCs induced OVA-specific IgM production by purified B cells within 48 hrs in the absence of T cells and T cell factors

If periodically arranged FDC-ICs can induce specific IgM in the absence of T cells or T cell factors; then purified FDCs should rapidly stimulate specific IgM by purified naïve B cells *in vitro* if they bear Ag in ICs but not with free TD Ag. FDC-B cell interactions are not MHC or species restricted and murine FDCs can stimulate human B cells effectively (56). Purified murine (Fig. 3-A) or human (Fig. 3-B) B cells in cultures lacking T cells and T cell factors produced OVA-specific IgM in 48 hrs when stimulated with FDCs bearing OVA ICs. Both the kinetics of the response and the IgM production are consistent with a T-independent response. Control conditions, that failed to produce a detectable response, included FDCs with B cells stimulated with free OVA that would have unfettered access to BCR.

Purified B cells were signaled by FDCs bearing anti-IgD-ICs as indicated by intracellular phosphotyrosine distribution, expression of activation marker GL-7, plasmablast differentiation, and B cell proliferation

If Ags in FDC-ICs promote simultaneous binding and cross-linking of multiple BCRs, as we hypothesize, then anti-IgD loaded on FDCs in the form of

Figure 1: ***Nude mice challenged with OVA ICs, but not with OVA, mounted OVA-specific immune responses in 48 h.*** *A*, Groups of *nu/nu* mice, pretreated with 50 μg of anti-Thy-1 to block residual T cell activity, were challenged with alum-precipitated OVA with *B. pertussis*, OVA-ICs, or OVA-ICs with *B. pertussis*. Serum anti-OVA IgM levels were determined 48 h, 1 wk, and 2 wk later, and results were recorded after subtracting background levels using preimmunization sera. As expected, anti-OVA was not detectible in animals immunized with OVA in adjuvant (baseline tracking). In marked contrast, OVA-specific IgM was present in the sera of all IC-injected animals with or without adjuvant in just 48 h and was maintained over a 7-wk assessment period. *B*, Phenotypically normal heterozygous *nu*/+ mice with competent T cell compartment also responded to ICs by producing OVA-specific IgM within 48 h, although these IgM levels declined over time. *C*, The phenotypically normal *nu*/+ also produced IgG, and the increase in this isotype correlated with a decrease in IgM. Note that neither class switching nor OVA-specific IgG was detectable in *nu/nu* mice lacking T cell help (baseline tracking). Data are represented as mean ± SD.

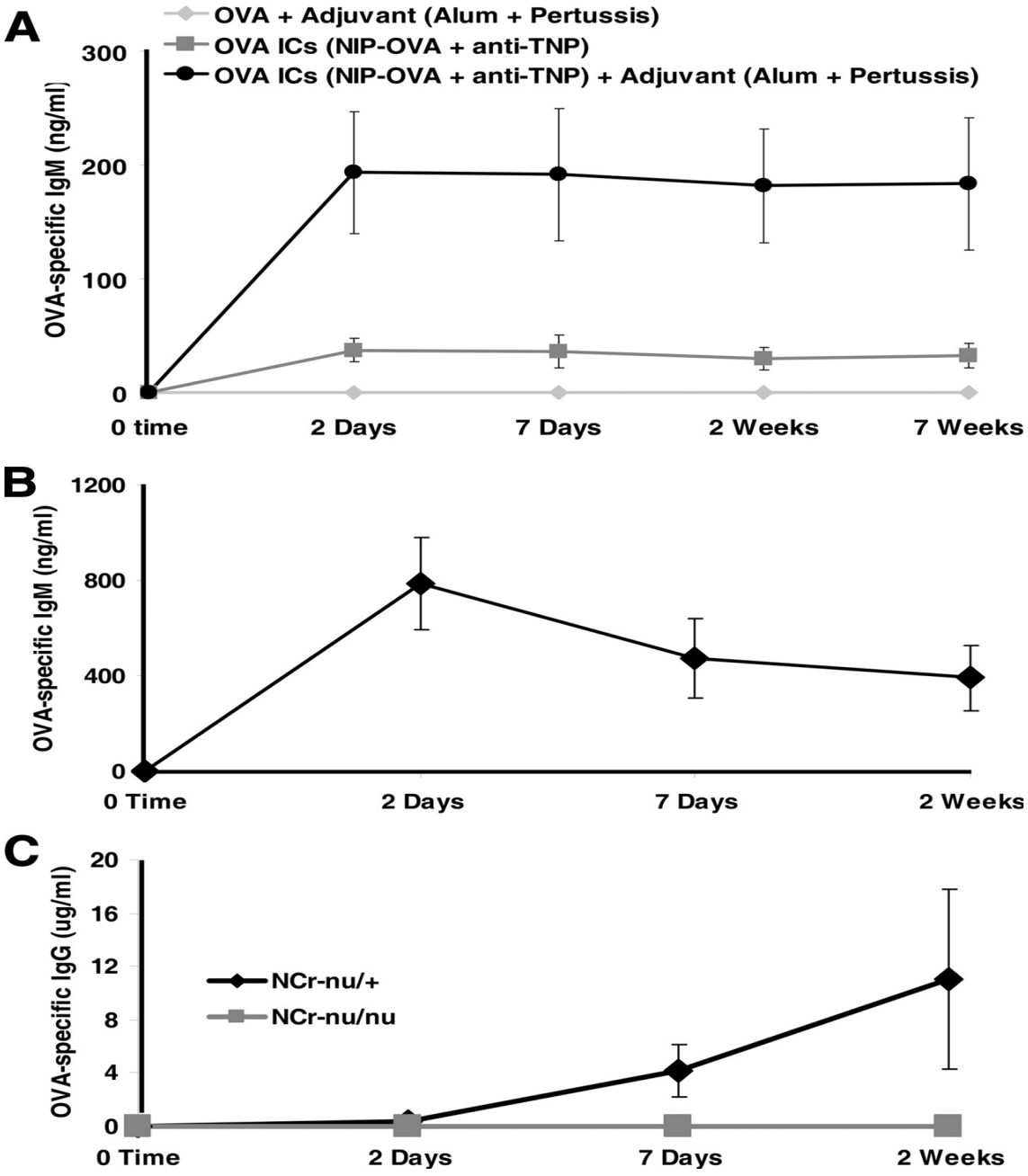
A
OVA + Adjuvant (Alum + Pertussis)
OVA ICs (NIP-OVA + anti-TNP)
OVA ICs (NIP-OVA + anti-TNP) + Adjuvant (Alum + Pertussis)
OVA-specific IgM (ng/ml)
300
200
100
0
0 time
2 Days
7 Days
2 Weeks
7 Weeks
B
OVA-specific IgM (ng/ml)
1200
800
400
0
0 Time
2 Days
7 Days
2 Weeks
C
OVA-specific IgG (ug/ml)
20
16
12
8
4
0
NCr-nu/+
NCr-nu/nu
0 Time
2 Days
7 Days
2 Weeks

Figure 2: ***Robust GC and plasmablast responses were induced in nude mice by OVA-ICs in 48 h and sustained for at least 1 wk in association with IC-retaining FDC-reticula.*** Groups of *nu/nu* mice were challenged with OVA-specific rabbit serum or normal (nonspecific) rabbit serum plus alum-precipitated OVA and *B. pertussis*. Two and 7 days later, mid-saggittal sections from axillary LNs were triple labeled with GL-7-FITC (green, GC-B cells), B220-Cy5.5 (magenta, pan-B cell marker), and Rhodamine Red X-goat anti-rabbit IgG (red, OVA-ICs in FDC-reticulum). GC-associated plasmablasts were labeled with anti-Blimp-1-PE (red). *A*, GCs were not detected in athymic *nu/nu* mice challenged with OVA and adjuvant at days 2 or 7. The B cell follicles labeled well with B220 (magenta) but not with the GC B cell marker GL-7 (green); thus, the overlay (B220/GL-7) was magenta. *B*, As early as 48 h, *nu/nu* mice challenged with OVA-ICs exhibited large GCs that were maintained at least for 1 wk. The GL-7^{bright} B cells (green) correspond with an area of $B220^{dim}$ labeling (magenta). The overlay (B220/GL-7) illustrates GL-7^{bright} GC B cells surrounded by a zone of resting $B220^{bright}$ B cells. *C*, Labeling with anti-rabbit IgG revealed well-developed, crescent-shaped, ARR (red) both at days 2 and 7. Funnel-shaped Ag transport site extending from the subcapsular sinus (indicated in this illustration by a red left bracket in the 7 day data) was seen in continuation with the ARR. In the overlay of the ARR and the GL-7, the GL-7^{+} GC B cells (green) were seen capped with the ARR (red) and the light zone of the GC where the FDC-ARR (red) overlapped with the GC B cells (green) appeared orange-yellow (areas between orange arrows). *D*, Blimp-1^{+} plasmablasts were found at the paracortical borders of multiple GCs (red arrowheads) both at days 2 and 7, and some migrated toward the medullary cords deeper in the node (green arrowheads). These cells were also GL-7^{+} (green) giving an orange overlay (yellow arrows).

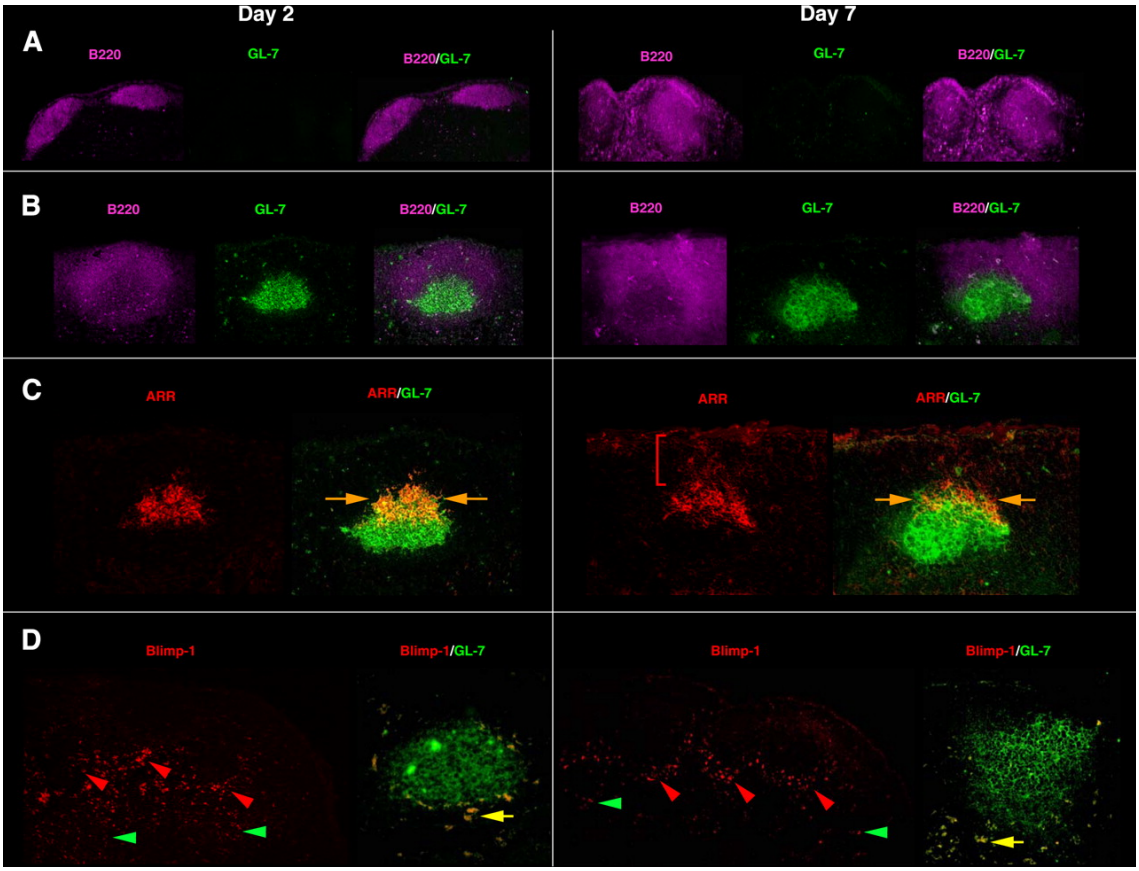
Day 2
Day 7
A
B220
GL-7
B220/GL-7
B220
GL-7
B220/GL-7
B
B220
GL-7
B220/GL-7
B220
GL-7
B220/GL-7
C
ARR
ARR/GL-7
ARR
ARR/GL-7
D
Blimp-1
Blimp-1/GL-7
Blimp-1
Blimp-1/GL-7

Figure 3: ***Purified OVA-IC-bearing FDCs induced OVA-specific IgM production by purified B cells within 48 h in the absence of T cells.*** Purified murine or human B cells were incubated with purified OVA-IC-loaded FDCs at a ratio of 1FDC:2B cells, and OVA-specific Abs were assessed after 48 h. Murine (*A*) and human (*B*) B cells stimulated with FDCs bearing OVA ICs produced OVA-specific IgM in 48 h. Control conditions that failed to produce a detectable response included FDCs with B cells stimulated with free OVA that would have had free access to BCRs. Data are represented as mean ± SD and are representative of two experiments of this type.

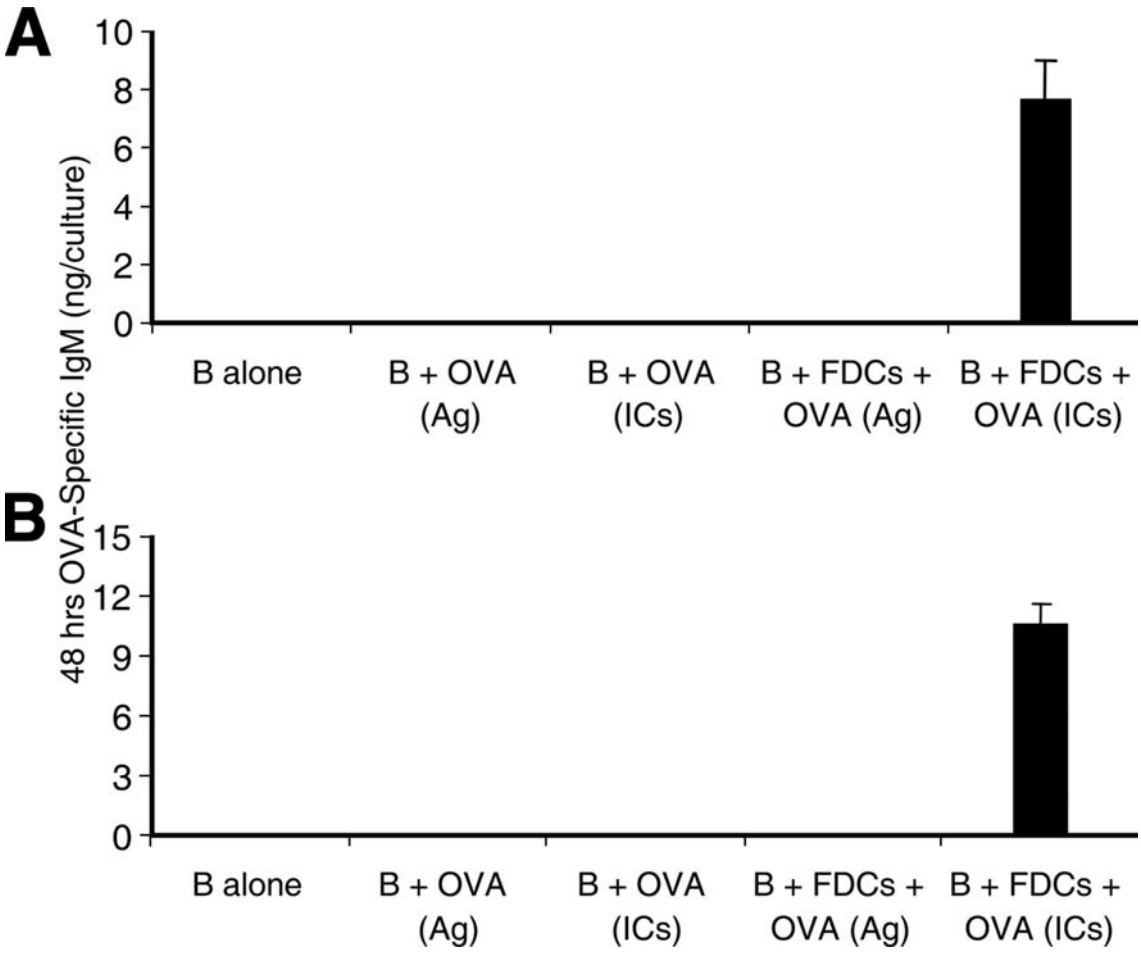
A
48 hrs OVA-Specific IgM (ng/culture)
10
8
6
4
2
0
B alone
B + OVA (Ag)
B + OVA (ICs)
B + FDCs + OVA (Ag)
B + FDCs + OVA (ICs)
B
15
12
9
6
3
0
B alone
B + OVA (Ag)
B + OVA (ICs)
B + FDCs + OVA (Ag)
B + FDCs + OVA (ICs)

ICs should engage multiple BCRs and induce signaling in the vast majority of B cells. B cell signaling may be indicated by increases in and redistribution of intracellular phosphotyrosine in the form of patches (patching) and owing to cell motility and cell surface fluidity such patches can aggregate to one pole of the cell in the form of caps (capping) (219,220). The anti-IgD mAb (rat anti-mouse IgD clone 11-26) was selected for study because, among a number of rat anti-mouse IgD mAbs tested, clone 11-26 does not induce B cell activation (216). This mAb was complexed with Fc-specific rabbit anti-rat IgG (leaving the Fabs free to engage BCRs) and loaded on the surface of FDCs. As shown in Fig. 4-A, phosphotyrosine labeling in unstimulated B cells was low and evenly distributed. In marked contrast, B cells stimulated with FDCs bearing anti-IgD ICs (Fig. 4-B) labeled more intensely and the phosphotyrosine was capped (fluorescence localized at one pole of the cell surface), or patched on the membrane indicating a marked redistribution. Most B cells exhibited the patched or capped intracellular phosphotyrosine pattern consistent with being signaled (Fig. 4-C). Moreover, flow cytometric analysis (Fig. 4-D) confirmed that the B cells exhibited higher levels of intracellular phosphotyrosine (increased MFI) and the entire B cell population had clearly shifted to the right suggesting that virtually the entire B cell population had been signaled by anti-IgD bearing FDCs. High magnification imaging revealed that the phosphotyrosine labeling (green) was intense at areas of contact between the B cell membrane and the AMCA-labeled IC-bearing FDCs (blue) (Fig. 4-E). In

addition, the activation marker GL-7 was induced when B cells were stimulated with anti-IgD IC-bearing FDCs *in vitro* (Fig. 4-F). Note the shift to the right, indicating increased GL-7 expression, when B cells were stimulated with anti-IgD IC-bearing FDCs. The MFI on the highest 33% of FDC-IC-stimulated B cells was almost 4 times that of the unstimulated B cell control. Blimp-1 expression was also induced by IC-bearing FDCs *in vitro* within 48 hrs. About 0.6% of B cells expressed Blimp-1 in control cultures lacking anti-IgD IC-bearing FDCs (Fig. 4-G), however, the addition of anti-IgD IC-bearing FDCs, (Fig. 4-H), induced a 4-fold increase (2.4%) and many cells showed high Blimp-1 levels. Moreover, B cell proliferation was induced by IC-bearing FDCs *in vitro* within 48 hrs. The response was IC-dependent since purified B cells cultured with FDCs alone (Fig. 4-I) or FDCs in addition to the mAb rat anti-m-IgD (Fig. 4-J) did not divide. In contrast, 30% of B cells stimulated with anti-IgD IC-bearing FDCs showed up to two rounds of division within 48 hrs in the absence of T cell and T cell factors (Fig. 4-K).

Purified B cells stimulated with anti-IgD-IC-bearing FDCs produced IgM within 48 hrs

Given that B cells are signaled by anti-IgD ICs on FDCs, we reasoned that the simultaneous engagement of multiple B cell receptors should signal, at least some B cells adequately, to rapidly produce IgM. Moreover, this should be possible in the absence of T cells or T cell factors as was seen in Fig. 3 with OVA ICs. As illustrated in Fig. 5-A, free anti-IgD, or anti-IgD-ICs alone, or in

the presence of complement-mediated accessory signals did not stimulate IgM production. Blockade of B cell-FcγRIIB to minimize ITIM signaling did not alter the lack of responsiveness. In marked contrast, anti-IgD-ICs loaded on FDCs stimulated polyclonal B cell IgM production within 48 hrs. This response was B cell number dependent ($1x10^4$ - $1x10^6$) as shown in Fig. 5-B but increasing doses of anti-IgD-ICs (0.1-10 μg/ml) did not improve IgM responses, indicating that 100 ng anti-IgD-ICs was an adequate agonist level.

Blockade of FDC-FcγRIIB, -C4BP, and –BAFF significantly inhibited IgM production by FDC-IC-stimulated B cells

We reasoned that the mechanism underpinning the TI FDC-dependent Ab response would require that FDCs deliver both primary and secondary signals to B cells. Periodically arranged Ag is thought to provide the first signal and FDC-FcγRIIB appears to be important in periodically arranging ICs such that extensive cross-linking of multiple BCRs can occur (34). As shown in Fig. 6, blockade of FDC-FcγRIIB with 2.4G2 and loading anti-IgD ICs on FDCs via complement receptors resulted in a significant inhibition of IgM production by FDC-IC-stimulated B cells (Fig. 6-A). Secondary signals in the form of FDC-C4BP and -BAFF are believed to promote B cell activation, proliferation and IgM secretion. Blockade of FDC-C4BP with FDC-M2 (Fig. 6-B) resulted in ~75% reduction in the IgM response suggesting that engagement of B cell CD40 is a critical part of the induction mechanism. Furthermore, FDCs produce BAFF and the level of FDC-BAFF produced was enhanced by the addition of OVA

ICs (Fig. 6-C), and this enhancement was abrogated by the FcR blocker 2.4G2 as previously reported for FDC-ICAM and VCAM (70). Addition of the decoy-BAFF-R-Fc (Fig 6-D) resulted in 20% inhibition of IgM production [from 633 $\pm$ 17 to 503 $\pm$ 58 with p value <0.02] by the FDC-IC-stimulated B cells indicating that FDC-BAFF, together with FDC-FcγRIIB and –C4BP, play important roles in the mechanism involved in the FDC-dependent induction of TI Ab responses to T-dependent Ags.

Figure 4: ***B cell signaling induced by FDC-anti-IgD-ICs in vitro was indicated by intracellular phosphotyrosine distribution, expression of activation marker GL-7, plasmablast differentiation, and B cell proliferation.*** Purified B cells were stimulated with anti-IgD-IC-bearing FDCs for 45 min, and the distribution of phosphotyrosine was analyzed. *A*, Phosphotyrosine labeling in unstimulated B cells was low and evenly distributed when visualization with confocal microscopy. *B*, FDC-ICs led to B cell signaling, as indicated by increases in and redistribution of intracellular phosphotyrosine in the form of patches (magenta arrowhead) and caps (yellow arrowhead). *C*, Most B cells exhibited the patched or capped intracellular phosphotyrosine pattern, consistent with being signaled. *D*, Flow cytometric analysis indicated that the entire B cell population had shifted to the right, suggesting that virtually all B cells had been signaled by anti-IgD-bearing FDCs, resulting in increased intracellular levels of phosphotyrosine. *E*, High magnification imaging revealed that the phosphotyrosine labeling (green) was intense at areas of contact (white arrowheads) between the B cell membrane and the 7-amino-4-methylcoumarin-3-acetic acid-labeled ICs on FDCs (blue). *F*, Purified B cells were stimulated with anti-IgD IC-bearing FDCs for 48 h and labeled with anti-GL-7 or isotype control, and GL-7 expression was assessed by flow cytometry. Compared with the isotype control (red, MFI = 2) and the unstimulated B cell control (black, MFI = 2.5), B cells stimulated with anti-IgD IC-bearing FDCs (green) shifted to the right indicating increased GL-7 expression and an MFI of 9.0 on the highest 33% of activated B cells. *G* and *H*, Purified B cells were incubated for 48 h alone or with anti-IgD IC-bearing FDCs and labeled with PE-conjugated anti-Blimp-1. Approximately 0.6% of the isolated B cells expressed Blimp-1 (*G*). However, the addition of anti-IgD IC-bearing FDCs (*H*) induced a 4-fold increase (2.4%), and many cells in *H* were in the second and third decades of the Blimp-1-PE (*y*)-axis, indicating high Blimp-1 expression. *I–K*, Purified B cells cultured with FDCs alone (*I*) or FDCs in addition to the mAb rat anti-m-IgD (*J*) did not divide, whereas 30% of B cells stimulated with anti-IgD IC-bearing FDCs showed up to two rounds of division within 48 h in the absence of T cell and T cell factors (*K*). All results are representative of at least three separate experiments.

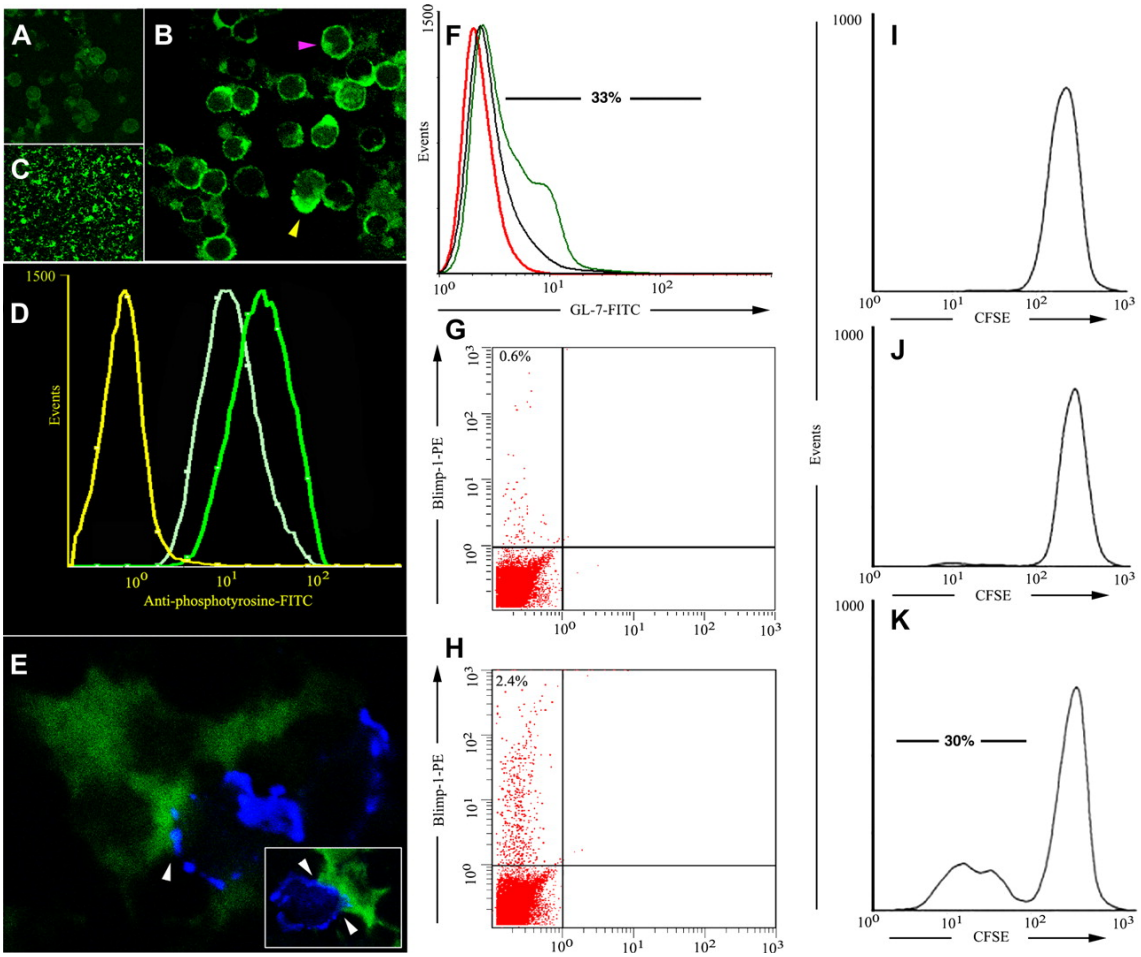
A
B
C
D
1500
Events
10^0
10^1
10^2
Anti-phosphotyrosine-FITC
E
F
1500
Events
33%
10^0
10^1
10^2
GL-7-FITC
G
0.6%
Blimp-1-PE
10^0
10^1
10^2
10^3
H
2.4%
Blimp-1-PE
I
1000
CFSE
J
1000
CFSE
K
1000
30%
CFSE
Events

Figure 5: ***Purified FDCs bearing anti-IgD-ICs on their surfaces induced IgM production by purified B cells within 48 h in a B cell number-dependent manner.*** The rat anti-mouse IgD mAb clone 11–26, which does not per se induce proliferation of mature B cells in vitro nor activate B cells in vivo, was complexed with Fc-specific rabbit anti-rat IgG. *A*, Purified B cells (10^5) were cultured under different conditions, and IgM production was assessed by ELISA 48 h later. As expected, free anti-IgD mAb (1 μg), or anti-IgD-ICs alone, or in the presence of complement-mediated accessory signals did not stimulate IgM production, and blockade of B cell-FcγRIIB to minimize ITIM signaling did not alter the lack of responsiveness. However, anti-IgD-ICs loaded on FDCs stimulated polyclonal B cell IgM production within 48 h. *B* shows that the IgM response was B cell number dependent and that 100 ng of anti-IgD loaded as ICs on FDCs was an adequate stimulus. Data are represented as mean ± SD and are representative of three experiments of this type.

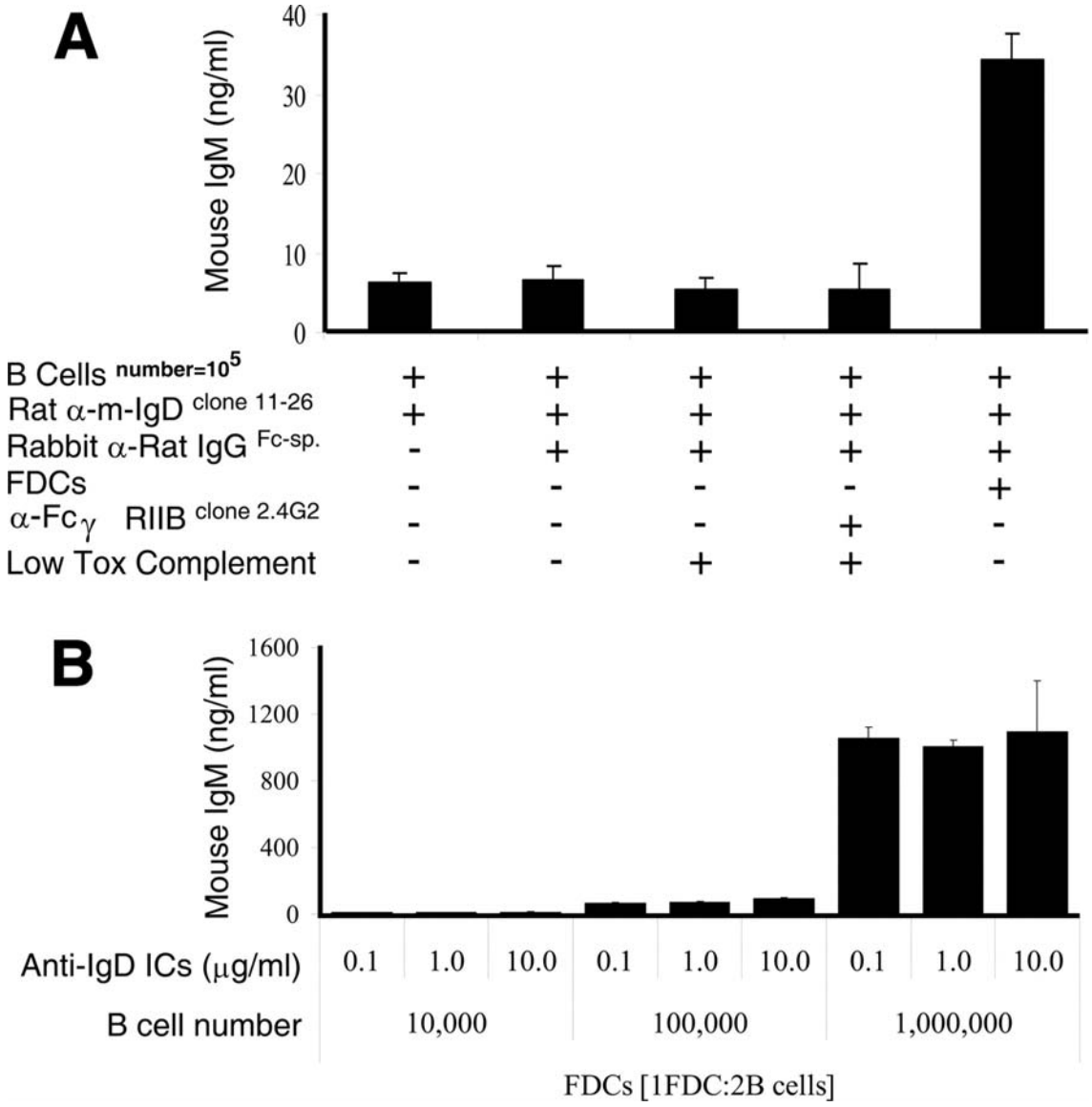
A
Mouse IgM (ng/ml)
40
30
20
10
0
B Cells number=10^5 + + + + +
Rat α-m-IgD clone 11-26 + + + + +
Rabbit α-Rat IgG Fc-sp. - + + + +
FDCs - - - - +
α-Fcγ RIIB clone 2.4G2 - - - + -
Low Tox Complement - - + + -
B
Mouse IgM (ng/ml)
1600
1200
800
400
0
Anti-IgD ICs (μg/ml) 0.1 1.0 10.0 0.1 1.0 10.0 0.1 1.0 10.0
B cell number 10,000 100,000 1,000,000
FDCs [1FDC:2B cells]

Figure 6: ***Blockade of FDC-FcγRIIB, -C4BP, and -BAFF significantly inhibited IgM production by FDC-IC-stimulated B cells.*** *A*, FDC-FcγRIIB was blocked with 2.4G2, and anti-IgD ICs, incubated in 10% Low Tox Complement, were trapped using complement receptors. Anti-IgD ICs did not stimulate B cells in the absence of FDCs, and IgM production by FDC-IC-stimulated B cells was significantly inhibited by blockade of FDC-FcγRIIB, which is involved in the periodicity of ICs. *B*, Half million B220-purified B cells were stimulated with 0.25×10^6 anti-IgD IC-bearing FDCs in the presence or absence of 1 μg/ml C4BP-blocking FDC-M2 for 48 h, then IgM production was assessed by ELISA. The addition of FDC-M2 resulted in ~75% reduction in IgM production. Control conditions of B cells alone, and B cells plus anti-IgD ICs, did not stimulate IgM production by purified B cells. *C*, One million FDCs were cultured for 48 h, and BAFF production was assessed. Addition of 100 ng/ml soluble OVA (OVA Ag) did not significantly increase BAFF production over levels produced by FDCs alone. Addition of OVA in the form of ICs significantly increased BAFF production by FDCs ($p < 0.001$). This enhancement was minimized by the addition 10 μg/ml FcR blocker 2.4G2 ($p < 0.005$ for FDCs + OVA-ICs vs FDCs + 2.4G2 + OVA-ICs). Replacement of 2.4G2 with its isotype control rat IgG2b restored the enhancement ($p = 0.2$ for FDCs + OVA-ICs vs FDCs + isotype Ctrl + OVA-ICs, and $p < 0.01$ for FDCs + 2.4G2 + OVA-ICs vs FDCs + isotype Ctrl + OVA-ICs). *D*, One million B220-purified B cells were stimulated with 0.5×10^6 anti-IgD IC-bearing FDCs in the presence or absence of 1 μg/ml decoy BAFF-R-Fc for 48 h; then, IgM production was assessed by ELISA. Addition of the decoy-BAFF-R-Fc resulted in 20% inhibition of IgM production (from 633 ± 17 to 503 ± 58 with $p < 0.02$). Control conditions of B cells alone, B cells plus anti-IgD mAb, B cells plus anti-IgD ICs, and B cells plus anti-IgD mAb plus FDCs did not result in B cell stimulation and IgM production, indicating the importance of FDC-ICs in the IgM response. Data are represented as mean ± SD and are representative of three experiments of this type.

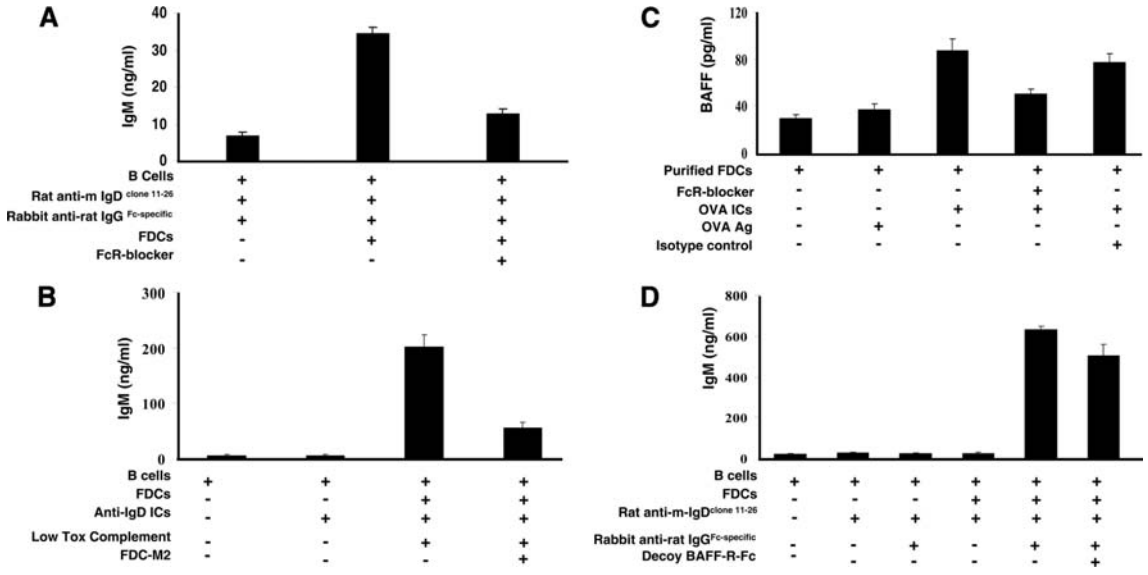
A
IgM (ng/ml)
40
30
20
10
0
B Cells
Rat anti-m IgD clone 11-26
Rabbit anti-rat IgG Fc-specific
FDCs
FcR-blocker
B
IgM (ng/ml)
300
200
100
0
B cells
FDCs
Anti-IgD ICs
Low Tox Complement
FDC-M2
C
BAFF (pg/ml)
120
80
40
0
Purified FDCs
FcR-blocker
OVA ICs
OVA Ag
Isotype control
D
IgM (ng/ml)
800
600
400
200
0
B cells
FDCs
Rat anti-m-IgD clone 11-26
Rabbit anti-rat IgG Fc-specific
Decoy BAFF-R-Fc

Discussion

The data presented here support the novel concept that FDCs can convert TD Ags into TI Ags capable of inducing specific IgM responses in 48 hrs or less. We were prompted to test this concept after: 1) observing TD-Ags in ICs on FDCs periodically spaced 200-500 Å apart (24,34), which is consistent with recurring epitopes 95-675 Å apart on the flexible backbone of an ideal TI-2 Ag (98,210); 2) noting the ability of FDCs to provide BAFF and C4BP which are known to support TI B cell activation (59-62,213,214). These relationships are illustrated in the model shown in Fig. 7, and more details are provided in the figure legend. We report here that nude mice, pre-treated with anti-Thy-1 to minimize any residual T cell activity, responded to ICs by producing specific IgM in 48 hrs while free Ag in adjuvant did not induce IgM in nude mice even after many weeks. In contrast, normal mice challenged with Ag in adjuvant induced detectible IgM in 4 days followed by IgG (Data not shown), and phenotypically normal *nu/+* mice injected with ICs exhibited the rapid IgM response followed by a switch to IgG, which we attribute to T cell help that is lacking in the *nu/nu* mice (Fig. 1). Moreover, the draining lymph nodes of IC-challenged nude mice exhibited well developed GL-7^+ GCs associated with ARR and Blimp-1^+ plasmablasts within 48 hrs that persisted for at least one week, further supporting the concept that B cells in the follicles are stimulated by the ICs on FDCs. In contrast, GCs and plasmablasts were lacking in Ag immunized nude controls where the B cells remained in the resting state

consistent with the lack of T cell help. TI-2 Ags have been used to load FDCs and induce GCs in animals lacking cognate T & B cell interactions. When mice with mutations that inactivate the *TCR Cβ* and *Cδ* genes were immunized with 4-hydroxy-3-nitrophenylacetyl (NP)-Ficoll, GCs with peanut agglutinin-binding B cells were observed in the splenic follicles. These GCs contained mature IC-bearing FDCs and although they were rapidly induced, their duration was short (104). We reason that engagement of FDC-FcγRIIB by IgG-TD Ag ICs induces FDC activation and production of FDC-BAFF and other trophic factors that maintain GCs. These *in vivo* studies were supported by *in vitro* experiments where highly purified IC-bearing FDCs and naïve B cells from humans or mice were co-cultured in the absence of T cells or T cell factors. B cells stimulated with IC-bearing FDCs in these cultures produced specific IgM in 48 hrs while no response was observed when ICs were replaced with free Ag. Both the kinetics of the response and the IgM production are consistent with TI responses. Furthermore, rat anti-mouse IgD mAb clone 11-26, which by itself does not activate B cells (216), became a potent B cell activator when loaded on FDCs in the form of ICs capable of simultaneously binding and cross-linking multiple BCRs. Within 48 hrs, activation was indicated by increased tyrosine phosphorylation in virtually all B cells along with patching and capping together with expression of the B cell activation marker GL-7, Blimp-1^{+} plasmablast differentiation, and B cell proliferation assessed by the CFSE dilution assay. Moreover, this signaling appeared to be productive in that FDCs bearing those

Figure 7: ***Model illustrating FDC-dependent, T-independent B cell activation and Ig production.*** *A*, Monomeric proteins generally express only a single copy of each antigenic determinant, making them unable to cross-link multiple BCRs and activate B cells in the absence of T cell help. *B*, TI-2 Ags contain numerous periodically arranged epitopes (green protrusions) attached to a flexible backbone (red curve). This arrangement allows extensive simultaneous cross-linking of BCRs (Y-shaped green). The multiple BCR cross-linking delivers a signal leading to B cell activation and Ig production. *C*, FDCs express high levels of FcγRIIB (red) and CRs (blue), which trap ICs containing TD Ags (multicolor clusters). ICs loaded via FcγRIIB alone exhibited periodicity of 200–500 Å apart (18), and we reasoned that this spatial arrangement would allow cross-linking of multiple BCRs specific for a single epitope, leading to B cell activation and Ig production as in *B. D*, Transmission electron micrograph showing HRP (a TD Ag) retained on the FDC surface in IC clusters 200–500 Å apart. This facilitates BCR cross-linking and B cell activation as explained in *B* and *C. E*, FDCs accessory activity includes secondary signals or cosignals that promote B cell activation and Ig production. Specifically, FDC-derived BAFF (22 44) ligates BAFF receptors on B cells, and FDC-derived C4BP (21) ligates B cell-CD40, which is a classical cosignal in B cell activation. *F*, B cells stimulated with IC-bearing FDCs, FDC-BAFF, and FDC-C4BP rapidly differentiate into plasma cells and secrete Ag-specific IgM.

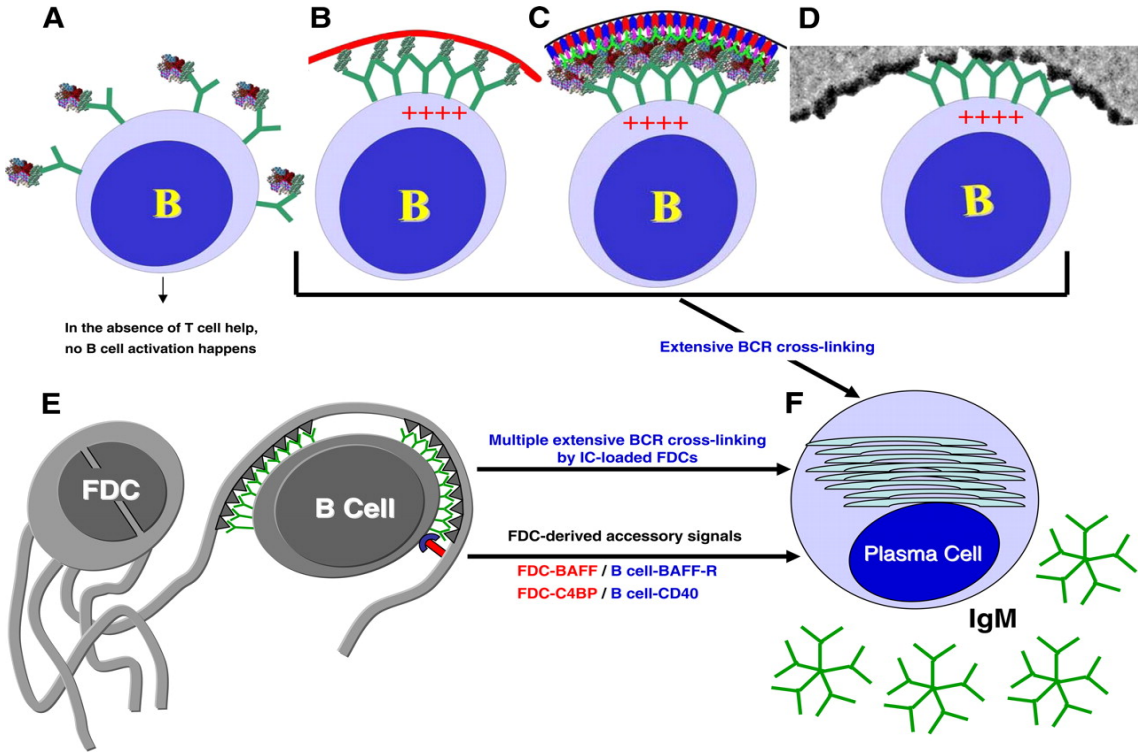
A
B
C
D
B
B
B
B
++++
++++
++++
In the absence of T cell help,
no B cell activation happens
Extensive BCR cross-linking
E
F
FDC
B Cell
Multiple extensive BCR cross-linking
by IC-loaded FDCs
FDC-derived accessory signals
FDC-BAFF / B cell-BAFF-R
FDC-C4BP / B cell-CD40
Plasma Cell
IgM

ICs induced polyclonal IgM in 48 hrs consistent with a TI response. Thus, we conclude that TD Ags in the form of ICs can induce specific IgM responses in an FDC-dependent but T cell independent fashion.

The concept that TD proteins can trigger B cells when appropriately arranged is supported by a number of reports in the literature. Studies on the requirements for generation of Ab responses to repetitive determinants on polymers, polysaccharides and higher order structures such as viral capsid proteins indicated that high molecular weight arrays of Ag are efficient in eliciting an Ab response independent of T-cell help, whereas their less ordered counterparts are less immunogenic and require T-cell help (97,221,221,222). Certain bacteria, viruses, mammalian cells, some polymeric proteins like collagen, and hapten-protein complexes have repeating antigenic determinants. The multivalent presentation of antigenic determinants extensively cross-links BCRs and leads to B cell activation, proliferation, and Ig secretion that is characteristic of TI-2 responses. For example, multimerization of monomeric proteins by aggregation facilitates presentation of their Ag determinants in a highly arrayed structure fit for cross-linking BCRs and inducing Ab responses in the absence of T cell help (222).

In addition, FDCs deliver secondary or co-stimulatory signals to B cells and the data presented here provide support for the involvement of FDC-C4BP that signals via B cell CD40, and FDC-BAFF that engages the B cell BAFF receptor. A role for other FDC molecules involved in signaling has not been

ruled out. For example, CD21L on FDCs engages CD21 in the B cell co-receptor complex and CD21L-CD21 interactions not only promote Ag specific recall responses but also polyclonal responses induced by LPS (29,223). In addition, FDC-8D6 as well as BAFF inhibit B cell apoptosis (60,63,65,114,115); FDCs block IC mediated ITIM signaling in B cells via FcγRIIB and minimize this inhibitory pathway (30,57,58), and FDCs provide IL-6 for terminal B cell differentiation (68).

Classic TI-2 Ags induce robust responses in splenic marginal zones (MZs) while lymph nodes are not heavily involved (224). In this respect, the reported FDC-dependent T-independent response appears to differ from classic TI-2 Ags. ICs are loaded on FDCs within minutes after Ag challenge (37) and follicular B cells appear to be heavily involved (Fig. 2). Lymph node responses are robust with GCs and plasmablasts apparent within 48 hrs. However, a role for other B cell subsets that can interact with the ICs in the FDC-ARR has not been ruled out. The anatomical proximity of the MZ to the splenic B cell follicles, where FDCs reside in the spleen, make it likely that a dynamic interaction between both compartments exists. An elegant commentary recently published on the follicular dimension of MZ B cells concluded with the a question whether MZ-B cells can be triggered to respond to Ags on FDCs when they visit the splenic follicles or not (225) and we plan to extend this work and test this possibility.

Responses to classical TI antigens appear to be more robust when T cells are present (97). The reported FDC-dependent TI response appears to be similar in that the 48 hr IgM responses in *nu/+* mice were higher than in *nu/nu* mice (Fig. 1). Moreover, IgM production induced by FDC-ICs *in vitro* was also significantly enhanced at 48 hrs in the presence of normal T cells (Data not shown). The enhanced IgM response that occurs within 48 hrs is not likely attributable to MHC class II-restricted T-cell help as a period of ~48 hrs is needed before primed T cells are able to provide cognate T cell help. However, cytokines and other T cell derived trophic factors may be present. For example, activated FDCs produce BAFF, IL-6, and IL-15 and these cytokines can rapidly induce cytokine production by conventional T cells (226-230). Moreover, NK T cells and γδT cells that mediate non-MHC class II-restricted non-cognate help may be a source of B cell activation factors within 48 hrs. We were impressed by the decline in IgM titers in *nu/+* mice and we suspect that this will continue and this contrasts with the *nu/nu* mice that maintained their IgM for 7 weeks.

The short time required to induce FDC-dependent TI IgM responses may have practical application. IgM is the first class of antibodies produced during a primary Ab response and it plays important roles in host protection [reviewed in (231)]. Moreover, its multimeric structure makes it a strong complement activator; a single bound IgM pentamer can trigger the classical pathway of complement activation and can lyse a red blood cell, while approximately a thousand IgG molecules are required to accomplish the same (232). In synergy

with complement, IgM offers immediate protection to systemic bacterial and viral infections (3) and patients with normal IgG levels but selective IgM deficiency suffer from morbid recurrent upper respiratory tract infections, asthma, celiac disease, and meningitis (233,234). Other potential applications include countering the negative effect of regulatory T cells and the non-responder state as a consequence of a limited MHC-II repertoire that may be unable to load certain peptides. We reason that individuals who fail to respond to a vaccine, as a consequence of problems with Ag presenting cells or the effect of T regulatory cells, should mount rapid specific IgM responses when immunized with appropriate ICs. The ICs should load on FDCs and bypass limitations imposed by MHC and T cells. Similarly, specific IgM responses should be inducible in animals or people with congenital and/or acquired T cell insufficiencies (235,236) including HIV infected (237), aged (238), diabetic (239), uremic (240) and neonates (241,242). We look forward to experiments designed to test these postulates.

CHAPTER 6

In vitro Induction of Human Primary Antibody Responses: A Novel Model for Rapid Vaccine Assessment

Introduction

In vivo studies of human immune responses to therapies and vaccines are limited by technical and ethical considerations. Studies with closely related non-human primates are confronted by problems such as the high cost, limited availability, paucity of genetic models for human diseases, and lack of genetically inbred strains suitable for stem cell or tissue transplantation. Studies in mice have been helpful in demonstrating the feasibility of stem cell transplantation and some other therapies; but, rodents are not humans, and human-related studies carried out solely in mice might not accurately predict the real outcome in humans.

Inspite of progress that has been achieved since the inception of these models, major limitations prevent them from being fully representative of the human immune system. For example, the mouse thymus lacks the expression of HLA class I and II, which is required for the selection of T cells after human stem cell (HSC) engraftment. And inspite of the recent approach of transgenic expression of human HLA molecules in mice engrafted with HSCs, the limited diversity in the human major and minor histocompatibility alleles that can be expressed in a mouse, renders these optimized models inadequate to fully represent the human system (243).

The initiation of an adaptive immune response in vivo is dependent not only on an efficient cross talk between the major players of the immune system, but also on a highly compatible and competent interaction between the immune

system cells and other molecules and non-immune cells, such as the stromal cells in primary and secondary lymphoid tissues. Despite the recent reports by the Garcia group, where humanized mice intrarectally infected with HIV showed depletion of T cells similar to humans, there was a significant difference in the phenotype of T cells in the humanized mice guts if compared to human gut CD4+T cells. T cells in the humanized mice guts showed low levels of CXCR4, compared to the co-expression of CCR5 and CXCR4 by human gut CD4+ T cells (244,245).

Several attempts have been made to further manipulate the humanized mouse model to render it physiologically close enough to fully represent the human systems. One approach was the addition of human endothelium, growth factors, and chemokines, which might help promote the appropriate trafficking and expansion of human cells. Another approach was to engraft artificial lymph nodes consisting of biocompatible scaffolds containing human stromal cells in the humanized mouse models (243).

However, even the optimized humanized mouse model does not solve the problem of the variation in the individual human immune responses to certain vaccines. Each person's immune cells would be needed in a separate mouse model to faithfully predict specifically his/her response to a tested vaccine. The inpracticality of this approach and the increased desire for the reduction of the number of animals used to test vaccines, the animal suffering, and finding replacement methods for the biological quality control testing of the

human vaccines argues for the development of an efficient human in vitro immune system response-testing model.

Unfortunately, induction of specific primary human antibody (Ab) responses *in vitro* has been challenging (246-252). This is attributable, at least in part, to the natural scarcity of antigen (Ag)-specific T and B cells in non-immune individuals as well as the complexity of circuits controlling lymphocyte activation and proliferation (253)..

The functional element of a human lymph node or spleen is the follicle, which develops a germinal center (GC) when stimulated by antigen (11,106,107,125,187,188,218,254-258). The GC is the "hot spot" in the lymph node or spleen where critical interactions take place in developing an effective humoral immune response. Upon antigen stimulation, follicles are replicated and an active human lymph node can have dozens of active follicles with functioning GCs. Interactions between B cells, T cells, and follicular dendritic cells (FDCs) take place in GCs. These interactions result in stimulation of Ab specific B cells, Ig class switching, somatic hypermutation, and the selection of high affinity B cells responsible for affinity maturation and the production of high quality Ab (35,39).

In this study, we sought to design *in vitro* GCs to examine humoral responses to vaccines. Succinctly, while T cells are necessary for B cell responses to T dependent Ags, they are not sufficient for the development of fully functional and mature Ab responses that are required to assess most

vaccines. FDCs provide critical assistance needed for the B cells to achieve their full potential and accessory functions of FDCs and regulation of these functions is critical to an understanding of fully functional and mature Ab responses (35,38,40,44,45,159,259).

Mature Ab responses involve dendritic cell (DC) maturation, Ag processing, MHC-restricted Ag presentation, $CD4^+$ T cell priming, B cell activation, immune complex (IC) formation, IC trapping by FDCs, FDC-B cell interactions leading to clonal selection, somatic hypermutation and affinity maturation. When responding to T cell dependent Ags *in vivo,* these processes reach maturity in GCs. Accordingly, we sought to generate primary Ab responses in temporally-controlled GC reactions (GCRs) *in vitro* by sequential integration of the activated cellular components (260-264).

Antibody responses are greatly influenced by the form of antigens and T cell help. Consequently, we started by characterizing the effect of these variables in well-defined test models prior to their integration in the *in vitro* model. Results showed that mature Ag-pulsed DCs are competent in priming $CD4^+$ T cells *in vitro*, while antigens trapped in the form of ICs on the surface of FDCs efficiently stimulated B cells. Moreover, B cell help by cognate Ag-specific T cells was an absolute necessity for class switching and affinity maturation.

To develop our *in vitro* model, immature monocyte-derived DCs (mDCs) were pulsed with Ovalbumin (OVA) or recombinant protective antigen of

Bacillus anthracis (rPA) for processing. Bacterial lipopolysaccharide (LPS) was used as maturation signals for mDCs. Negatively selected $CD4^+$ T cells were added for priming and ten days later, naïve B cells and FDCs bearing Ags in the form of ICs were added. Ag specific IgM and IgG were assessed by ELISA at different intervals, affinity maturation was assessed by salt dissociation, and cultures were microscopically examined for morphological alterations and cluster formation. Preliminary results show the clustering of $CD4^+$ T cells with DCs through the 10 days of priming and fusion with FDC-B cell clusters when GCRs were induced. An initial response dominated by Ag-specific IgM was observed in the first week followed by class switching to a dominant IgG response in the second week. In addition, preliminary results suggest an increase in Ag specific IgG affinity in the second week and imply the increased efficiency of this *in vitro* model in predicting the human immune response to certain antigens like HIV-gp120 than experimental murine models.

In summary, Ag specific affinity matured primary human Ab responses, with class switching from specific IgM to IgG was generated in GCRs entirely *in vitro* thus providing the means for individually and safely assessing emerging vaccines and therapeutics in a human immune system.

Materials and Methods

Mice

Normal 8–12 wk old BALB/c mice were purchased from the National Cancer Institute (Frederick, MD) or The Jackson Laboratory (Bar Harbor, ME). The mice were housed in standard plastic shoebox cages with filter tops and maintained under specific pathogen-free conditions in accordance with VCU Animal Care and Use guidelines. Food and water were supplied *ad libitum*.

Germinal center reactions in vitro

To induce a human antigen-specific GCR *in vitro*, the different cellular components of the GC were prepared as follows:

(1) Peripheral blood mononuclear cells (PBL) were obtained from heparinized blood by density centrifugation using Lymphocyte Separation Medium (ICN, Aurora, OH). Cells were centrifuged at 400 x *g* for 20 minutes, the cells were collected from the interface and washed three times in RPMI 1640 media (Cellgro, VA). After washing the cells were suspended in RPMI-1640 supplemented with 10% of fetal calf serum (HyClone, Logan, Utah) and antibiotics for cell culture.

(2) $CD14^+$ human monocytes were isolated on MACS columns from the PBLs using CD14 MicroBeads, human, (Miltenyi Biotech, # 130-050-201).

(3) Monocyte-derived dendritic cells (mDCs) were generated by treating 10^7 $CD14^+$ cells with a mixture of IL-4 (50 ng/ml) and GM-CSF (50 ng/ml). Two days later the cells were fed with another dose of the cytokines to enhance

their differentiation. On day 5, LPS was added at 1 μg/ml concentration together with 1 μg/ml OVA or rPA to provide Ag for processing and LPS for DC maturation.

(4) After 8 hours, 20 x 10^6 $CD4^+$ T cells isolated by Naïve $CD4^+$ T Cell Isolation Kit II, human, (Miltenyi Biotech, #130-094-131) were added and left for 5 days for DCs to present OVA and prime the $CD4^+$ T cells.

(5) At the end of the 5 days the T cells and remaining DCs were spun down and 15 x 10^6 naïve B lymphocytes were isolated and added to them together with FDCs loaded with 5 μg OVA or rPA in ICs.

(6) Murine FDCs were isolated from lymph nodes (axillary, lateral axillary, inguinal, popliteal, mesenteric, and paraaortic) of normal young adult mice as previously described (130). In brief, One day before isolation, mice were irradiated with 1000 rad to eliminate most lymphocytes, and one day later mice were killed, and LNs were collected, opened, and treated with 1.5 ml of collagenase D (22 mg/ml, C-1088882; Roche), 0.5 ml of DNase I (5000 U/ml, D-4527; Sigma-Aldrich), and 2 ml of DMEM with 20 mM HEPES buffer. After 45 min at 37°C in a CO2 incubator, released cells were washed in 5 ml of DMEM with 10% FCS. Cells were then sequentially incubated with FDC-specific Ab (FDC-M1) for 45 min, 1 μg of biotinylated anti-rat kL chain for 45 min, and 20 μl of anti-biotin microbeads (Miltenyi Biotec) for 15–20 min on ice. The cells were layered on a MACS LS column and washed with 10 ml of ice-

cold MACS buffer. The column was removed from the VarioMACS, and the bound FDCs were released with 5 ml of MACS buffer.

Cultures were assessed microscopically and differentiated cells were tracked with specific mAbs and examined with confocal microscopy. Culture supernatant fluids were collected one and two weeks later and OVA- and rPA-specific IgG and IgM were assessed by ELISA.

Affinity maturation in vitro

Generation of high affinity antibodies is important for efficient immune responses. To test for affinity maturation *in vitro* we used a simple salt dissociation method for human cultures. In the salt dissociation method, we let OVA-specific IgG produced in 5 and 10 days old *in vitro* cultures to bind OVA coated plates. Two hours later, 1/16M-4M NaCl was used to dissociate the bound Abs for an hour on a shaker. Plates were washed and the remaining bound Abs (higher affinities) were detected using alkaline phosphatase labeled anti-human IgG and the optical densities (ODs) were obtained using an ELISA reader.

In vitro GCRs versus animal models in predicting human immune responses

Animal models and *in vitro* models may be equally valid in testing the human response to antigens that do not directly modify the response of the immune cells. However, antigens that have species-specific effects may be tested in animals but the results cannot be extrapolated from one species to the other. For example, gp120 is a glycoprotein exposed on the surface of the HIV

that binds human but not murine CD4 on CD4-expressing T cells (265-268). We reasoned that gp120 would block the T cell help if tested on human cells, whereas, a normal response would be generated if tested in BALB/c mice. To test our reasoning and consequently the efficiency of our *in vitro* human model, we immunized BALB/c mice with gp120 and tested their sera for mouse anti-gp120, 7 and 14 days later using ELISA. In parallel, we generated human *in vitro* GCRs against gp120 and tested the culture supernatant fluids for human anti-gp120, 7 and 14 days later and both assessment techniques were compared.

Results

Germinal center-like in vitro clusters

Preliminary results showed the clustering of mature antigen-loaded monocyte-derived dendritic cells with CD4 T cells, and we reason this promted T cell priming. Preliminary confocal microscopy studies showed well-developed clusters of antigen-specific CD4 T cells associated with DCs. Additionally, B cells clustered with FDCs, and formed a B cell zone of FDCs and B cells segregated from the T cell zone in the GCR. Moreover, B cell proliferation resulted in the development of a high density and low density compartments similar to the dark and light zones of GCs *in vivo* (data not shown).

Induction of primary human immune responses to OVA and rPA in vitro

As shown in Fig. 1, GCRs *in vitro* were productive only in the presence of OVA-specific T cells and OVA-IC-loaded FDCs indicating the importance of specific T and FDC help to the antigen-specific B cells. Responses were typical of a T cell-dependent response in that, Ag-specific IgM dominated in the first week and that was followed by class-switching to Ag-specific IgG in the second week. Preliminary results with rPA showed a specific response similar to that of Ova (data not shown).

Affinity maturation in vitro

Preliminary studies using a simple salt dissociation method showed that the human *in vitro* immune responses exhibited higher affinity of Ag-specific Abs as they progress from the first week (5 days) to the second week (10 days).

(data not shown), at all molar concentrations of NaCl, bound Abs that resisted dissociation by the addition of salt (high affinity Abs) were higher at day 10 as compared to day 5 (data not shown).

HIV-gp120 failed to induce Ag-specific IgG responses in human in vitro GRCs despite the generation of normal responses in BALB/c mice

Our preliminary results showed that challenging BALB/c with gp120 induced a normal T cell dependent response dominated by Ag-specific IgM in the first week that switched to gp120-specific IgG in the second week. In contrast, gp120 failed to induce class switching even after two weeks of setting up *in vitro* human GCRs (data not shown). The gp120 binds human CD4 T cells specifically, and inhibits T cell priming and we reason that this resulted in a lack of class switching in these cultures. The fact that FDCs bear ICs in a periodic arrangement capable of engaging multiple BCRs and induction of T-cell independent responses can explain production of gp120-specific IgM in the first week that persisted through the second week (34).

Figure 1: ***Induction of primary human immune responses to OVA.*** Germinal centers developed *in vitro* where productive only in the presence of OVA-specific T cells and OVA IC-loaded FDCs indicating the importance of specific T and FDC help to the antigen-specific B cells. Responses were typical of a T cell-dependent nature. They were dominated by OVA-specific IgM **(A)** in the first week that class-switched to OVA-specific IgG in the second week **(B)**.

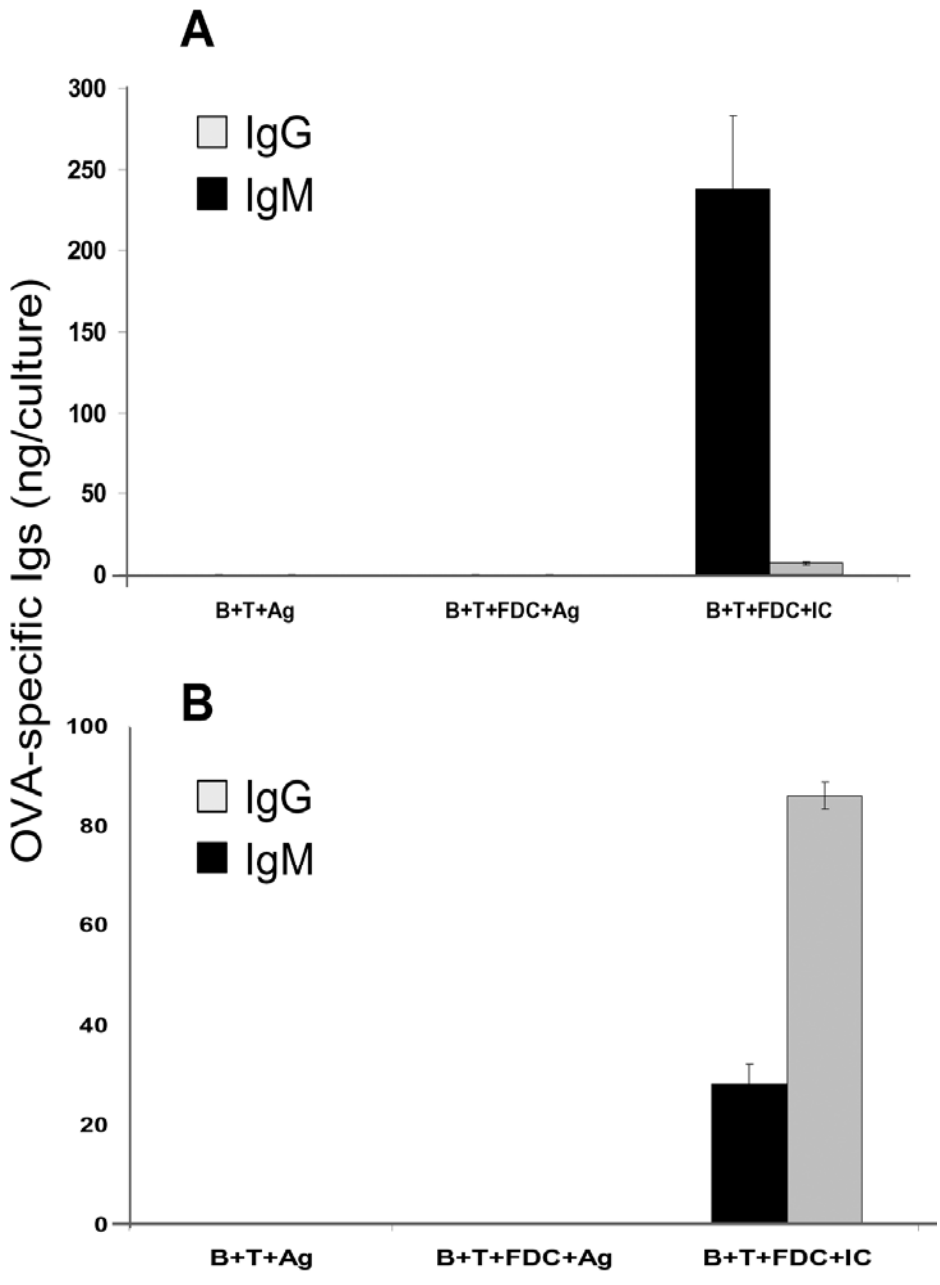
A
300
250
200
150
100
50
0
IgG
IgM
OVA-specific Igs (ng/culture)
B+T+Ag
B+T+FDC+Ag
B+T+FDC+IC
B
100
80
60
40
20
0
IgG
IgM
B+T+Ag
B+T+FDC+Ag
B+T+FDC+IC

Discussion

The data presented here support the novel concept that Ag specific primary human Ab responses, including Ig class switching can be generated in GCRs entirely *in vitro*. We report here that mature Ag-pulsed mDCs, primed MHC-matched human naïve CD4 T cells *in vitro*. Naïve B cells helped by IC-bearing FDCs produced Ag-specific Abs dominated by IgM in the first week followed by class switching to a dominant IgG response in the second week and an increase in the affinity of Ag specific IgG. Preliminary data suggest the induction of affinity maturation and compartementalization in these GCRs in vitro.

Traditionally, new vaccines and therapeutics are tested in animals like mice, rabbits or, in some cases in higher primates, like monkeys. Animal testing is time-consuming, expensive, controversial, and carries the risk of being untranslatable in humans. No matter how well an experimental vaccine works in animals, the application in humans is riddled with uncertainty and unforeseeable complications. Here, we report an *in vitro* model that may sidestep such devastating setbacks by allowing researchers to test vaccines and possibly therapeutics in human immune systems constructed *in vitro*.

Speed and flexibility are two major advantages of the reported model. The need for speed has come about in response to emerging infectious diseases like SARS or avian flu. If a disease is spreading quickly and is highly virulent, time is of the essence and animal testing would take too long to be helpful.

Flexibility is a landmark of this model. Previous trials to induce human *in vitro* antibody responses were restricted to certain antigens for which primed cells can be isolated from immune human subjects like TT or HBV. In this model we bypassed this limitation by priming naïve human CD4 T cells *in vitro* using mature Ag-pulsed DCs. This allows screening of antigens from different sources including bacteria, fungi, parasites and viruses. In fact, the use of naïve cells gives the model flexibility as wide as the diversity of the B cell and T cell repertoires.

The model can predict issues not apparent in studies conducted in animal models. For example, in contrast to the expected normal response of the murine model to HIV-gp120 exhibiting classic T-cell dependent class switching from Ag-specific IgM to IgG, the human cells *in vitro* may not switch to IgG, owing to the inhibitory effect of gp120 on the human but not the murine CD4 T-cell activity.

The dose-dependent immuno-modulatory effects of certain drugs like chemotherapeutic agents can be simultaneously tested for toxicity without risk to human health using this model. Although, humanized SCID mice models have been traditionally developed for this purpose, their responses are low, they use a lot more human cells, they take more time (a month or more), they are expensive, and need special facilities for containment. More importantly, FDCs, the major B-cell co-stimulators in GCs, take 8 weeks or more to develop in SCID mice and humanized SCID mice would not be expected to work rapidly

by means of immune complexes being trapped on FDCs as we demonstrated in these chimeras.

We are excited by the prospect of reconstructing GCRs *in vitro* where the important events for productive humoral immune responses take place and this is of utmost importance to critically assess vaccines. For example, it is not uncommon to find non-responders to particular vaccine and these people are put at risk when given a live vaccine. It may be possible to identify these people by setting up their immune system *in vitro* and determining their non-responsive or poor responsive state before they were challenged with a live vaccine capable of causing disease. In addition some therapeutic agents and industrial chemicals are toxic to the immune system and the *in vitro* immune system could be helpful in determining immunotoxicity in the context of the human immune system. The ability to get potent responses *in vitro* may even be useful in the production of human monoclonal Abs reactive against toxic agents and pathogens. In short, we report generation of primary human antibody responses entirely *in vitro.* The reported model can be used for the assessment of vaccines and therapeutics in a fast, flexible, and accurate way.

Summary and conclusion

FDC-FcγRIIB levels are up-regulated 1-3 days after challenge of actively immunized mice with Ag. This kinetics suggested that memory cells are not driving this response, prompting the hypothesis that IC-FDC interactions lead to FDC activation. To test this, mice passively immunized with anti-OVA Ab were OVA challenged to produce ICs. After 3 days, levels of ICs, FcγRIIB, ICAM-1, and VCAM-1 on FDC were analyzed. FDC were also stimulated with ICs *in vitro*, and mRNA for FcγRIIB, ICAM-1, and VCAM-1 was quantified by quantitative RT-PCR. IC labeling in passively immunized WT and FcγRIIB$^{-/-}$ mice revealed five to six FDC-reticula per LN midsagittal section. In WT mice, these IC-bearing FDC-reticula corresponded with FDC-reticula labeling for FcγRIIB, ICAM-1, and VCAM-1. Increases in these molecules on IC-stimulated FDC were confirmed by flow cytometry. FcγRIIB$^{-/-}$ mice showed normal trapping of ICs on FDC-reticula; mediated by CR, however, no increase in VCAM-1 or ICAM-1 was seen either on IC-bearing FDC-reticula or on purified FDCs. Addition of ICs *in vitro* resulted in a dramatic increase in mRNA for FcγRIIB, ICAM-1 and VCAM-1 in WT FDC, but not in FDC from FcγRIIB$^{-/-}$ mice, 2.4G2-pretreated WT FDC, B cells, or macrophages. Thus, although FDC-FcγRIIB was not essential for IC trapping, engagement of FDC-FcγRIIB with ICs initiated an FDC activation pathway.

Microbial molecular patterns engage TLRs and activate dendritic cells and other accessory cells. FDCs exist in resting and activated states, but are activated in GCs, where they provide accessory function. We reasoned that FDCs might express TLRs and that TLR-engagement might activate FDCs leading to the up-regulation of molecules important for accessory activity. To test this hypothesis, TLR4 expression on FDCs was

studied in situ with immunohistochemistry, followed by flow cytometry and RT-PCR analysis. TLR4 was expressed on FDC reticula in situ, and flow cytometry indicated that TLR4 was expressed on surface membranes and TLR4 message was readily apparent in FDCs by RT-PCR. Injecting mice or treating purified FDCs with LPS up-regulated molecules important for accessory activity, including FDC-FcγRIIB, FDC-ICAM-1, and FDC-VCAM-1. Treatment of purified FDCs with LPS also induced intracellular phospho-IκB-α, indicating NF-κB activation, and that correlated with increased FcγRIIB, ICAM-1, and VCAM-1. FDCs in C3H/HeJ mice were not activated with LPS even when mice were reconstituted with C3H/HeN leukocytes, suggesting that engagement of FDC-TLR4 is necessary for activation. Moreover, activated FDCs exhibited increased accessory activity in anti-OVA recall responses in vitro, and the FDC number could be reduced 4-fold if they were activated. In short, we report expression of TLR4 on FDCs for the first time and that engagement of FDC-TLR4 activated NF-κB, up-regulated expression of molecules important in FDC accessory function, including FcγRIIB, ICAM-1, and VCAM-1, as well as FDC accessory activity in promoting recall IgG responses.

FDCs reside in GCs in which their dendrites interdigitate and form non-mobile networks. FDC purification requires the use of collagenase and selection columns and leaves FDCs without detectable dendrites; the cardinal morphological feature of FDCs, when examined by light microscopy. We have reasoned that isolated FDCs might reattach to a collagen matrix, extend their processes, and form immobile networks in vitro. As a test for this, cells were plated on collagen type I, laminin, biglycan, and hyaluronan. After 12 h, 80%–90% of FDCs adhered to all tested matrices but not to

plastic. Within 2 weeks, FDCs adhering to type I collagen had spread out and had begun to acquire processes with occasional interconnections. By day 30, most FDCs had fine processes that formed networks through interdigitation with neighboring cells. FDC identity was confirmed by FDC-M1 labeling, immune complex trapping, and retention by FDCs in the networks. Scanning electron microscopy confirmed that groups of FDCs were in networks composed of convolutions and branching dendrites emanating from FDC cell bodies. In vivo, collagen type I was co-localized with FDCs, 5 h after challenge of immune mice with antigen. However, 2 days later, the collagen type I fibers were largely found at the periphery of the active follicles. Flow cytometry established the expression of CD29 and CD44 on FDCs; this may have partly mediated FDC-collagen interactions. Thus, we report, for the first time, that FDCs attach to collagen type I in vitro and regenerate their processes and networks with features in common with networks present in vivo

The contribution of IL-6 to terminal B cell differentiation has long been recognized and reports that FDCs produce IL-6 prompted the hypotheses that ICs induce FDCs to produce IL-6 and that FDC-IL-6 promotes GCRs, SHM and IgG production. FDCs were activated *in vitro* by addition of ICs and FDC-IL-6 production was determined. WT and IL-6 KO mice, as well as chimeras with WT and IL-6 KO cells, were immunized with NP-CGG and used to study anti-NIP responses, GC formation, and SHM in the VH186.2 gene segment in Ig-gamma. FDC-IL-6 increased when FDCs encountered ICs. At low immunogen dose, 1 μg NP-CGG/mouse, the IgG anti-NIP response in IL-6 KO mice was low and immunohistochemistry revealed a reduction in

both the number and size of GCs. The physiological relevance of FDC-IL-6 was apparent in the chimeric mice where total splenocytes from WT mice were unable to provide the IL-6 needed for normal IgG and GC responses in IL-6 KO animals with IL-6-defective FDCs. Moreover, the rate of mutation decreased from 18 to 8.9 mutations/1000 bases ($P < 0.001$) in WT vs. IL-6 KO mice. Addition of anti-IL-6 to GCRs *in vitro* reduced Ab levels and SHM from 3.5 to 0.65 mutations/1000 bases ($P < 0.02$). Thus, the absence of FDC-IL-6 correlated with a reduction in SHM that coincided with the reduction in GCs and specific anti-NIP. This is the first study to document that ICs induce FDC-IL-6 and that FDC-derived IL-6 is physiologically relevant in generating optimal GCRs, SHM, and IgG levels.

FDCs periodically arrange membrane-bound ICs of T-dependent Ags 200–500Å apart, and in addition to Ag, they provide B cells with co-stimulatory signals. This prompted the hypothesis that Ag in FDC-ICs can simultaneously cross-link multiple BCRs and induce TI B cell activation. TI responses are characterized by rapid IgM production. OVA-IC-bearing FDCs induced OVA-specific IgM in anti-Thy-1-pretreated nude mice and by purified murine and human B cells in vitro within just 48 h. Moreover, nude mice immunized with OVA-ICs exhibited well-developed GL-7^+ GCs with IC-retaining FDC-reticula and Blimp-1^+ plasmablasts within 48 h. In contrast, FDCs with unbound-OVA, which would have free access to BCRs, induced no GCs, plasmablasts, or IgM. Engagement of BCRs with rat-anti-mouse IgD (clone 11–26) does not activate B cells even when cross-linked. However, B cells were activated when anti-IgD-ICs, formed with Fc-specific rabbit anti-rat IgG, were loaded on FDCs. B cell activation was

indicated by high phosphotyrosine levels in caps and patches, expression of GL-7 and Blimp-1, and B cell proliferation within 48 h after stimulation with IC-bearing FDCs. Moreover, anti-IgD-IC-loaded FDCs induced strong polyclonal IgM responses within 48 h. Blockade of FDC-FcγRIIB inhibited the ability of FDC-ICs to induce T-independent IgM responses. Similarly, neutralizing FDC-C4BP or -BAFF, to minimize these FDC-costimulatory signals, also inhibited this FDC-dependent IgM response. This is the first report of FDC-dependent but TI responses to T cell-dependent Ags.

Induction of potent primary human Ab responses entirely *in vitro* is challenging, although such *in vitro* responses could be helpful in assessing vaccines and therapeutics without jeopardizing human health. Given that DCs prime T cells and that FDCs promote B cell responses, and that the four players are indispensible for the induction of a primary Ab response, we hypothesized that a primary Ab response can be induced in temporally-controlled GCRs *in vitro*. To test this, human monocyte derived-DCs were given OVA, anthrax rPA or HIV-gp120 for processing, matured with LPS, and $CD4^+$ T cells were added for priming. Ten days later, naïve B cells and OVA, rPA or gp120 IC-bearing FDCs were added and Ab production was subsequently assayed by ELISA. The $CD4^+$ T cells clustered with DCs through the 10 days of priming and fused with FDC-B cell clusters when GCRs were induced. IgM dominated the primary human immune response to OVA and rPA in the first week then declined as class switching to IgG was induced by the Ag-specific T cells. Moreover, high affinity Abs detectable in the second week replaced the low affinity Abs of the first week indicating affinity maturation. In contrast, antibodies against gp120 did not classswitch, which we attribute to the inhibitory activity

of gp120 on $CD4^+$ T cells (265-268). Consequently, gp120 would be a problematic vaccine in humans inspite of its effective induction of an effective immune response in mice. In short, Ag specific primary human Ab responses, including Ig class switching from specific IgM to IgG and affinity maturation, can be generated in GCRs entirely *in vitro*. Thus, potential vaccines can be rapidly and safely assessed using the human immune system in an accurate and flexible way.

Reference List

1. Cose, S., C. Brammer, K. M. Khanna, D. Masopust, and L. Lefrancois. 2006. Evidence that a significant number of naive T cells enter non-lymphoid organs as part of a normal migratory pathway. *Eur.J Immunol* 36:1423-1433.

2. Junt, T., E. Scandella, and B. Ludewig. 2008. Form follows function: lymphoid tissue microarchitecture in antimicrobial immune defence. *Nat.Rev.Immunol* 8:764-775.

3. Ochsenbein, A. F., T. Fehr, C. Lutz, M. Suter, F. Brombacher, H. Hengartner, and R. M. Zinkernagel. 1999. Control of early viral and bacterial distribution and disease by natural antibodies. *Science.* 286:2156-2159.

4. Junt, T., E. A. Moseman, M. Iannacone, S. Massberg, P. A. Lang, M. Boes, K. Fink, S. E. Henrickson, D. M. Shayakhmetov, N. C. Di Paolo, N. van Rooijen, T. R. Mempel, S. P. Whelan, and U. H. von Andrian. 2007. Subcapsular sinus macrophages in lymph nodes clear lymph-borne viruses and present them to antiviral B cells. *Nature* 450:110-114.

5. Cervantes-Barragan, L., R. Zust, F. Weber, M. Spiegel, K. S. Lang, S. Akira, V. Thiel, and B. Ludewig. 2007. Control of coronavirus infection through plasmacytoid dendritic-cell-derived type I interferon. *Blood* 109:1131-1137.

6. Stoll, S., J. Delon, T. M. Brotz, and R. N. Germain. 2002. Dynamic imaging of T cell-dendritic cell interactions in lymph nodes. *Science* 296:1873-1876.

7. Mempel, T. R., S. E. Henrickson, and U. H. von Andrian. 2004. T-cell priming by dendritic cells in lymph nodes occurs in three distinct phases. *Nature* 427:154-159.

8. Schluns, K. S. and L. Lefrancois. 2003. Cytokine control of memory T-cell development and survival. *Nat.Rev.Immunol* 3:269-279.

9. Gretz, J. E., A. O. Anderson, and S. Shaw. 1997. Cords, channels, corridors and conduits: critical architectural elements facilitating cell interactions in the lymph node cortex. *Immunol Rev.* 156:11-24.

10. Batista, F. D. and N. E. Harwood. 2009. The who, how and where of antigen presentation to B cells. *Nat.Rev.Immunol* 9:15-27.

11. Nieuwenhuis, P. and D. Opstelten. 1984. Functional anatomy of germinal centers. *Am.J.Anat.* 170:421-435.

12. Allen, C. D., T. Okada, and J. G. Cyster. 2007. Germinal-center organization and cellular dynamics. *Immunity.* 27:190-202.

13. Berek, C., A. Berger, and M. Apel. 1991. Maturation of the immune response in germinal centers. *Cell* 67:1121-1129.

14. Jacob, J., G. Kelsoe, K. Rajewsky, and U. Weiss. 1991. Intraclonal generation of antibody mutants in germinal centres. *Nature* 354:389-392.

15. Wang, Y., G. Huang, J. Wang, H. Molina, D. D. Chaplin, and Y. X. Fu. 2000. Antigen persistence is required for somatic mutation and affinity maturation of immunoglobulin. *Eur.J.Immunol.* 30:2226-2234.

16. Okada, T., M. J. Miller, I. Parker, M. F. Krummel, M. Neighbors, S. B. Hartley, A. O'Garra, M. D. Cahalan, and J. G. Cyster. 2005. Antigen-engaged B cells undergo chemotaxis toward the T zone and form motile conjugates with helper T cells. *PLoS.Biol.* 3:e150.

17. MacLennan, I. C., A. Gulbranson-Judge, K. M. Toellner, M. Casamayor-Palleja, E. Chan, D. M. Sze, S. A. Luther, and H. A. Orbea. 1997. The changing preference of T and B cells for partners as T-dependent antibody responses develop. *Immunol Rev.* 156:53-66.

18. Garside, P., E. Ingulli, R. R. Merica, J. G. Johnson, R. J. Noelle, and M. K. Jenkins. 1998. Visualization of specific B and T lymphocyte interactions in the lymph node. *Science* 281:96-99.

19. Jacob, J., R. Kassir, and G. Kelsoe. 1991. In situ studies of the primary immune response to (4-hydroxy-3-nitrophenyl)acetyl. I. The architecture and dynamics of responding cell populations. *J.Exp.Med.* 173:1165-1175.

20. Wang, Y. and R. H. Carter. 2005. CD19 regulates B cell maturation, proliferation, and positive selection in the FDC zone of murine splenic germinal centers. *Immunity.* 22:749-761.

21. Szakal, A. K. and M. G. Hanna, Jr. 1968. The ultrastructure of antigen localization and viruslike particles in mouse spleen germinal centers. *Exp.Mol.Pathol.* 8:75-89.

22. Hanna, M. G., Jr. and A. K. Szakal. 1968. Localization of 125I-labeled antigen in germinal centers of mouse spleen: histologic and ultrastructural autoradiographic studies of the secondary immune reaction. *J.Immunol.* 101:949-962.

23. Tew, J. G., G. J. Thorbecke, and R. M. Steinman. 1982. Dendritic cells in the immune response: characteristics and recommended nomenclature (A report from the Reticuloendothelial Society Committee on Nomenclature). *J.Reticuloendothel.Soc.* 31:371-380.

24. Szakal, A. K., R. L. Gieringer, M. H. Kosco, and J. G. Tew. 1985. Isolated follicular dendritic cells: cytochemical antigen localization, Nomarski, SEM, and TEM morphology. *J.Immunol.* 134:1349-1359.

25. Burton, G. F., M. H. Kosco, A. K. Szakal, and J. G. Tew. 1991. Iccosomes and the secondary antibody response. *Immunology* 73:271-276.

26. Szakal, A. K. and J. G. Tew. 1991. Significance of iccosomes in the germinal centre reaction. *Res.Immunol.* 142:261-263.

27. Wu, J., D. Qin, G. F. Burton, A. K. Szakal, and J. G. Tew. 1995. Iccosomes and induction of specific antibody production in vitro. *Adv.Exp.Med.Biol.* 378:309-311.

28. Szakal, A. K., M. H. Kosco, and J. G. Tew. 1988. A novel in vivo follicular dendritic cell-dependent iccosome-mediated mechanism for delivery of antigen to antigen-processing cells. *J.Immunol.* 140:341-353.

29. Qin, D., J. Wu, M. C. Carroll, G. F. Burton, A. K. Szakal, and J. G. Tew. 1998. Evidence for an important interaction between a complement-derived CD21 ligand on follicular dendritic cells and CD21 on B cells in the initiation of IgG responses. *J.Immunol.* 161:4549-4554.

30. Qin, D., J. Wu, K. A. Vora, J. V. Ravetch, A. K. Szakal, T. Manser, and J. G. Tew. 2000. Fc gamma receptor IIB on follicular dendritic cells regulates the B cell recall response. *J.Immunol.* 164:6268-6275.

31. Tew, J. G., E. J. Greene, and M. H. Makoski. 1976. In vitro evidence indicating a role for the Fc region of IgG in the mechanism for the long-term maintenance and regulation of antibody levels in vivo. *Cell Immunol.* 26:141-152.

32. Tew, J. G., T. E. Mandel, and G. A. Miller. 1979. Immune retention: immunological requirements for maintaining an easily degradable antigen in vivo. *Aust.J.Exp.Biol.Med.Sci.* 57:401-414.

33. Smith-Franklin, B. A., B. F. Keele, J. G. Tew, S. Gartner, A. K. Szakal, J. D. Estes, T. C. Thacker, and G. F. Burton. 2002. Follicular dendritic cells and the persistence of HIV infectivity: the role of antibodies and Fcgamma receptors. *J.Immunol.* 168:2408-2414.

34. Sukumar, S., M. E. El Shikh, J. G. Tew, and A. K. Szakal. 2008. Ultrastructural study of highly enriched follicular dendritic cells reveals their morphology and the periodicity of immune complex binding. *Cell Tissue Res.* 332:89-99.

35. Wu, Y., S. Sukumar, M. E. El Shikh, A. M. Best, A. K. Szakal, and J. G. Tew. 2008. Immune complex-bearing follicular dendritic cells deliver a late antigenic signal that promotes somatic hypermutation. *J.Immunol.* 180:281-290.

36. Szakal, A. K., Y. Aydar, P. Balogh, and J. G. Tew. 2002. Molecular interactions of FDCs with B cells in aging. *Semin.Immunol.* 14:267-274.

37. Szakal, A. K., K. L. Holmes, and J. G. Tew. 1983. Transport of immune complexes from the subcapsular sinus to lymph node follicles on the surface of nonphagocytic cells, including cells with dendritic morphology. *J.Immunol.* 131:1714-1727.

38. Tew, J. G., J. Wu, D. Qin, S. Helm, G. F. Burton, and A. K. Szakal. 1997. Follicular dendritic cells and presentation of antigen and costimulatory signals to B cells. *Immunol.Rev.* 156:39-52.

39. Aydar, Y., S. Sukumar, A. K. Szakal, and J. G. Tew. 2005. The influence of immune complex-bearing follicular dendritic cells on the IgM response, Ig class switching, and production of high affinity IgG. *J.Immunol.* 174:5358-5366.

40. Burton, G. F., D. H. Conrad, A. K. Szakal, and J. G. Tew. 1993. Follicular dendritic cells and B cell costimulation. *J.Immunol.* 150:31-38.

41. Schnizlein, C. T., A. K. Szakal, and J. G. Tew. 1984. Follicular dendritic cells in the regulation and maintenance of immune responses. *Immunobiology* 168:391-402.

42. Szakal, A. K., M. H. Kosco, and J. G. Tew. 1989. Microanatomy of lymphoid tissue during humoral immune responses: structure function relationships. *Annu.Rev.Immunol.* 7:91-109.

43. Szakal, A. K., J. K. Taylor, J. P. Smith, M. H. Kosco, G. F. Burton, and J. J. Tew. 1990. Kinetics of germinal center development in lymph nodes of young and aging immune mice. *Anat.Rec.* 227:475-485.

44. Tew, J. G., J. Wu, M. Fakher, A. K. Szakal, and D. Qin. 2001. Follicular dendritic cells: beyond the necessity of T-cell help. *Trends Immunol.* 22:361-367.

45. Tew, J. G., G. F. Burton, S. Helm, J. Wu, D. Qin, E. Hahn, and A. K. Szakal. 1995. Murine follicular dendritic cells: accessory activities in vitro. *Curr.Top.Microbiol.Immunol.* 201:93-104.

46. Tew, J. G., M. H. Kosco, G. F. Burton, and A. K. Szakal. 1990. Follicular dendritic cells as accessory cells. *Immunol.Rev.* 117:185-211.

47. Tew, J. G., M. H. Kosco, and A. K. Szakal. 1989. The alternative antigen pathway. *Immunol.Today* 10:229-232.

48. Maeda, K., G. F. Burton, D. A. Padgett, D. H. Conrad, T. F. Huff, A. Masuda, A. K. Szakal, and J. G. Tew. 1992. Murine follicular dendritic cells and low affinity Fc receptors for IgE (Fc epsilon RII). *J.Immunol.* 148:2340-2347.

49. Payet-Jamroz, M., S. L. Helm, J. Wu, M. Kilmon, M. Fakher, A. Basalp, J. G. Tew, A. K. Szakal, N. Noben-Trauth, and D. H. Conrad. 2001. Suppression of IgE responses in CD23-transgenic animals is due to expression of CD23 on nonlymphoid cells. *J.Immunol.* 166:4863-4869.

50. Sukumar, S., D. H. Conrad, A. K. Szakal, and J. G. Tew. 2006. Differential T cell-mediated regulation of CD23 (Fc epsilonRII) in B cells and follicular dendritic cells. *J.Immunol.* 176:4811-4817.

51. Tew, J. G., R. P. Phipps, and T. E. Mandel. 1980. The maintenance and regulation of the humoral immune response: persisting antigen and the role of follicular antigen-binding dendritic cells as accessory cells. *Immunol.Rev.* 53:175-201.

52. Tew, J. G., T. Mandel, A. Burgess, and J. D. Hicks. 1979. The antigen binding dendritic cell of the lymphoid follicles: evidence indicating its role in the maintenance and regulation of serum antibody levels. *Adv.Exp.Med.Biol.* 114:407-410.

53. Tew, J. G. and T. Mandel. 1978. The maintenance and regulation of serum antibody levels: evidence indicating a role for antigen retained in lymphoid follicles. *J.Immunol.* 120:1063-1069.

54. Mandel, T. E., R. P. Phipps, A. Abbot, and J. G. Tew. 1980. The follicular dendritic cell: long term antigen retention during immunity. *Immunol.Rev.* 53:29-59.

55. Allen, C. D. and J. G. Cyster. 2008. Follicular dendritic cell networks of primary follicles and germinal centers: phenotype and function. *Semin.Immunol* 20:14-25.

56. Fakher, M., J. Wu, D. Qin, A. Szakal, and J. Tew. 2001. Follicular dendritic cell accessory activity crosses MHC and species barriers. *Eur.J.Immunol.* 31:176-185.

57. Aydar, Y., J. Wu, J. Song, A. K. Szakal, and J. G. Tew. 2004. FcgammaRII expression on follicular dendritic cells and immunoreceptor tyrosine-based inhibition motif signaling in B cells. *Eur.J.Immunol.* 34:98-107.

58. Aydar, Y., P. Balogh, J. G. Tew, and A. K. Szakal. 2003. Altered regulation of Fc gamma RII on aged follicular dendritic cells correlates with immunoreceptor

tyrosine-based inhibition motif signaling in B cells and reduced germinal center formation. *J.Immunol.* 171:5975-5987.

59. Gaspal, F. M., F. M. McConnell, M. Y. Kim, D. Gray, M. H. Kosco-Vilbois, C. R. Raykundalia, M. Botto, and P. J. Lane. 2006. The generation of thymus-independent germinal centers depends on CD40 but not on CD154, the T cell-derived CD40-ligand. *Eur.J.Immunol.* 36:1665-1673.

60. Hase, H., Y. Kanno, M. Kojima, K. Hasegawa, D. Sakurai, H. Kojima, N. Tsuchiya, K. Tokunaga, N. Masawa, M. Azuma, K. Okumura, and T. Kobata. 2004. BAFF/BLyS can potentiate B-cell selection with the B-cell coreceptor complex. *Blood* 103:2257-2265.

61. Magliozzi, R., S. Columba-Cabezas, B. Serafini, and F. Aloisi. 2004. Intracerebral expression of CXCL13 and BAFF is accompanied by formation of lymphoid follicle-like structures in the meninges of mice with relapsing experimental autoimmune encephalomyelitis. *J.Neuroimmunol.* 148:11-23.

62. Zhang, X., C. S. Park, S. O. Yoon, L. Li, Y. M. Hsu, C. Ambrose, and Y. S. Choi. 2005. BAFF supports human B cell differentiation in the lymphoid follicles through distinct receptors. *Int.Immunol.* 17:779-788.

63. Ng, L. G., C. R. Mackay, and F. Mackay. 2005. The BAFF/APRIL system: life beyond B lymphocytes. *Mol.Immunol.* 42:763-772.

64. Schneider, P. 2005. The role of APRIL and BAFF in lymphocyte activation. *Curr.Opin.Immunol.* 17:282-289.

65. Li, L., S. O. Yoon, D. D. Fu, X. Zhang, and Y. S. Choi. 2004. Novel follicular dendritic cell molecule, 8D6, collaborates with CD44 in supporting lymphomagenesis by a Burkitt lymphoma cell line, L3055. *Blood.* 104:815-821.

66. Estes, J. D., T. C. Thacker, D. L. Hampton, S. A. Kell, B. F. Keele, E. A. Palenske, K. M. Druey, and G. F. Burton. 2004. Follicular dendritic cell regulation of CXCR4-mediated germinal center CD4 T cell migration. *J.Immunol.* 173:6169-6178.

67. Cyster, J. G., K. M. Ansel, K. Reif, E. H. Ekland, P. L. Hyman, H. L. Tang, S. A. Luther, and V. N. Ngo. 2000. Follicular stromal cells and lymphocyte homing to follicles. *Immunol.Rev.* 176:181-193.

68. Kopf, M., S. Herren, M. V. Wiles, M. B. Pepys, and M. H. Kosco-Vilbois. 1998. Interleukin 6 influences germinal center development and antibody production via a contribution of C3 complement component. *J.Exp.Med.* 188:1895-1906.

69. Kosco, M. H., E. Pflugfelder, and D. Gray. 1992. Follicular dendritic cell-dependent adhesion and proliferation of B cells in vitro. *J.Immunol.* 148:2331-2339.

70. El Shikh, M. E., R. El Sayed, A. K. Szakal, and J. G. Tew. 2006. Follicular dendritic cell (FDC)-FcgammaRIIB engagement via immune complexes induces the activated FDC phenotype associated with secondary follicle development. *Eur.J.Immunol.* 36:2715-2724.

71. El Shikh, M. E., R. M. El Sayed, Y. Wu, A. K. Szakal, and J. G. Tew. 2007. TLR4 on follicular dendritic cells: an activation pathway that promotes accessory activity. *J.Immunol.* 179:4444-4450.

72. El Shikh, M. E., R. M. El Sayed, J. G. Tew, and A. K. Szakal. 2007. Follicular dendritic cells stimulated by collagen type I develop dendrites and networks in vitro. *Cell Tissue Res.* 329:81-89.

73. El Shikh, M. E., R. M. El Sayed, A. K. Szakal, and J. G. Tew. 2009. T-independent antibody responses to T-dependent antigens: a novel follicular dendritic cell-dependent activity. *J.Immunol.* 182:3482-3491.

74. El Shikh, M. E., R. M. El Sayed, J. G. Tew, and G. F. Burton. 2009. Follicular Dendritic Cells (B Lymphocyte Stimulating). *Encyclopedia of Life Sciences* In Press.

75. Miller, J. F. 2004. Events that led to the discovery of T-cell development and function--a personal recollection. *Tissue Antigens* 63:509-517.

76. MACLEAN, L. D., S. J. ZAK, R. L. VARCO, and R. A. Good. 1957. The role of the thymus in antibody production; an experimental study of the immune response in thymectomized rabbits. *Transplant.Bull.* 4:21-22.

77. Miller, J. F. 1961. Immunological function of the thymus. *Lancet* 2:748-749.

78. MARTINEZ, C., J. KERSEY, B. W. PAPERMASTER, and R. A. Good. 1962. Skin homograft survival in thymectomized mice. *Proc.Soc.Exp.Biol.Med.* 109:193-196.

79. Parrott, D. M. and J. EAST. 1964. THE THYMUS AND IMMUNITY. THE IMMUNOLOGICAL STATUS OF THYMECTOMIZED ANIMALS. A SURVEY. *Proc.R.Soc.Med.* 57:147-151.

80. JANKOVIC, B. D., B. H. WAKSMAN, and B. G. ARNASON. 1962. Role of the thymus in immune ractions in rats. I. The immunologic response to bovine serum albumin (antibody formation, Arthus reactivity, and delayed hypersensitivity) in

rats thymectomized or splenectomized at various times after birth. *J Exp.Med.* 116:159-176.

81. ARCHER, O. K., J. C. PIERCE, B. W. PAPERMASTER, and R. A. Good. 1962. Reduced antibody response in thymectomized rabbits. *Nature* 195:191-193.

82. MARTINEZ, C., A. P. DALMASSO, and R. A. Good. 1964. EFFECT OF THYMECTOMY ON DEVELOPMENT OF IMMUNOLOGICAL COMPETENCE IN MICE. *Ann.N.Y.Acad.Sci.* 113:933-946.

83. Humphrey, J. H., D. M. Parrott, and J. EAST. 1964. STUDIES ON GLOBULIN AND ANTIBODY PRODUCTION IN MICE THYMECTOMIZED AT BIRTH. *Immunology* 7:419-439.

84. Parrott, D. M. and M. A. de Sousa. 1966. Changes in the thymus-dependent areas of lymph nodes after immunological stimulation. *Nature* 212:1316-1317.

85. Metcalf, D. 1960. The effect of thymectomy on the lymphoid tissues of the mouse. *Br.J Haematol.* 6:324-333.

86. Parrott, D. M. and M. De Sousa. 1971. Thymus-dependent and thymus-independent populations: origin, migratory patterns and lifespan. *Clin.Exp.Immunol* 8:663-684.

87. Parrott, D. V., M. A. de Sousa, and J. EAST. 1966. Thymus-dependent areas in the lymphoid organs of neonatally thymectomized mice. *J Exp.Med.* 123:191-204.

88. Parrott, D. M. and M. A. de Sousa. 1967. The persistence of donor-derived cells in thymus grafts, lymph nodes and spleens of recipient mice. *Immunology* 13:193-200.

89. Micklem, H. S., C. E. Ford, E. P. Evans, and J. Gray. 1966. Interrelationships of myeloid and lymphoid cells: studies with chromosome-marked cells transfused into lethally irradiated mice. *Proc.R.Soc.Lond B Biol.Sci.* 165:78-102.

90. Davies, A. J., R. L. Carter, E. Leuchars, and V. Wallis. 1969. The morphology of immune reactions in normal, thymectomized and reconstituted mice. II. The response to oxazolone. *Immunology* 17:111-126.

91. Davies, A. J., R. L. Carter, E. Leuchars, V. Wallis, and P. C. Koller. 1969. The morphology of immune reactions in normal, thymectomized and reconstituted mice. I. The response to sheep erythrocytes. *Immunology* 16:57-69.

92. Miller, J. F. and G. F. Mitchell. 1969. Thymus and antigen-reactive cells. *Transplant.Rev.* 1:3-42.

93. Claman, H. N. and E. A. Chaperon. 1969. Immunologic complementation between thymus and marrow cells--a model for the two-cell theory of immunocompetence. *Transplant.Rev.* 1:92-113.

94. Parish, C. R. 1975. Separation and functional analysis of subpopulations of lymphocytes bearing complement and Fc receptors. *Transplant.Rev.* 25:98-120.

95. Mond, J. J., A. Lees, and C. M. Snapper. 1995. T cell-independent antigens type 2. *Annu.Rev.Immunol.* 13:655-92.:655-692.

96. Zubler, R. H. 2001. Naive and memory B cells in T-cell-dependent and T-independent responses. *Springer Semin.Immunopathol.* 23:405-419.

97. Vos, Q., A. Lees, Z. Q. Wu, C. M. Snapper, and J. J. Mond. 2000. B-cell activation by T-cell-independent type 2 antigens as an integral part of the humoral immune response to pathogenic microorganisms. *Immunol.Rev.* 176:154-70.:154-170.

98. Dintzis, H. M., R. Z. Dintzis, and B. Vogelstein. 1976. Molecular determinants of immunogenicity: the immunon model of immune response. *Proc.Natl.Acad.Sci.U.S.A.* 73:3671-3675.

99. Dintzis, R. Z., B. Vogelstein, and H. M. Dintzis. 1982. Specific cellular stimulation in the primary immune response: experimental test of a quantized model. *Proc.Natl.Acad.Sci.U.S.A.* 79:884-888.

100. Brunswick, M., F. D. Finkelman, P. F. Highet, J. K. Inman, H. M. Dintzis, and J. J. Mond. 1988. Picogram quantities of anti-Ig antibodies coupled to dextran induce B cell proliferation. *J.Immunol.* 140:3364-3372.

101. Brunswick, M., A. Burkhardt, F. Finkelman, J. Bolen, and J. J. Mond. 1992. Comparison of tyrosine kinase activation by mitogenic and nonmitogenic anti-IgD antibodies. *J.Immunol.* 149:2249-2254.

102. Sulzer, B. and A. S. Perelson. 1997. Immunons revisited: binding of multivalent antigens to B cells. *Mol.Immunol.* 34:63-74.

103. de Vinuesa, C. G., M. C. Cook, J. Ball, M. Drew, Y. Sunners, M. Cascalho, M. Wabl, G. G. Klaus, and I. C. MacLennan. 2000. Germinal centers without T cells. *J.Exp.Med.* 191:485-494.

104. Lentz, V. M. and T. Manser. 2001. Cutting edge: germinal centers can be induced in the absence of T cells. *J.Immunol.* 167:15-20.

105. Kayhty, H., V. Karanko, H. Peltola, and P. H. Makela. 1984. Serum antibodies after vaccination with Haemophilus influenzae type b capsular polysaccharide and

responses to reimmunization: no evidence of immunologic tolerance or memory. *Pediatrics* 74:857-865.

106. Weissman, I. L., G. A. Gutman, S. H. Friedberg, and L. Jerabek. 1976. Lymphoid tissue architecture. III. Germinal centers, T cells, and thymus-dependent vs thymus-independent antigens. *Adv.Exp.Med.Biol.* 66:229-237.

107. Nahm, M. H., F. G. Kroese, and J. W. Hoffmann. 1992. The evolution of immune memory and germinal centers. *Immunol.Today* 13:438-441.

108. Szomolanyi-Tsuda, E. and R. M. Welsh. 1998. T-cell-independent antiviral antibody responses. *Curr.Opin.Immunol.* 10:431-435.

109. Fehr, T., M. F. Bachmann, E. Bucher, U. Kalinke, F. E. Di Padova, A. B. Lang, H. Hengartner, and R. M. Zinkernagel. 1997. Role of repetitive antigen patterns for induction of antibodies against antibodies. *J.Exp.Med.* %19;185:1785-1792.

110. Tanaka, S., M. Fakher, S. E. Barbour, H. A. Schenkein, and J. G. Tew. 2006. Influence of proinflammatory cytokines on Actinobacillus actinomycetemcomitans specific IgG responses. *J.Periodontal Res.* 41:1-9.

111. Lindhout, E., M. L. Mevissen, J. Kwekkeboom, J. M. Tager, and C. de Groot. 1993. Direct evidence that human follicular dendritic cells (FDC) rescue germinal centre B cells from death by apoptosis. *Clin.Exp.Immunol.* 91:330-336.

112. Lindhout, E. and C. de Groot. 1995. Follicular dendritic cells and apoptosis: life and death in the germinal centre. *Histochem.J.* 27:167-183.

113. Liu, Y. J., D. Y. Mason, G. D. Johnson, S. Abbot, C. D. Gregory, D. L. Hardie, J. Gordon, and I. C. MacLennan. 1991. Germinal center cells express bcl-2 protein after activation by signals which prevent their entry into apoptosis. *Eur.J.Immunol.* 21:1905-1910.

114. Schwarz, Y. X., M. Yang, D. Qin, J. Wu, W. D. Jarvis, S. Grant, G. F. Burton, A. K. Szakal, and J. G. Tew. 1999. Follicular dendritic cells protect malignant B cells from apoptosis induced by anti-Fas and antineoplastic agents. *J.Immunol.* 163:6442-6447.

115. Qin, D., J. Wu, G. F. Burton, A. K. Szakal, and J. G. Tew. 1999. Follicular dendritic cells mediated maintenance of primary lymphocyte cultures for long-term analysis of a functional in vitro immune system. *J.Immunol.Methods* 226:19-27.

116. Wysocki, L., T. Manser, and M. L. Gefter. 1986. Somatic evolution of variable region structures during an immune response. *Proc.Natl.Acad.Sci.U.S.A.* 83:1847-1851.

117. Pepys, M. B. 1974. Role of complement in induction of antibody production in vivo. Effect of cobra factor and other C3-reactive agents on thymus-dependent and thymus-independent antibody responses. *J.Exp.Med.* 140:126-145.

118. Pepys, M. B. 1972. Role of complement in induction of the allergic response. *Nat.New Biol.* 237:157-159.

119. Papamichail, M., C. Gutierrez, P. Embling, P. Johnson, E. J. Holborow, and M. B. Pepys. 1975. Complement dependence of localisation of aggregated IgG in germinal centres. *Scand.J.Immunol.* 4:343-347.

120. Klaus, G. G. and J. H. Humphrey. 1977. The generation of memory cells. I. The role of C3 in the generation of B memory cells. *Immunology.* 33:31-40.

121. Carroll, M. C. 1998. The role of complement and complement receptors in induction and regulation of immunity. *Annu.Rev.Immunol* 16:545-568.

122. Bolland, S. and J. V. Ravetch. 1999. Inhibitory pathways triggered by ITIM-containing receptors. *Adv.Immunol.* 72:149-77.:149-177.

123. Ott, V. L. and J. C. Cambier. 2000. Activating and inhibitory signaling in mast cells: new opportunities for therapeutic intervention? *J.Allergy Clin.Immunol.* 106:429-440.

124. Dal Porto, J. M., S. B. Gauld, K. T. Merrell, D. Mills, A. E. Pugh-Bernard, and J. Cambier. 2004. B cell antigen receptor signaling 101. *Mol.Immunol.* 41:599-613.

125. MacLennan, I. C. 1994. Germinal centers. *Annu.Rev.Immunol.* 12:117-39.:117-139.

126. Li, L., X. Zhang, S. Kovacic, A. J. Long, K. Bourque, C. R. Wood, and Y. S. Choi. 2000. Identification of a human follicular dendritic cell molecule that stimulates germinal center B cell growth. *J.Exp.Med.* 191:1077-1084.

127. Zhang, X., L. Li, J. Jung, S. Xiang, C. Hollmann, and Y. S. Choi. 2001. The distinct roles of T cell-derived cytokines and a novel follicular dendritic cell-signaling molecule 8D6 in germinal center-B cell differentiation. *J Immunol* 167:49-56.

128. Victoratos, P., J. Lagnel, S. Tzima, M. B. Alimzhanov, K. Rajewsky, M. Pasparakis, and G. Kollias. 2006. FDC-specific functions of p55TNFR and IKK2 in the development of FDC networks and of antibody responses. *Immunity.* 24:65-77.

129. Dhodapkar, K. M., J. L. Kaufman, M. Ehlers, D. K. Banerjee, E. Bonvini, S. Koenig, R. M. Steinman, J. V. Ravetch, and M. V. Dhodapkar. 2005. Selective

blockade of inhibitory Fcgamma receptor enables human dendritic cell maturation with IL-12p70 production and immunity to antibody-coated tumor cells. *Proc.Natl.Acad.Sci.U.S.A* 102:2910-2915.

130. Sukumar, S., A. K. Szakal, and J. G. Tew. 2006. Isolation of functionally active murine follicular dendritic cells. *J.Immunol.Methods* 313:81-95.

131. Livak, K. J. and T. D. Schmittgen. 2001. Analysis of relative gene expression data using real-time quantitative PCR and the 2(-Delta Delta C(T)) Method. *Methods* 25:402-408.

132. Balogh, P., Y. Aydar, J. G. Tew, and A. K. Szakal. 2002. Appearance and phenotype of murine follicular dendritic cells expressing VCAM-1. *Anat.Rec.* 268:160-168.

133. Koopman, G., H. K. Parmentier, H. J. Schuurman, W. Newman, C. J. Meijer, and S. T. Pals. 1991. Adhesion of human B cells to follicular dendritic cells involves both the lymphocyte function-associated antigen 1/intercellular adhesion molecule 1 and very late antigen 4/vascular cell adhesion molecule 1 pathways. *J Exp.Med.* 173:1297-1304.

134. Balogh, P., Y. Aydar, J. G. Tew, and A. K. Szakal. 2001. Ontogeny of the follicular dendritic cell phenotype and function in the postnatal murine spleen. *Cell Immunol.* 214:45-53.

135. Rennert, P. D., J. L. Browning, R. Mebius, F. Mackay, and P. S. Hochman. 1996. Surface lymphotoxin alpha/beta complex is required for the development of peripheral lymphoid organs. *J.Exp.Med.* 184:1999-2006.

136. Mackay, F. and J. L. Browning. 1998. Turning off follicular dendritic cells. *Nature* 395:26-27.

137. Kosco-Vilbois, M. H., H. Zentgraf, J. Gerdes, and J. Y. Bonnefoy. 1997. To 'B' or not to 'B' a germinal center? *Immunol Today* 18:225-230.

138. Matsumoto, M., Y. X. Fu, H. Molina, G. Huang, J. Kim, D. A. Thomas, M. H. Nahm, and D. D. Chaplin. 1997. Distinct roles of lymphotoxin alpha and the type I tumor necrosis factor (TNF) receptor in the establishment of follicular dendritic cells from non-bone marrow-derived cells. *J Exp.Med.* 186:1997-2004.

139. Chaplin, D. D. and Y. Fu. 1998. Cytokine regulation of secondary lymphoid organ development. *Curr.Opin.Immunol.* 10:289-297.

140. Gonzalez, M., F. Mackay, J. L. Browning, M. H. Kosco-Vilbois, and R. J. Noelle. 1998. The sequential role of lymphotoxin and B cells in the development of splenic follicles. *J Exp.Med.* 187:997-1007.

141. Endres, R., M. B. Alimzhanov, T. Plitz, A. Futterer, M. H. Kosco-Vilbois, S. A. Nedospasov, K. Rajewsky, and K. Pfeffer. 1999. Mature follicular dendritic cell networks depend on expression of lymphotoxin beta receptor by radioresistant stromal cells and of lymphotoxin beta and tumor necrosis factor by B cells. *J.Exp.Med.* 189:159-168.

142. Sinclair, N. R. 2000. Immunoreceptor tyrosine-based inhibitory motifs on activating molecules. *Crit Rev.Immunol* 20:89-102.

143. Gessner, J. E., H. Heiken, A. Tamm, and R. E. Schmidt. 1998. The IgG Fc receptor family. *Ann.Hematol.* 76:231-248.

144. Ravetch, J. V. and S. Bolland. 2001. IgG Fc receptors. *Annu.Rev.Immunol* 19:275-290.

145. Janeway, C. A., Jr. 1989. Approaching the asymptote? Evolution and revolution in immunology. *Cold Spring Harb.Symp.Quant.Biol.* 54 Pt 1:1-13.:1-13.

146. Janeway, C. A., Jr. 1992. The immune system evolved to discriminate infectious nonself from noninfectious self. *Immunol.Today.* 13:11-16.

147. Medzhitov, R. and C. A. Janeway, Jr. 2002. Decoding the patterns of self and nonself by the innate immune system. *Science.* 296:298-300.

148. Matzinger, P. 1994. Tolerance, danger, and the extended family. *Annu.Rev.Immunol.* 12:991-1045.:991-1045.

149. Matzinger, P. 2002. The danger model: a renewed sense of self. *Science.* 296:301-305.

150. Lemaitre, B., E. Nicolas, L. Michaut, J. M. Reichhart, and J. A. Hoffmann. 1996. The dorsoventral regulatory gene cassette spatzle/Toll/cactus controls the potent antifungal response in Drosophila adults. *Cell.* 20;86:973-983.

151. Medzhitov, R., P. Preston-Hurlburt, and C. A. Janeway, Jr. 1997. A human homologue of the Drosophila Toll protein signals activation of adaptive immunity. *Nature.* 388:394-397.

152. Medzhitov, R. and C. Janeway, Jr. 2000. The Toll receptor family and microbial recognition. *Trends Microbiol.* 8:452-456.

153. Kimbrell, D. A. and B. Beutler. 2001. The evolution and genetics of innate immunity. *Nat.Rev.Genet.* 2:256-267.

154. Aderem, A. and R. J. Ulevitch. 2000. Toll-like receptors in the induction of the innate immune response. *Nature.* 406:782-787.

155. Beutler, B. 2000. Endotoxin, toll-like receptor 4, and the afferent limb of innate immunity. *Curr.Opin.Microbiol.* 3:23-28.

156. Takeda, K., T. Kaisho, and S. Akira. 2003. Toll-like receptors. *Annu.Rev.Immunol.* 21:335-76. Epub;2001 Dec;19.:335-376.

157. Mitchell, J. and A. Abbot. 1965. Ultrastructure of the antigen-retaining reticulum of lymph node follicles as shown by high-resolution autoradiography. *Nature* 208:500-502.

158. Schriever, F. and L. M. Nadler. 1992. The central role of follicular dendritic cells in lymphoid tissues. *Adv.Immunol* 51:243-284.

159. Wu, J., D. Qin, G. F. Burton, A. K. Szakal, and J. G. Tew. 1996. Follicular dendritic cell-derived antigen and accessory activity in initiation of memory IgG responses in vitro. *J.Immunol.* 157:3404-3411.

160. Steinman, R. M. and H. Hemmi. 2006. Dendritic cells: translating innate to adaptive immunity. *Curr.Top.Microbiol.Immunol.* 311:17-58.:17-58.

161. Poltorak, A., X. He, I. Smirnova, M. Y. Liu, C. Van Huffel, X. Du, D. Birdwell, E. Alejos, M. Silva, C. Galanos, M. Freudenberg, P. Ricciardi-Castagnoli, B. Layton, and B. Beutler. 1998. Defective LPS signaling in C3H/HeJ and C57BL/10ScCr mice: mutations in Tlr4 gene. *Science.* 282:2085-2088.

162. Akira, S., K. Takeda, and T. Kaisho. 2001. Toll-like receptors: critical proteins linking innate and acquired immunity. *Nat.Immunol.* 2:675-680.

163. Kalinski, P., C. M. Hilkens, E. A. Wierenga, and M. L. Kapsenberg. 1999. T-cell priming by type-1 and type-2 polarized dendritic cells: the concept of a third signal. *Immunol.Today.* 20:561-567.

164. Szakal, A. K., M. H. Kosco, and J. G. Tew. 1988. FDC-iccosome mediated antigen delivery to germinal center B cells, antigen processing and presentation to T cells. *Adv.Exp.Med.Biol.* 237:197-202.

165. Akashi, S., R. Shimazu, H. Ogata, Y. Nagai, K. Takeda, M. Kimoto, and K. Miyake. 2000. Cutting edge: cell surface expression and lipopolysaccharide signaling via the toll-like receptor 4-MD-2 complex on mouse peritoneal macrophages. *J.Immunol.* 164:3471-3475.

166. Nossal, G. J., A. Abbot, J. Mitchell, and Z. Lummus. 1968. Antigens in immunity. XV. Ultrastructural features of antigen capture in primary and secondary lymphoid follicles. *J.Exp.Med.* 127:277-290.

167. Thorbecke, G. J., A. R. Amin, and V. K. Tsiagbe. 1994. Biology of germinal centers in lymphoid tissue. *FASEB J.* 8:832-840.

168. KAPLAN, M. E., A. H. COONS, and H. W. DEANE. 1950. Localization of antigen in tissue cells; cellular distribution of pneumococcal polysaccharides types II and III in the mouse. *J.Exp.Med.* 91:15-30, 4.

169. Schriever, F., A. S. Freedman, G. Freeman, E. Messner, G. Lee, J. Daley, and L. M. Nadler. 1989. Isolated human follicular dendritic cells display a unique antigenic phenotype. *J.Exp.Med.* 169:2043-2058.

170. Yoshida, K., T. K. van den Berg, and C. D. Dijkstra. 1993. Two functionally different follicular dendritic cells in secondary lymphoid follicles of mouse spleen, as revealed by CR1/2 and FcR gamma II-mediated immune-complex trapping. *Immunology.* 80:34-39.

171. Balogh, P., G. Horvath, and A. K. Szakal. 2004. Immunoarchitecture of distinct reticular fibroblastic domains in the white pulp of mouse spleen. *J.Histochem.Cytochem.* 52:1287-1298.

172. Tsunoda, R., M. Nakayama, K. Onozaki, E. Heinen, N. Cormann, C. Kinet-Denoel, and M. Kojima. 1990. Isolation and long-term cultivation of human tonsil follicular dendritic cells. *Virchows Arch.B Cell Pathol.Incl.Mol.Pathol.* 59:95-105.

173. Donaldson, S. L., M. H. Kosco, A. K. Szakal, and J. G. Tew. 1986. Localization of antibody-forming cells in draining lymphoid organs during long-term maintenance of the antibody response. *J.Leukoc.Biol.* 40:147-157.

174. Gelse, K., E. Poschl, and T. Aigner. 2003. Collagens--structure, function, and biosynthesis. *Adv.Drug Deliv.Rev.* 55:1531-1546.

175. Raspanti, M., T. Congiu, and S. Guizzardi. 2002. Structural aspects of the extracellular matrix of the tendon: an atomic force and scanning electron microscopy study. *Arch.Histol.Cytol.* 65:37-43.

176. Isacke, C. M. and H. Yarwood. 2002. The hyaluronan receptor, CD44. *Int.J.Biochem.Cell Biol.* 34:718-721.

177. Lu, L., J. Woo, A. S. Rao, Y. Li, S. C. Watkins, S. Qian, T. E. Starzl, A. J. Demetris, and A. W. Thomson. 1994. Propagation of dendritic cell progenitors from normal mouse liver using granulocyte/macrophage colony-stimulating factor and their maturational development in the presence of type-1 collagen. *J.Exp.Med.* 179:1823-1834.

178. Tasaki, A., N. Yamanaka, M. Kubo, K. Matsumoto, H. Kuroki, K. Nakamura, C. Nakahara, H. Onishi, H. Kuga, E. Baba, M. Tanaka, T. Morisaki, and M. Katano.

2004. Three-dimensional two-layer collagen matrix gel culture model for evaluating complex biological functions of monocyte-derived dendritic cells. *J.Immunol.Methods.* 287:79-90.

179. Boyd, P. J., J. Doyle, E. Gee, S. Pallan, and T. L. Haas. 2005. MAPK signaling regulates endothelial cell assembly into networks and expression of MT1-MMP and MMP-2. *Am.J.Physiol Cell Physiol.* 288:C659-C668.

180. Ma, W., W. Fitzgerald, Q. Y. Liu, T. J. O'Shaughnessy, D. Maric, H. J. Lin, D. L. Alkon, and J. L. Barker. 2004. CNS stem and progenitor cell differentiation into functional neuronal circuits in three-dimensional collagen gels. *Exp.Neurol.* 190:276-288.

181. Castanos-Velez, E., P. Biberfeld, and M. Patarroyo. 1995. Extracellular matrix proteins and integrin receptors in reactive and non-reactive lymph nodes. *Immunology.* 86:270-278.

182. Bofill, M., A. N. Akbar, and P. L. Amlot. 2000. Follicular dendritic cells share a membrane-bound protein with fibroblasts. *J.Pathol.* 191:217-226.

183. Ansel, K. M., V. N. Ngo, P. L. Hyman, S. A. Luther, R. Forster, J. D. Sedgwick, J. L. Browning, M. Lipp, and J. G. Cyster. 2000. A chemokine-driven positive feedback loop organizes lymphoid follicles. *Nature* 406:309-314.

184. Taga, T. and T. Kishimoto. 1992. Role of a two-chain IL-6 receptor system in immune and hematopoietic cell regulation. *Crit Rev.Immunol.* 11:265-280.

185. Berek, C. and M. Ziegner. 1993. The maturation of the immune response. *Immunol.Today* 14:400-404.

186. MacLennan, I. C. and D. Gray. 1986. Antigen-driven selection of virgin and memory B cells. *Immunol.Rev.* 91:61-85.

187. Liu, Y. J., F. Malisan, O. de Bouteiller, C. Guret, S. Lebecque, J. Banchereau, F. C. Mills, E. E. Max, and H. Martinez-Valdez. 1996. Within germinal centers, isotype switching of immunoglobulin genes occurs after the onset of somatic mutation. *Immunity.* 4:241-250.

188. Kelsoe, G. 1996. The germinal center: a crucible for lymphocyte selection. *Semin.Immunol.* 8:179-184.

189. Tsunoda, R., N. Cormann, E. Heinen, K. Onozaki, P. Coulie, Y. Akiyama, K. Yoshizaki, C. Kinet-Denoel, L. J. Simar, and M. Kojima. 1989. Cytokines produced in lymph follicles. *Immunol.Lett.* 22:129-134.

190. Clark, E. A., K. H. Grabstein, and G. L. Shu. 1992. Cultured human follicular dendritic cells. Growth characteristics and interactions with B lymphocytes. *J.Immunol.* 148:3327-3335.

191. Orscheschek, K., H. Merz, B. Schlegelberger, and A. C. Feller. 1994. An immortalized cell line with features of human follicular dendritic cells. Antigen and cytokine expression analysis. *Eur.J.Immunol.* 24:2682-2690.

192. Husson, H., S. M. Lugli, P. Ghia, A. Cardoso, A. Roth, K. Brohmi, E. G. Carideo, Y. S. Choi, J. Browning, and A. S. Freedman. 2000. Functional effects of TNF and lymphotoxin alpha1beta2 on FDC-like cells. *Cell Immunol.* 203:134-143.

193. Butch, A. W., G. H. Chung, J. W. Hoffmann, and M. H. Nahm. 1993. Cytokine expression by germinal center cells. *J.Immunol.* 150:39-47.

194. Toellner, K. M., D. Scheel-Toellner, R. Sprenger, M. Duchrow, L. H. Trumper, M. Ernst, H. D. Flad, and J. Gerdes. 1995. The human germinal centre cells, follicular dendritic cells and germinal centre T cells produce B cell-stimulating cytokines. *Cytokine* 7:344-354.

195. Schriever, F., G. Freeman, and L. M. Nadler. 1991. Follicular dendritic cells contain a unique gene repertoire demonstrated by single-cell polymerase chain reaction. *Blood* 77:787-791.

196. Jacob, J., J. Przylepa, C. Miller, and G. Kelsoe. 1993. In situ studies of the primary immune response to (4-hydroxy-3-nitrophenyl)acetyl. III. The kinetics of V region mutation and selection in germinal center B cells. *J.Exp.Med.* 178:1293-1307.

197. Higgins, D. G. and P. M. Sharp. 1988. CLUSTAL: a package for performing multiple sequence alignment on a microcomputer. *Gene* 73:237-244.

198. Higgins, D. G. 1994. CLUSTAL V: multiple alignment of DNA and protein sequences. *Methods Mol.Biol.* 25:307-318.

199. Decker, D. J., P. J. Linton, S. Zaharevitz, M. Biery, T. R. Gingeras, and N. R. Klinman. 1995. Defining subsets of naive and memory B cells based on the ability of their progeny to somatically mutate in vitro. *Immunity.* 2:195-203.

200. Furukawa, K., A. Akasako-Furukawa, H. Shirai, H. Nakamura, and T. Azuma. 1999. Junctional amino acids determine the maturation pathway of an antibody. *Immunity.* 11:329-338.

201. Jack, R. S., T. Imanishi-Kari, and K. Rajewsky. 1977. Idiotypic analysis of the response of C57BL/6 mice to the (4-hydroxy-3-nitrophenyl)acetyl group. *Eur.J.Immunol.* 7:559-565.

202. Makela, O., K. Karjalainen, S. T. Ju, and A. Nisonoff. 1977. Two str1cturally similar haptens each induce a different inherited idiotype. *Eur.J.Immunol.* 7:831-835.

203. Makela, O. and K. Karjalainen. 1977. Inheritance of antibody specificity. IV. Control of related molecular species by one VH gene. *Cold Spring Harb.Symp.Quant.Biol.* 41 Pt 2:735-741.

204. Makela, O. and K. Karjalainen. 1977. Inherited immunoglobulin idiotypes of the mouse. *Immunol.Rev.* 34:119-138.

205. Cumano, A. and K. Rajewsky. 1985. Structure of primary anti-(4-hydroxy-3-nitrophenyl)acetyl (NP) antibodies in normal and idiotypically suppressed C57BL/6 mice. *Eur.J.Immunol.* 15:512-520.

206. Jacob, J. and G. Kelsoe. 1992. In situ studies of the primary immune response to (4-hydroxy-3-nitrophenyl)acetyl. II. A common clonal origin for periarteriolar lymphoid sheath-associated foci and germinal centers. *J.Exp.Med.* 176:679-687.

207. Song, H., X. Nie, S. Basu, M. Singh, and J. Cerny. 1999. Regulation of VH gene repertoire and somatic mutation in germinal centre B cells by passively administered antibody. *Immunology* 98:258-266.

208. Matsumoto, M., S. F. Lo, C. J. Carruthers, J. Min, S. Mariathasan, G. Huang, D. R. Plas, S. M. Martin, R. S. Geha, M. H. Nahm, and D. D. Chaplin. 1996. Affinity maturation without germinal centres in lymphotoxin-alpha-deficient mice. *Nature* 382:462-466.

209. Lesinski, G. B. and M. A. Westerink. 2001. Novel vaccine strategies to T-independent antigens. *J.Microbiol.Methods* 47:135-149.

210. Dintzis, R. Z., M. H. Middleton, and H. M. Dintzis. 1983. Studies on the immunogenicity and tolerogenicity of T-independent antigens. *J.Immunol.* 131:2196-2203.

211. Tsiagbe, V. K., P. J. Linton, and G. J. Thorbecke. 1992. The path of memory B-cell development. *Immunol.Rev.* 126:113-141.

212. Helm, S. L., G. F. Burton, A. K. Szakal, and J. G. Tew. 1995. Follicular dendritic cells and the maintenance of IgE responses. *Eur.J.Immunol.* 25:2362-2369.

213. Groom, J. R., C. A. Fletcher, S. N. Walters, S. T. Grey, S. V. Watt, M. J. Sweet, M. J. Smyth, C. R. Mackay, and F. Mackay. 2007. BAFF and MyD88 signals promote a lupuslike disease independent of T cells. *J.Exp.Med.* 204:1959-1971.

214. Shulga-Morskaya, S., M. Dobles, M. E. Walsh, L. G. Ng, F. Mackay, S. P. Rao, S. L. Kalled, and M. L. Scott. 2004. B cell-activating factor belonging to the TNF family acts through separate receptors to support B cell survival and T cell-independent antibody formation. *J.Immunol.* 173:2331-2341.

215. Kapasi, Z. F., G. F. Burton, L. D. Shultz, J. G. Tew, and A. K. Szakal. 1993. Induction of functional follicular dendritic cell development in severe combined immunodeficiency mice. Influence of B and T cells. *J.Immunol.* 150:2648-2658.

216. Goroff, D. K., J. M. Holmes, H. Bazin, F. Nisol, and F. D. Finkelman. 1991. Polyclonal activation of the murine immune system by an antibody to IgD. XI. Contribution of membrane IgD cross-linking to the generation of an in vivo polyclonal antibody response. *J.Immunol.* 146:18-25.

217. Taylor, P. R., M. C. Pickering, M. H. Kosco-Vilbois, M. J. Walport, M. Botto, S. Gordon, and L. Martinez-Pomares. 2002. The follicular dendritic cell restricted epitope, FDC-M2, is complement C4; localization of immune complexes in mouse tissues. *Eur.J.Immunol.* 32:1888-1896.

218. Han, S., B. Zheng, Y. Takahashi, and G. Kelsoe. 1997. Distinctive characteristics of germinal center B cells. *Semin.Immunol.* 9:255-260.

219. Tolar, P., H. W. Sohn, and S. K. Pierce. 2008. Viewing the antigen-induced initiation of B-cell activation in living cells. *Immunol.Rev.* 221:64-76.:64-76.

220. Raff, M. C., M. Sternberg, and R. B. Taylor. 1970. Immunoglobulin determinants on the surface of mouse lymphoid cells. *Nature.* 225:553-554.

221. Bachmann, M. F. and R. M. Zinkernagel. 1997. Neutralizing antiviral B cell responses. *Annu.Rev.Immunol.* 15:235-70.:235-270.

222. Rosenberg, A. S. 2006. Effects of protein aggregates: an immunologic perspective. *AAPS.J.* 8:E501-E507.

223. Carter, R. H., G. M. Doody, J. B. Bolen, and D. T. Fearon. 1997. Membrane IgM-induced tyrosine phosphorylation of CD19 requires a CD19 domain that mediates association with components of the B cell antigen receptor complex. *J.Immunol.* 158:3062-3069.

224. Liu, Y. J., S. Oldfield, and I. C. MacLennan. 1988. Thymus-independent type 2 responses in lymph nodes. *Adv.Exp.Med.Biol.* 237:113-117.

225. MacLennan, I. C. 2008. B cells: the follicular dimension of the marginal zone. *Immunol.Cell Biol.* 86:219-220.

226. Heijink, I. H., E. Vellenga, P. Borger, D. S. Postma, J. G. de Monchy, and H. F. Kauffman. 2002. Interleukin-6 promotes the production of interleukin-4 and interleukin-5 by interleukin-2-dependent and -independent mechanisms in freshly isolated human T cells. *Immunology* 107:316-324.

227. Huard, B., P. Schneider, D. Mauri, J. Tschopp, and L. E. French. 2001. T cell costimulation by the TNF ligand BAFF. *J.Immunol.* 167:6225-6231.

228. Huard, B., L. Arlettaz, C. Ambrose, V. Kindler, D. Mauri, E. Roosnek, J. Tschopp, P. Schneider, and L. E. French. 2004. BAFF production by antigen-presenting cells provides T cell co-stimulation. *Int.Immunol.* 16:467-475.

229. Park, C. S., S. O. Yoon, R. J. Armitage, and Y. S. Choi. 2004. Follicular dendritic cells produce IL-15 that enhances germinal center B cell proliferation in membrane-bound form. *J.Immunol.* 173:6676-6683.

230. Mori, A., M. Suko, O. Kaminuma, S. Inoue, T. Ohmura, Y. Nishizaki, T. Nagahori, Y. Asakura, A. Hoshino, Y. Okumura, G. Sato, K. Ito, and H. Okudaira. 1996. IL-15 promotes cytokine production of human T helper cells. *J.Immunol.* 156:2400-2405.

231. Boes, M. 2000. Role of natural and immune IgM antibodies in immune responses. *Mol.Immunol.* 37:1141-1149.

232. Cooper, N. R. 1985. The classical complement pathway: activation and regulation of the first complement component. *Adv.Immunol.* 37:151-216.:151-216.

233. Goldstein, M. F., A. L. Goldstein, E. H. Dunsky, D. J. Dvorin, G. A. Belecanech, and K. Shamir. 2006. Selective IgM immunodeficiency: retrospective analysis of 36 adult patients with review of the literature. *Ann.Allergy Asthma Immunol.* 97:717-730.

234. Goldstein, M. F., A. L. Goldstein, E. H. Dunsky, D. J. Dvorin, G. A. Belecanech, and K. Shamir. 2008. Pediatric selective IgM immunodeficiency. *Clin.Dev.Immunol.* 2008:624850. Epub;%2008 Nov 24.:624850.

235. Buckley, R. H. 2002. Primary cellular immunodeficiencies. *J.Allergy Clin.Immunol.* 109:747-757.

236. Grunebaum, E., N. Sharfe, and C. M. Roifman. 2006. Human T cell immunodeficiency: when signal transduction goes wrong. *Immunol.Res.* 35:117-126.

237. Cowley, S. 2001. The biology of HIV infection. *Lepr.Rev.* 72:212-220.

238. Fulop, T., A. Larbi, A. Wikby, E. Mocchegiani, K. Hirokawa, and G. Pawelec. 2005. Dysregulation of T-cell function in the elderly : scientific basis and clinical implications. *Drugs Aging.* 22:589-603.

239. Spatz, M., N. Eibl, S. Hink, H. M. Wolf, G. F. Fischer, W. R. Mayr, G. Schernthaner, and M. M. Eibl. 2003. Impaired primary immune response in type-1 diabetes. Functional impairment at the level of APCs and T-cells. *Cell Immunol.* 221:15-26.

240. Moser, B., G. Roth, M. Brunner, T. Lilaj, R. Deicher, E. Wolner, J. Kovarik, G. Boltz-Nitulescu, A. Vychytil, and H. J. Ankersmit. 2003. Aberrant T cell activation and heightened apoptotic turnover in end-stage renal failure patients: a comparative evaluation between non-dialysis, haemodialysis, and peritoneal dialysis. *Biochem.Biophys.Res.Commun.* 308:581-585.

241. Garcia, A. M., S. A. Fadel, S. Cao, and M. Sarzotti. 2000. T cell immunity in neonates. *Immunol.Res.* 22:177-190.

242. Velilla, P. A., M. T. Rugeles, and C. A. Chougnet. 2006. Defective antigen-presenting cell function in human neonates. *Clin.Immunol.* 121:251-259.

243. Macchiarini, F., M. G. Manz, A. K. Palucka, and L. D. Shultz. 2005. Humanized mice: are we there yet? *J Exp.Med.* 202:1307-1311.

244. Suematsu, S. and T. Watanabe. 2004. Generation of a synthetic lymphoid tissue-like organoid in mice. *Nat.Biotechnol.* 22:1539-1545.

245. Sun, Z., P. W. Denton, J. D. Estes, F. A. Othieno, B. L. Wei, A. K. Wege, M. W. Melkus, A. Padgett-Thomas, M. Zupancic, A. T. Haase, and J. V. Garcia. 2007. Intrarectal transmission, systemic infection, and CD4+ T cell depletion in humanized mice infected with HIV-1. *J Exp.Med.* 204:705-714.

246. Verdier, F. 2002. Non-clinical vaccine safety assessment. *Toxicology* 174:37-43.

247. Torvaldsen, S. and P. B. McIntyre. 2002. Observational methods in epidemiologic assessment of vaccine effectiveness. *Commun.Dis.Intell.* 26:451-457.

248. Rothman, A. L., Y. Yamada, J. Jameson, J. Cruz, K. West, S. Green, and F. A. Ennis. 1998. Assessment of human CD4+ and CD8+ T lymphocyte responses in experimental viral vaccine studies. *Dev.Biol.Stand.* 95:95-104.

249. Hogrefe, W. R. 2005. Biomarkers and assessment of vaccine responses. *Biomarkers* 10 Suppl 1:S50-S57.

250. Goncalves, G. 2008. Herd immunity: recent uses in vaccine assessment. *Expert.Rev.Vaccines.* 7:1493-1506.

251. Cho, M. W. 2000. Assessment of HIV vaccine development: past, present, and future. *Adv.Pharmacol.* 49:263-314.

252. Burns, M. J. and A. M. O'Connor. 2008. Assessment of methodological quality and sources of variation in the magnitude of vaccine efficacy: a systematic review of studies from 1960 to 2005 reporting immunization with Moraxella bovis vaccines in young cattle. *Vaccine* 26:144-152.

253. Reitan, L. J. and C. J. Secombes. 1997. In vitro methods for vaccine evaluation. *Dev.Biol.Stand.* 90:293-301.

254. Tew, J. G., G. F. Burton, L. I. Kupp, and A. Szakal. 1993. Follicular dendritic cells in germinal center reactions. *Adv.Exp.Med.Biol.* 329:461-465.

255. Liu, Y. J., G. Grouard, O. de Bouteiller, and J. Banchereau. 1996. Follicular dendritic cells and germinal centers. *Int.Rev.Cytol.* 166:139-179.

256. Liu, Y. J., J. Zhang, P. J. Lane, E. Y. Chan, and I. C. MacLennan. 1991. Sites of specific B cell activation in primary and secondary responses to T cell-dependent and T cell-independent antigens. *Eur.J.Immunol.* 21:2951-2962.

257. Cozine, C. L., K. L. Wolniak, and T. J. Waldschmidt. 2005. The primary germinal center response in mice. *Curr.Opin.Immunol.* 17:298-302.

258. Chen, L. L., J. C. Adams, and R. M. Steinman. 1978. Anatomy of germinal centers in mouse spleen, with special reference to "follicular dendritic cells". *J.Cell Biol.* 77:148-164.

259. Szakal, A. K. and J. G. Tew. 1992. Follicular dendritic cells: B-cell proliferation and maturation. *Cancer Res.* 52:5554s-5556s.

260. Kelsoe, G. 2000. Studies of the humoral immune response. *Immunol.Res.* 22:199-210.

261. Przylepa, J., C. Himes, and G. Kelsoe. 1998. Lymphocyte development and selection in germinal centers. *Curr.Top.Microbiol.Immunol.* 229:85-104.

262. Wolniak, K. L., S. M. Shinall, and T. J. Waldschmidt. 2004. The germinal center response. *Crit Rev.Immunol.* 24:39-65.

263. Chappell, C. P. and J. Jacob. 2007. Germinal-center-derived B-cell memory. *Adv.Exp.Med.Biol.* 590:139-148.

264. Cozine, C. L., K. L. Wolniak, and T. J. Waldschmidt. 2005. The primary germinal center response in mice. *Curr.Opin.Immunol.* 17:298-302.

265. Herbeuval, J. P. and G. M. Shearer. 2006. Are blockers of gp120/CD4 interaction effective inhibitors of HIV-1 immunopathogenesis? *AIDS Rev.* 8:3-8.

266. Herbeuval, J. P. and G. M. Shearer. 2007. HIV-1 immunopathogenesis: how good interferon turns bad. *Clin.Immunol.* 123:121-128.

267. Espert, L., M. Denizot, M. Grimaldi, V. Robert-Hebmann, B. Gay, M. Varbanov, P. Codogno, and M. Biard-Piechaczyk. 2007. Autophagy and CD4+ T lymphocyte destruction by HIV-1. *Autophagy.* 3:32-34.

268. Alimonti, J. B., T. B. Ball, and K. R. Fowke. 2003. Mechanisms of CD4+ T lymphocyte cell death in human immunodeficiency virus infection and AIDS. *J.Gen.Virol.* 84:1649-1661.

Vita

Rania Mohamed El Sayed was born on January 6, 1974 in Cairo, Egypt. She received her Bachelors degree in Sciences from Ain Shams University, Cairo, Egypt in 1995, and a pre-master degree in Microbiology in 1996. She worked as an Assistant Researcher in Microbiology in The Regional Center for Mycology and Biotechnology, Al-Azhar University, Cairo, Egypt in 1995. In 1998, she joined the Department of Plant Studies, Faculty of Science, Helwan University, Cairo, Egypt as a Demonstrator of Microbiology. In 1999, she worked in Food Microbiology in The Agricultural Research Center, Cairo, Egypt as a Research Assistant, as Deputy for Technical Manager in 2000 and then as a Technical Manager in 2003. She joined the Departement of Microbiology and Immunology at Medical Colledge of Virginia campus of Virginia Commonwealth University as a Laboratory Assistant in March 2005 and as a Doctoral Student in 2006.